



**PONTIFICIA UNIVERSIDAD CATÓLICA DE CHILE**  
**Facultad de Ciencias Biológicas**  
**Programa Doctorado en Ciencias Biológicas**  
**Departamento Genética Molecular y Microbiología**

**“Engineering multicellular domains in  
*M. polymorpha* from internal phytohormone  
gradients”**

Tesis entregada a la Pontificia Universidad Católica de Chile en cumplimiento parcial  
de los requisitos para optar al Grado de Doctor en Ciencias con mención en  
Genética Molecular y Microbiología

**Ariel Patricio Cerda Rojas**  
**Tutor: Dr. Fernán Federici**

¿Pero qué no ves que toda vida,  
toda creación en el campo que sea,  
todo acto de amor,  
no es más que una rebeldía frente a la extinción,  
no importa que sea falsa o verdadera,  
que dé resultados o no?

**José Donoso, Coronación (1957)**



FACULTAD DE CIENCIAS BIOLÓGICAS  
PONTIFICIA UNIVERSIDAD CATÓLICA DE CHILE

**ACTA DEFENSA FINAL DE TESIS**

Don Ariel Patricio Cerda Rojas, estudiante del Programa de Doctorado en Ciencias Biológicas Mención Genética Molecular y Microbiología, ha presentado la Defensa Pública de Tesis.

En consideración a los conocimientos generales sobre Genética Molecular y Microbiología, y la defensa de la Tesis Doctoral, titulada **"Engineering multicellular domains in M. polymorpha from internal phytohormone gradients"**, el Comité de Tesis a resuelto calificar esta actividad académica como Aprobada y con nota .....<sup>7,0 (siete)</sup>.....

Se firma la presente acta en la ciudad de Santiago, el día 27 de abril de 2022.

Dr. Juan Correa M.  
Decano  
Facultad de Ciencias Biológicas-UC

Dr. Luis Larrondo C.  
Coordinador de Comité de Tesis  
Facultad de Ciencias Biológicas-UC

Dr. Fernán Federici N.  
Director de Tesis  
Facultad de Ciencias Biológicas-UC

Dr. Rodrigo Gutiérrez I.  
Miembro Comité de Tesis  
Facultad de Ciencias Biológicas-UC

Dr. Diego Orzaez C.  
Miembro Externo Comité de Tesis  
Universidad de Valencia-España

## AGRADECIMIENTOS

Primero que todo agradezco a mi laboratorio, especialmente a mi tutor Fernán, quien me proporciono un ambiente lleno de desafíos intelectuales (y amor por Boca). Tengo suerte de haber encontrado ese espacio donde la ciencia siempre estuvo presente en armonía con el arte, la política y la filosofía. Sin lugar a duda ahí he crecido como científico, pero también como persona. Agradezco también a sus integrantes y amigos: Alejo, Isaac, Tamara, Maca, Aníbal, Kevin, Coti, Daniel y Sev.

Agradezco al Dr. Rodrigo Gutiérrez y todas las personas que conocí en su laboratorio. Siempre se aseguraron de hacerme sentir parte de su espacio sin ningún cuestionamiento alguno. Sin su ayuda me hubiera sido imposible desarrollar mi Tesis Doctoral ni desarrollar mi carrera profesional. Agradezco en especial a mis amigos y colegas: Seba, Grace, Tomas, Su, Valentina, Jhonny, Meli, Laura, Karem, Andrea, Eleo, Vivi, Jose, Isas, Pancha, Lili, Alvaro y Jenny.

A mis compañeros de doctorado por su amistad y compañía en todos estos años. Me siento orgulloso de haber compartido con tan grandes (y curiosas) personas. Sin Uds. hubiera perdido el rumbo en tan largo camino. Gracias a Benja, Brenda, Carlitos, Diana, Leo, Marlene y Jose.

A mi familia, principalmente mis padres y hermanas. Por su amor y paciencia. Pero por sobre todo por permitirme, apoyarme y motivarme durante todo este tiempo a seguir haciendo lo que amo.

A mis tatas y tío que ya no están, por todos los abrazos que nos dimos y aquellos que no alcanzamos a darnos. Me hubiera gustado compartir con Uds. la culminación de este proceso.

A mis amigos de la vida, por los momentos de ocio que ayudaron a aliviar la carga e incluso a desarrollar nuevos proyectos (o nuevas obsesiones). Por su apoyo incondicional y su constante motivación a mirar hacia adelante. Gracias a Mati, Carla, Nicole, Dey, Talo, Rolo, Fran, Aliosha, Juanjo, Pablo, Titi, Paula, Chilo, Jocy y Clau,

A mi Rena, mi hijo. Motivación constante para ser mejor persona y papá. Por todo el amor que día a día me entrega y por todos esos momentos que nos quedan por compartir.

A mi Joy, por su compañía incondicional durante todos estos últimos años. Por ser una compañera, una amiga y una excelente científica. Por ser un pilar fundamental de mi vida y por ser una inspiración constante en mi vida. Gracias por tu amor y por Bowie.

## INDEX

|   |            |
|---|------------|
| <b>ACKNOWLEDGMENT.....</b>                          | <b>3</b>   |
| <b>INDEX.....</b>                                   | <b>4</b>   |
| <b>RESUMEN.....</b>                                 | <b>5</b>   |
| <b>ABSTRACT.....</b>                                | <b>6</b>   |
| <b>INTRODUCTION.....</b>                            | <b>7</b>   |
| <b>HYPOTHESIS.....</b>                              | <b>16</b>  |
| <b>OBJECTIVES.....</b>                              | <b>16</b>  |
| <b>MATERIAL AND METHODS .....</b>                   | <b>17</b>  |
| <b>RESULTS.....</b>                                 | <b>26</b>  |
| <b>DISCUSSION.....</b>                              | <b>74</b>  |
| <b>CONCLUSIONS.....</b>                             | <b>83</b>  |
| <b>BIBLIOGRAPHY.....</b>                            | <b>84</b>  |
| <b>APPENDIX I: Plasmids .....</b>                   | <b>100</b> |
| <b>APPENDIX II: Equations and Assumptions. ....</b> | <b>126</b> |

## RESUMEN

La biología sintética es un campo multidisciplinario emergente que involucra a la biología, la ingeniería, y la física en el desarrollo de abstracciones, herramientas y modelos para diseñar sustratos biológicos de manera reproducible, escalable y eficiente. Uno de los temas más desafiantes corresponde a la programación de comportamientos emergentes y procesos de autoorganización en sistemas multicelulares, campo denominado ingeniería morfogénica. Las plantas son una plataforma atractiva para estudiar cómo la formación de patrones contribuye al desarrollo y la morfogénesis, así como para definir principios morfogénicos. Un modelo atractivo para abordar estos desafíos y reducir la brecha entre la facilidad de manejo de los organismos unicelulares y la complejidad de las plantas superiores es la hepática *Marchantia Polymorpha* (Marchantia). Marchantia presenta características prometedoras para la biología sintética, como un ciclo de vida más corto, una fase de gametofito haploide dominante, un genoma secuenciado con baja redundancia genética, una propagación clonal sencilla y robusta a través del subcultivo de gemas y una transformación de alta eficiencia para la manipulación genética. La ingeniería morfogénica en plantas debe enfrentar constantemente la escasez de herramientas fundacionales y componentes genéticos estandarizados, y su progreso se ha visto retrasado por la falta de información sobre los elementos funcionales de ADN. En este trabajo, nuestro objetivo es crear funciones elementales para la ingeniería de patrones en plantas mediante el establecimiento de dominios artificiales de estados celulares, utilizando gradientes internos (fitohormonas) como entradas para nuestros circuitos formadores de patrones. Para lograrlo, creamos nuevas herramientas para la construcción rápida, modular y combinatoria de circuitos genéticos en plantas, probamos elementos genéticos para construir estos circuitos y propusimos formalismos matemáticos para el desarrollo de modelos morfogénicos. Todo esto se hizo utilizando Marchantia y sus ventajas como chasis para la biología sintética.

## ABSTRACT

Synthetic biology is an emerging multidisciplinary field involving biology, physics, and mathematics in developing abstractions, tools, and models for engineering biological substrate in a reproducible, scalable, and efficient way. One of the most interesting topics corresponds to the programming of emergent behavior and self-organizing processes in multicellular systems, field called morphogenetic engineering. Plants are an attractive platform to study how pattern formation contributes to development and morphogenesis as well as to define engineering morphogenetic principles. An attractive model to address these challenges and reduce the gap between unicellular organisms' handiness and complexity of higher plants is the liverwort *Marchantia Polymorpha* (Marchantia). Marchantia has promising features for synthetic biology such as a shorter life cycle, dominant haploid gametophyte phase, sequenced genome with low genetic redundancy, easy and robust non-chimeric clonal propagation through the subculture of gemmae, and high-efficiency transformation for genetic manipulation. Performing morphogenetic engineering on plants must constantly face the scarcity of foundational tools and standardized genetic components, and its progress has been delayed by a lack of information about functional DNA elements. In this work, we aim to create elementary functions for pattern engineering in plants through the establishment of artificial domains of cellular states, using internal gradients (phytohormones) as inputs for our pattern-forming circuits. To achieve this, we created new tools for the rapid, modular and combinatorial construction of plant genetic circuits, tested genetic elements to build these circuits and proposed mathematical formalisms for the development of predictive models. All this was done using *Marchantia polymorpha* and its advantages as a testbed for synthetic biology.

## INTRODUCTION

### **Synthetic biology as an interdisciplinary field.**

The origin of synthetic biology starts with the assertion that engineering approaches could be applied to biology with the aim of both discovering principles that explain biological functioning and allowing the engineering of artificial biosystems of high complexity, predictability and scale. Nowadays, synthetic biology is an emerging multidisciplinary field involving biology, physics, and mathematics in developing abstractions, tools, and models for engineering biological substrate in a reproducible, scalable and efficient way. Guided by these models, this discipline uses techniques and tools of molecular biology to move from high-level abstractions and logical designs to the physical implementation of these in biological systems (Cameron et al., 2014). Additionally, this discipline includes biological systems redesign to adapt them to new applications for industrial, medical, or social interest (Khalil and Collins, 2010; Slomovic et al., 2015; Dobrin et al., 2016; Haellman and Fussenegger, 2016). Engineering principles such as standardization, characterization, modular design, and abstraction have been essential to implementing living systems engineering (Endy, 2005). Characterization attempts to assign parameters to the parts (e.g., transcription and degradation rate, RBS and terminator strength, etc.) intending to generate abstractions and design specifications with correspondence with mathematical or algorithmic design tools. This is highly desirable since having well-defined standard parts allows us to predict their modes of connectivity with others and therefore facilitate their reuse and readaptation in the creation of synthetic biological circuits. Despite all the efforts made over the past decade, the complexity and unpredictability of living cells engineering cause the parts to still fail to function predictably when taken out of their original biological context or function improperly when placed into circuits with

other parts (Purnick and Weiss, 2009; Kwok, 2010). Even so, a clear example of engineering and computation that can be performed in living cells is 'Cello', an end-to-end computer-assisted design system for logic circuit construction in *E. coli* (Nielsen et al., 2016). Cello uses electronic design specifications of combinational logic to automatically design a DNA sequence encoding the desired and fully-functional circuit in bacterial cells. This work showed that some of the challenges of engineering biological systems could be overcome and that cells could in principle be programmed in a similar way we wire up electronic circuits. Synthetic Biology finds inspiration in this electrical engineering dogma. Therefore, it is not a surprise that the first gene regulatory circuits, i.e., toggle switch (Gardner et al., 2000) and oscillator (Elowitz and Leibler, 2000), were built to carry out functions inspired by electrical circuits. Moreover, the general guidelines and experimental features of the field have allowed the development of a wide range of synthetic biological circuits such as molecular counters or memory devices (Friedland et al., 2009; Bonnet et al., 2012; Siuti et al., 2013; Farzadfard and Lu, 2014; Chen et al., 2021), logic gates (Wang et al., 2011; Ausländer et al., 2012; Moon et al., 2012; Miyamoto et al., 2013; Shis and Bennett, 2013; Gander et al., 2017), analog signal processors (Daniel et al., 2013), cellular classifiers (Xie et al., 2011; You et al., 2015), and recording devices (Sheth et al., 2017; Shipman et al., 2017).

## **Engineering pattern formation through synthetic biology.**

Currently, synthetic biology embraces cell-free (Perez et al., 2016; Tinafar et al., 2019; Arce et al., 2021), bacterial (Khalil and Collins, 2010; Nuñez et al., 2017), mammalian (Lienert et al., 2014; Wroblewska et al., 2015; Mathur et al., 2017; Kitada et al., 2018) and multicellular systems (Glass and Riedel-Kruse, 2018; Toda et al., 2018). Regarding the latter, a topic that has gained increasing interest is the programming of emergent behavior and self-organizing processes (i.e., self-assembly and self-regulation) in multicellular systems (Teague et al., 2016). This field, called morphogenetic engineering, seeks to explore the design, implementation, and control of the complex system agents that autonomously and reproducibly generate large heterogeneous architectures which will support a set of desired functionalities (Doursat et al., 2013). In multicellular organisms, the agents are living cells that execute cell proliferation, migration, and differentiation through genetically programmed rules giving rise to a hierarchical structural organization typically composed of tissues, organs, and systems. Furthermore, it has been proposed that this rewiring of modular cellular behaviors in multicellular systems has incorporated a new layer in the Synthetic Biology abstraction hierarchy (Federici et al., 2013). This layer opens new applications related to programmable artificial tissues and organs (Todhunter et al., 2015; Johnson et al., 2017), engineered living materials (Gilbert and Ellis, 2019), and complex morphogenetic systems (Blain and Szostak, 2014; Göpfrich et al., 2018; Weiss et al., 2018). This subject is also crucial for understanding of pattern formation in cell populations and tissues (Scholes and Isalan, 2017; Santos-Moreno and Schaerli, 2019). Pattern formation is a developmental process by which cells become differentiated spatially. After that, they acquire different identities through a nonrandom gene expression program that will eventually lead to a particular physical

form or spatially-structured functions. Pattern formation has been studied through diverse genetically-encoded synthetic approaches to autonomously establish a specific spatial arrangement. These approaches mainly include i) Lewis Wolpert's "positional information" model (so-called the "French Flag" model), where a spatial gradient of an external morphogen triggers differential gene expression according to each cell's position within this gradient (Basu et al., 2005; Isalan et al., 2005; Sohka et al., 2009; Greber and Fussenegger, 2010; Schaerli et al., 2014; Grant et al., 2016; Grant et al., 2020). ii) Turing or "reaction-diffusion" model in which repetitive patterns emerge due to a unique interaction between two diffusible species; an activator that favors the production of itself and a second species, while the second acts as a repressor inhibiting the activator (Karig et al., 2018; Sekine et al., 2018). iii) Phase separation models in which the cells become spatially segregated according to their differential adhesion properties, resulting in complete segregation or a complex pattern of patches if cells are constrained (Cachat et al., 2016; Glass and Riedel-Kruse, 2018; Toda et al., 2018; Toda et al., 2020). iv) Rule-based mechanisms that rely on physicochemical forces and properties, capable of forming fractal-like or branching structures through cell division and growth (Rudge et al., 2013; Nuñez et al., 2017; Smith et al., 2017). All these mechanisms are crucial in developmental biology, and the use of synthetic approaches can largely contribute to unveiling generic mechanisms.

## **Morphogenetic engineering in plants.**

Plants are an attractive platform to study how pattern formation contributes to development and morphogenesis as well as to define engineering morphogenetic principles. Pattern formation allows organ and tissue development in the correct spatiotemporal distribution through the concerted behavior of cell populations (Niklas et al., 2019). This behavior is shaped by feedback and interplay between local and whole-plant processes that involve mechanical stress, hormone flux, cell growth, cell wall biosynthesis, and cell division (Tsukaya, 2003; Somerville et al., 2004; Baskin, 2005; Hamant et al., 2008; Nakayama et al., 2012; Sampathkumar et al., 2014). Plant plasticity, body plan diversity and modularity, specialized structures for photosynthesis, and secondary metabolite production make them excellent candidates for morphogenetic reprogramming (Boehm et al., 2017; Patron, 2020). Moreover, plants present labor compartmentalization due to cellular differentiation that can be exploited by reprogramming pattern formation. Modular organization of the ABC model that specifies the different flower organs at the early stages of flower development through the integration of 3 classes of genes (Alvarez-Buylla et al., 2010) and compartmentalization of C4 photosynthesis between mesophyll and bundle sheath cells (Hatch, 1987; Sage, 2004) are remarkable examples of the relevance of spatially-distributed processes in biology. Despite the opportunities, our ability to modify the shape and structure of plants is hampered by our lack of knowledge and control of multicellular processes during morphogenesis. Besides, plant synthetic biology lags behind its microbial counterpart due to considerably slower growth, long life cycles, low transformation efficiencies, specialized equipment requirements, low availability of genetic manipulation tools, and the intrinsic complexity of working with multicellular organisms and larger genomes.

## **Marchantia as an ideal model for morphogenetic reprogramming.**

One of the best models to address these challenges and reduce the gap between unicellular organisms' handiness and complexity of higher plants is the liverwort *Marchantia Polymorpha* (Marchantia). Marchantia has promising features for synthetic biology such as a shorter life cycle, dominant haploid gametophyte phase, sequenced genome with low genetic redundancy, easy and robust non-chimeric clonal propagation through the subculture of gemmae, and high-efficiency sporeling transformation for genetic manipulation (Ishizaki et al., 2016; Boehm et al., 2017; Bowman et al., 2017). Marchantia is an ideal model to investigate plant development and morphology due to its simple, non-vascular, and flat sheet-like structure. Its characteristics allow tracking physiological and morphogenetic changes at the scale of whole-organism through the entire life cycle within a Petri dish. This is particularly evident for spores and gemmae, the reproductive propagules of Marchantia. Unicellular spores allow direct visualization of all early development processes because of the absence of testa (O'Hanlon, 1926) and may be stored at - 80°C for several years without a significant decrease in survival rate (Nakazato et al., 1999). Gemmae represent interesting models for engineering morphology owing to their robustness, plasticity, and accessibility (Boehm et al., 2017). Marchantia gemmae are held in specialized receptacles known as gemma cups and are viable for up to one year if stored at 4 ° C in agar or stored dehydrated in a - 80°C freezer (Miller, 1964; Tanaka et al., 2016). Additionally, the above-mentioned make Marchantia a rapid prototyping system for synthetic circuits with significant implications for crop production and metabolism engineering (Ishizaki et al., 2016).

## **Foundations for synthetic biology in plant systems.**

Although the plant biology community has been relatively slow to adopt the principles of synthetic biology, this field is following a similar path to the beginnings of microbial-focused synthetic biology (Liu and Stewart, 2015). In addition, performing morphogenetic engineering on plants must constantly face the scarcity of foundational tools and standardized genetic components. On top of that, its progress has been delayed by a lack of information about functional DNA elements (mainly regulatory elements), single-cell expression data for multiple organs, and directed evolution methods in plant cell cultures (Patron et al., 2020). Nevertheless, synthetic biology has also been strongly driven by technological innovations and improvements in engineering practices that have allowed significant progress in all relevant areas to discipline (Purnick and Weiss, 2009). The development of one-step assembly methods, such as Gibson Assembly (Gibson et al., 2009) and Golden Gate (Engler et al., 2008), coupled to the reduced cost of DNA synthesis has greatly facilitated and accelerated the methodical assembly of biological parts into larger circuits. This has even led to the *de novo* synthesis of entire bacterial genomes (Gibson et al., 2010) or yeast chromosomes (Annaluru et al., 2014). On the other hand, the Registry of Standard Biological Parts (RSBP, <http://parts.igem.org>) was created to deal with the exponential increase in biological parts. This registry has to date more than 20,000 well-documented standard parts (Briobricks) organized by part type, function, chassis, etc. (Knight, 2003; Shetty et al., 2008). However, almost all these efforts have been made in microbial models (mainly *E. coli* and *S. cerevisiae*) or mammalian cells, therefore more standardized components and methodologies are still needed for plant organisms. Coupled with this, a biological platform that allows us a rapid characterization and performance evaluation of synthetic genetic circuits in a plant

organism context is also needed. One of the first initiatives to meet those needs was the creation of OpenPlant, a collaborative initiative between the University of Cambridge, the John Innes Centre, and the Sainsbury Laboratory. This initiative promotes interdisciplinary exchange, open technologies for innovation, and responsible innovation for sustainable agriculture and conservation (<http://openplant.org/>). In addition, plants-specialized repositories of modular and standardized parts as MoClo (Weber et al., 2011; Engler et al., 2014) and GoldenBraid (Sarrion-Perdigones et al., 2011; Sarrion-Perdigones et al., 2013; Vazquez-Vilar et al., 2017) have been created. Both systems are based on the ability of type IIS restriction enzymes (REs) to assemble in a modular and efficient way multiple DNA fragments in a defined linear order by means of the Golden Gate assembly method. Several techniques of *in vitro* assembly allow the building of large DNA constructs from multiple parts; however, these involve *ad hoc* methods for primers and sequences design for each vector, increasing the manufacturing cost. Furthermore, the presence of repetitive elements in sequences such as binding sites of transcriptional regulators may interfere with the assembly of highly homologous fragments. To circumvent this problem, Torella et al. (2014) have created a computational approach to design synthetic, biologically inactive unique nucleotide sequences (UNSeqs) that facilitate accurate ordered assembly.

Based on the antecedents mentioned above we propose to create elementary artificial functions for pattern engineering in plants. In particular, we intent to create a simple system for the establishment of artificial domains of cellular states. In contrast to the most common approaches that use externally-added (e.g., Schaerli et al., 2014) or “sender” cells (e.g., Basu et al., 2004, Grant et al., 2016) of orthogonal signals, we want to exploit internal gradients as inputs for our pattern-forming circuits. Thus, we

aim to develop simple modules for the generation of artificial discrete domains from continuous gradients of phytohormones. The use of these internal gradients responds to the lack of artificial cell-to-cell signals that can be used to break symmetry in plants. As a proof-of-concept, we propose to use phytohormones internal gradients. Phytohormones control various aspects of plant growth, representing a robust internal framework for signal distribution to start from (Schaller et al., 2015). These hormones act through well-described response elements in the target genes promoters, allowing us to design synthetic promoters capable of interacting with internal distributions of these hormones. To achieve this, we focus on obtaining the following: a) New tools for the rapid, modular and combinatorial construction of plant genetic circuits. b) Standardized and characterized genetic elements to build these circuits. c) Mathematical formalisms for the development of predictive models. All this was done using *Marchantia polymorpha* and its advantages mentioned above as a testbed for synthetic biology.

## **HYPOTHESIS**

I/O characterization of genetic components allows the fabrication of artificial multicellular domains for application in morphogenetic engineering of *Marchantia polymorpha*

## **OBJECTIVES**

### **GENERAL OBJECTIVE**

To create elementary functions for the generation of multicellular domains from internal asymmetries of phytohormones distribution in *Marchantia polymorpha*

### **SPECIFIC OBJECTIVES**

1. To generate techniques and resources for fast, modular, and combinatorial construction of genetic circuits for plants.
2. To design and construct foundational components for the development of plant circuits.
3. To construct and characterize synthetic promoters for synthetic gene network engineering *in planta*.
4. To develop morphogenetic models based on internal gradients mediated by phytohormones.

## **MATERIAL AND METHODS**

### **Plant material and growth conditions**

Male (Cam-1) and female (Cam-2) *Marchantia* accessions were used in this study. Plants were grown and maintained on half-strength Gamborg's B5 medium plus vitamins (1.3% agar, pH 5.8, PhytoTech) at 22°C under white light (75  $\mu\text{mol m}^{-2} \text{s}^{-1}$ ) and long photoperiod (16 h light/ 8 h darkness). Wild type and transgenic *Marchantia* plants were asexually maintained and propagated through gemmae growth as previously described (Takenaka et al., 2000).

### **Construction of Loop assembly backbones**

The pOdd and pEven vectors of Loop were constructed using the Gibson Assembly (Gibson et al., 2009). As a starting point, a series of modifications were made to the pGreenII vector (Hellens et al, 2000) to generate the backbones. Recognition sites for the *Bsa*I and *Sap*I type-IIS restriction enzymes were removed using silent mutations when possible. The original pGreenII ColEI-derived origin of replication was mutated in two nucleotides to revert it to the medium-low copy number pBR322 replication origin. The region that comprised from the T-DNA left border to hygromycin resistance was replaced by the sequence contained between bases 2851 and 3527 of the pET15 vector (Haseloff, 1999), specifically from the *nptII* nosT terminator to the UASGAL4 promoter. In the pEven vectors, spectinomycin resistance was replaced by the *nptII* cassette to provide a microbial selection marker. UNSes were cloned into all pOdd and pEven vectors just after the 3' end of the pET15 vector sequence and the right border. Finally, the *Bsa*I and *Sap*I recognition sites, overhangs and the *lacZ* $\alpha$  cassette were cloned between the UNSes to achieve the final versions of Loop. The L0 plasmids were assembled using Gibson Assembly into a modified pUDP2 vector

(BBa\_P10500), which contained a random 20-bp sequence (5'-TAGCCGGTCGAGTGATACA CTGAAGTCTC-3') downstream of the 3' of the BsaI convergent site and upstream of the BioBrick suffix, to provide non-homologous flanking regions for the correct orientation during Gibson assembly. The L0 parts used for DNA construction and their sequences are described in Appendix I.

### **Loop Type IIS assembly protocol**

The Golden Gate-mediated Loop Assembly protocol was adapted from Patron (2016) and its specifications can be found at the following link: <https://www.protocols.io/view/loop-and-uloop-assembly-yxnfxfme>. In a 0.2 ml tube, 15 fmol of each part and 7.5 fmol of the specific receiver plasmid were added, completing a total volume of 5  $\mu$ l with nuclease-free water (Thermo Fisher) and keeping on ice until use. Then, a reaction mix was prepared depending on whether it consisted of an even or odd assembly. For assemblies in pOdd plasmids, the mix consisted of 1  $\mu$ l of T4 DNA ligase buffer 10x (NEB), 0.5  $\mu$ l of diluted Bovine Serum Albumin (BSA, 1 mg/mL, NEB), 0.25  $\mu$ l of T4 DNA ligase (400 U/ $\mu$ l, NEB), 0.25  $\mu$ l of BsaI-HFv2 (10 U/ $\mu$ l, NEB) and 3  $\mu$ l of nuclease-free water. While for pEven plasmid assemblies, the mix consisted of 0.5  $\mu$ l of Cutsmart 10X buffer (supplied with restriction enzymes, NEB), 0.5  $\mu$ l of T4 DNA ligase buffer (NEB), 0.25  $\mu$ l of T4 DNA ligase (400 U/ $\mu$ l, NEB), 0.25  $\mu$ l of SapI (10 U/ $\mu$ l, NEB), and 3.5  $\mu$ l of nuclease-free water. After that, the 5  $\mu$ l of DNA mix were mixed by pipetting with the corresponding reaction mix for a reaction volume of 10  $\mu$ l. The samples were placed in a thermocycler, alternating 37°C (3 min) and 16°C (4 min) for 30 cycles, ending with a temperature of 50°C (5 min) and 80°C (10 min). Subsequently, 1  $\mu$ l of the reaction mix was added to 50  $\mu$ l of chemically competent TOP10 cells. Then, they were incubated at 42°C for 1 min and transferred to ice for 10 min. After that time, 250  $\mu$ l of LB or SOC medium were added

and the cells were incubated for 1 h at 37°C. Finally, 5 µL of X-Gal (Sigma-Aldrich) dissolved in DMSO were added and the cells were plated in selective LB-agar medium (kanamycin or spectinomycin as appropriate) supplemented with 1 mM of IPTG (Sigma-Aldrich). All plasmids assembled by Loop, regardless of level and method, are listed in **Appendix I**.

### **Agrobacterium-mediated Marchantia transformation.**

Marchantia spore transformation was performed by modifying the protocol of Ishizaki et al. (2008). For the generation of Marchantia spores, male (CAM1) and female (CAM2) individuals were grown in separate boxes until the sexual organs developed. Plants were grown at 22°C under 75 µmol m<sup>-2</sup> s<sup>-1</sup> of white fluorescent light supplement with far-red light using high-intensity LEDs for growth chambers (PLGL-L, Epsilon Networks) and long-day conditions (16 hours light / 8 hours dark). Four to six weeks later, the male and female reproductive organs developed, and fertilization was performed. For this, a drop of water was placed with a sterile plastic pipette on the male reproductive organs (antheridium) to later be transferred to the female organs (archegonium). After 3-4 weeks, mature sporangia were visible and ready to be collected, dried with silica beads, and stored at -80°C until use. For spore sterilization, sporangia (1 per transformation reaction, 8 recommended per tube) were transferred to a 50 ml tube and triturated using a 1000 µl micropipette tip. Then, 1 ml of sterile water per sporangium was added and the resulting solution was filtered using a 40 µm cell strainer (Falcon). Sterile water was added to the tube with the filtered spores up to a total volume of 25 mL, and a Milton mini-sterilising tablet (Milton Pharmaceutical UK) was dissolved in the solution. Spore solution was incubated for 20 min at 150 rpm and then centrifuged at 4500 rpm for 2 min. The supernatant was carefully discarded, leaving at least 100 µl per sporangium used, in order to distribute concentrated spore

solution in 50 ml tubes with 20-25 ml of half-strength Gamborg's B5 medium (PhytoTech) supplemented with 2% sucrose (100 µl per tube). The spores were incubated at 22°C, 120 rpm and constant white light for 5 days, and then co-cultured with the *A. tumefaciens* clone GV2260 carrying the plasmid of interest for two days. To achieve that was necessary to grow the *Agrobacterium* clone at least two days before co-culture and then centrifuged (15 min at 3000 rpm) and resuspend in half-strength Gamborg's B5 medium supplemented with 2% sucrose and acetosyringone (100 µM, Sigma-Aldrich) for 6 h at 28°C. At least 1-2 ml of *Agrobacterium* solution was added per 50 mL tube. While for the thallus transformation, the protocol of Kubota et al. modified (2013) was used. *Marchantia gemmae* were grown for two weeks at 22°C at low light intensity (75 µmol m<sup>-2</sup> s<sup>-1</sup>) and long photoperiod (16 h light/ 8 h darkness). The apical portions (2-3 mm including the four meristems) were cut from each thallus. Once the meristems were eliminated, the remaining fragments were grouped into approximately 20-30 fragments and were incubated for 3 days in half-strength Gamborg's B5 medium with 1.3% agar at 22°C. Finally, the fragments are placed in 0M51C liquid medium together with the *A. tumefaciens* GV2260 clone of interest for 3 days at 22°C, 120 rpm and constant light. Once the co-culture was finished, in both protocols (spore and thallus), the tissue was washed five times with sterile water and once with 300 µg/ml of Timentin (PhytoTech) to eliminate the excess of *Agrobacterium*. The tissue was left for 30 min in a sterile water solution containing 300 µg/ml of Timentin. After that time, spores or thalli were spread on half-strength Gamborg's B5 medium plates with 1.3% agar, 250 µg/ml Timentin and 10 µg/ml hygromycin and were grown for 1 month at 22°C, low light intensity (75 µmol m<sup>-2</sup> s<sup>-1</sup>) and long photoperiod (16 h light/ 8 h darkness).

### **Epifluorescence microscopy**

Transfected *Arabidopsis* protoplasts and transformed *Marchantia* plants were visualized using a Nikon Ni microscope equipped with 49021 ET-EBFP2/Coumarin/Attenuated DAPI (excitation, 405/20 nm; dichroic, 425 nm; emission, 460/50 nm), 96227 AT-EYFP (excitation, 495/20 nm; dichroic, 515 nm; emission, 540/30 nm), 96223 AT-ECFP/C (excitation, 435/20 nm; dichroic, 455 nm; emission, 480/30 nm), 96343 EN-GFP (excitation, 470/40 nm; dichroic, 495 nm; emission, 525/50 nm) and 96312 G-2E/C (excitation, 540/20 nm; dichroic, 565 nm; emission, 620/60 nm) filter cubes.

### **Laser scanning confocal microscopy**

*Marchantia gemmae* were fitted in a microscope slide with 65  $\mu$ l of Gene Frame (ThermoFisher) and 65  $\mu$ l of dH<sub>2</sub>O were placed in the center. Gemmae were deposited on the dH<sub>2</sub>O using an inoculation loop or sterilized wooden toothpicks and a round coverslip 6mm #0 (0.08-0.12mm) was attached to the Gene Frame. To validate Loop assembly, slides were visualized in a Leica TCS SP8 confocal microscope platform equipped with a white-light laser (WLL) device. The images were obtained with a sequential scanning mode with laser wavelengths of 405, 488 and 515 nm, capturing emitted fluorescence at 450–482-, 492–512- and 520–550-nm windows, respectively, in each sequential scan. Z-stacks were collected every 5  $\mu$ m for the complete volume range and maximum intensity projections were processed using ImageJ software. To validate the localization of the fusion proteins, it was used an inverted Nikon Eclipse C2 Confocal microscope with a Nikon spectral detector and four solid-state lasers at 405 nm, 488 nm, 561 nm and 640 nm with intensity modulation through the AOTF system. The spectral detector was used to separate those fluorophores with close

emission/excitation ranges (resolution of 5 nm and scanning speed of 0.5 fps at 512x512 pixels).

### **Transient expression in Arabidopsis mesophyll protoplasts**

Well-expanded leaves from 3- to 4-week-old Arabidopsis plants (Columbia-0) were used for protoplast transfection. Plants were grown at 22°C in low-light (75  $\mu\text{mol m}^{-2} \text{s}^{-1}$ ) and short-photoperiod (12h:12h, light:dark) conditions. Protoplasts were isolated and polyethylene glycol (PEG) transfected according to Yoo et al. (2007). For transfection, 6  $\mu\text{l}$  of Loop L2 plasmids (2  $\mu\text{g } \mu\text{l}^{-1}$ ), isolated by a NucleoBond Xtra Midi/Maxi purification kit (Macherey-Nagel), were used. Transfected protoplasts were incubated for 12 h in light and then visualized by epifluorescent microscopy in a Neubauer chamber (Hirschmann).

### **Validation by sequencing and restriction endonuclease digestion**

All L0 and L1 plasmids were sequenced using a standard sequencing service (Macrogen). For L0 plasmids, pUPD-F3 (5'-TCACGAGGCAGAATTTTCAGA-3') and pUPD-R3 (5'-AGCCTGCATAACGCGAAGTA-3') primers were used. While, for L1 plasmids, LKS (5'-AGCTATGACCATGATTACGCCAAGC-3') and UNS-X reverse primer (**Table I**) were used. In order to validate Loop, the first assembled L2 and L3 plasmids were verified by complete sequencing using 150-base pair paired-end reads on an Illumina MiSeq platform and can be found in the EMBL-ENA database grouped under study PRJEB29863. Libraries were prepared using the Nextera XT DNA Library Prep Kit (Illumina), using the manufacturer's protocol modified to a one in four dilution. Reads were filtered and trimmed for low-quality bases and mapped to plasmids using the 'map to reference tool' from GENEIOUS 8.1.8 software (<https://www.geneious.com>;Kearse et al., 2012), with standard parameters. Sequence

fidelity was determined manually. After this validation, L2 and L3 plasmids were verified by restriction analysis. Generally, XbaI (NEB) and XhoI (NEB) restriction enzymes were sufficient to have a restriction profile that allowed comparison with the expected sizes pattern. Enzymatic digestions were performed according to the instructions of the manufacturers.

### **Plant UNSes design**

We designed 40 bp sequences to be used as UNSes in plants, inspired by Torella et al. (2014). We generated a list of 500,000 random 40mers and filtered them using the following criteria: (i) The complete sequence, or at least the 14 nucleotides at the 5' or 3' end, should not have a bit score greater than 35 when BLAST was performed against the Arabidopsis TAIR10 genome and *E.coli* genome., (ii) TGC Distribution: 45 % ≤ GC content ≤ 55 %. No tracts of > 4 AT-only or GC-only sequences; 1–2 G/C nucleotides at each terminus., (iii) Contain no start codons (ATG/TTG/CTG) since any randomly occurring RBS sequence will only be active if it is close to a start codon., (iv) Not contain the following common multiple cloning site (MCS) restriction sites: EcoNI, ClaI, XbaI, NcoI, BglII, SpeI, BamHI, NheI, PstI, HindIII, NotI, XhoI, AvrII, BlnI, Bsu36I, AgeI, AflII., (v) Not contain the following restriction sites commonly used for assemblies: AscI, SapI, MauBI, BbsI, MreI, AvrII, BpmI, BsaI., (vi) Hairpin T<sub>m</sub> < 40 °C assuming 10 mM NaCl and 10 mM Mg<sup>2+</sup>, tested with 'oligoprop' in MATLAB. Strong hairpins are predicted to be common because of high Mg<sup>2+</sup> concentrations in isothermal assembly reactions. Five already existing UNS (Torella et al., 2014) were reused because they met all the criteria. Plant UNS1 and UNS2 correspond to bacterial UNS1 and UNS2, respectively. Plant UNS3, UNS4 and UNS5 are equivalent to bacterial UNS5, UNS6 and UNS7. Plant UNSX was selected among the 40mers

that passed the filters mentioned above. All the UNSes used in this work are described in Table I.

**Table I.** Plant-UNSes sequences contained in Loop assembly plasmids

| UNS | Sequence                                 | Forward primer (5'→3') | Reverse primer (5'→3') |
|-----|--|------------------------|------------------------|
| 1   | CATTACTCGCATCCATTCTCAGGCTGTCTCGTCTCGTCTC | CATTACTCGCATCCATTCTC   | GAGACGAGACGAGACAGCCT   |
| 2   | GCTGGGAGTTCGTAGACGGAAACAAACGCAGAATCCAAGC | GCTGGGAGTTCGTAGACGGA   | GCTTGGATTCTGCGTTTGT    |
| 3   | GAGCCAACTCCCTTTACAACCTCACTCAAGTCCGTTAGAG | GAGCCAACTCCCTTTACAAC   | CTCTAACGGACTTGAGTGAG   |
| 4   | CTCGTTCGCTGCCACCTAAGAATACTCTACGGTCACATAC | CTCGTTCGCTGCCACCTAAG   | GTATGTGACCGTAGAGTATT   |
| 5   | CAAGACGCTGGCTCTGACATTTCCGCTACTGAACTACTCG | CAAGACGCTGGCTCTGACAT   | CGAGTAGTTCAGTAGCGGAA   |
| X   | CTACAACGCTAACTACGCTCTACACTACGATCTTCCAAG  | CTACAACGCTAACTACGCTC   | CTTGGGAAGATCGTAGTGTA   |

### Assembly of multi-TUs using Gibson Assembly.

Plasmids with multiple TUs used in protoplast transfection were constructed using Gibson Assembly. Each TU was amplified using Phusion polymerase (NEB) and primers specific for each UNSes indicated in **Table I**. Primer conditions were 60°C of annealing temperature and 35 cycles in a total volume of 50 µl at the concentrations recommended by the supplier. DNA fragments were visualized using SYBR Safe DNA Gel Stain (Thermo Fisher) in a blue LED light transilluminator (IORodeo). Purification of the PCR fragments was performed with NucleoSpin Gel and PCR Clean-up purification kit (Macherey-Nagel). About 10 to 100 ng of each DNA fragment to be assembled were mixed in a final volume of 3 µl. The volumes were added in equimolar amounts according to the size and number of fragments used in the assembly (Gibson, 2009). Subsequently, 1.5 µl of the mixture of fragments were placed in 0.2 mL tubes previously chilled on ice. Finally, 4.5 ul of a master mix were added, whose composition was; T5 exonuclease (1 U/µl, NEB), Phusion DNA polymerase (2 U/µl, Thermo Fisher), Taq DNA ligase (40 U/µl, NEB), 216.75 µl nuclease-free water (Thermo Fisher) and a 5X isothermal reaction buffer (25% PEG-8000, 500 mM Tris-HCl pH 7.5, 50 mM MgCl<sub>2</sub>, 50 mM DTT, 1 mM dATP, 1 mM dTTP, 1 mM dCTP, 1 mM dGTP and 5 mM NAD<sup>+</sup>). The ice-cold tubes were incubated immediately at 50°C for

1 h and the total volume (6 ul) was transformed into chemically competent TOP10 bacteria.

### **DNA spacers.**

The 200-bp spacers were obtained through a random sequence generator (<https://www.faculty.ucr.edu/~mmaduro/random.htm>). The 20-bp and 40-bp spacers were obtained using the same criteria for the plant UNSes design, adding the Marchantia genome to the BLAST criteria. In addition, those sequences that contained known binding sites for transcription factors described for Arabidopsis and Marchantia were eliminated. The spacers were ordered as dsDNA and ssDNA (IDT), respectively, and assembled using Gibson assembly.

### **Statistical Analysis.**

In all experiments that needed to determine significant differences between lines, data were analyzed using a two-tailed unpaired Student's t test with Welch's correction (GraphPad Prism 8).

### **Determination of area and fluorescence intensity.**

Total thallus area and fluorescence intensity were obtained from epifluorescence microscopy images (4x and 10x objective). Images were processed using a custom Python script that uses the image processing algorithm packages scikit-image (van der Walt et al., 2014) and scipy.ndimage (Virtanen et al., 2020). The codes are available at the following link <https://github.com/Arielinx/Plant-SynBio-PhD-Thesis> in the 'Image Processing' folder.

## RESULTS

### Objective 1

#### Design and use of Loop Assembly.

The construction of genetic circuits is becoming a regular procedure owing to high-efficiency DNA assembly methods, allowing complex designs and bigger scales. However, these approaches have a steep learning curve because they require customization, skills and intricate vector sets for the different assembly stages, making them highly operator-dependent. In this first objective, we develop Loop assembly, a versatile, straightforward, and efficient DNA assembly method based on a recursive approach. Loop assembly comprises two sets of plasmids that cyclically allow the incorporation of multiple genetic modules or transcriptional units (TUs) in a higher-level arrangement. The assembly of the genetic modules occurs as a result of Type IIS REs, BsaI and SapI, which are used alternately to incorporate the modules into odd or even receivers plasmids (pOdd and pEven plasmids, respectively) depending on the level required. In each assembly step, four genetic modules are combined into one receiver plasmid leading to an even level construct (L2, L4,...) if a pEven plasmid was used as receiver or an odd level construct (L1, L3,...) if a pOdd plasmid was used instead (**Figure 1a**). Additionally, pOdd and pEven plasmids carry alternating antibiotic resistant markers (kanamycin and spectinomycin, respectively) to discriminate the donor and receiver plasmid in a one-pot one-step 'Golden Gate' reaction (Engler et al., 2008). To move to the next level of assembly, four donor plasmids from the previous level are needed, except in L1 where TUs are assembled from L0 parts. Therefore, we can obtain an increment in the number of TUs described by a geometric series in which each term is given by multiplying the previous term by 4 (**Figure 1b**).

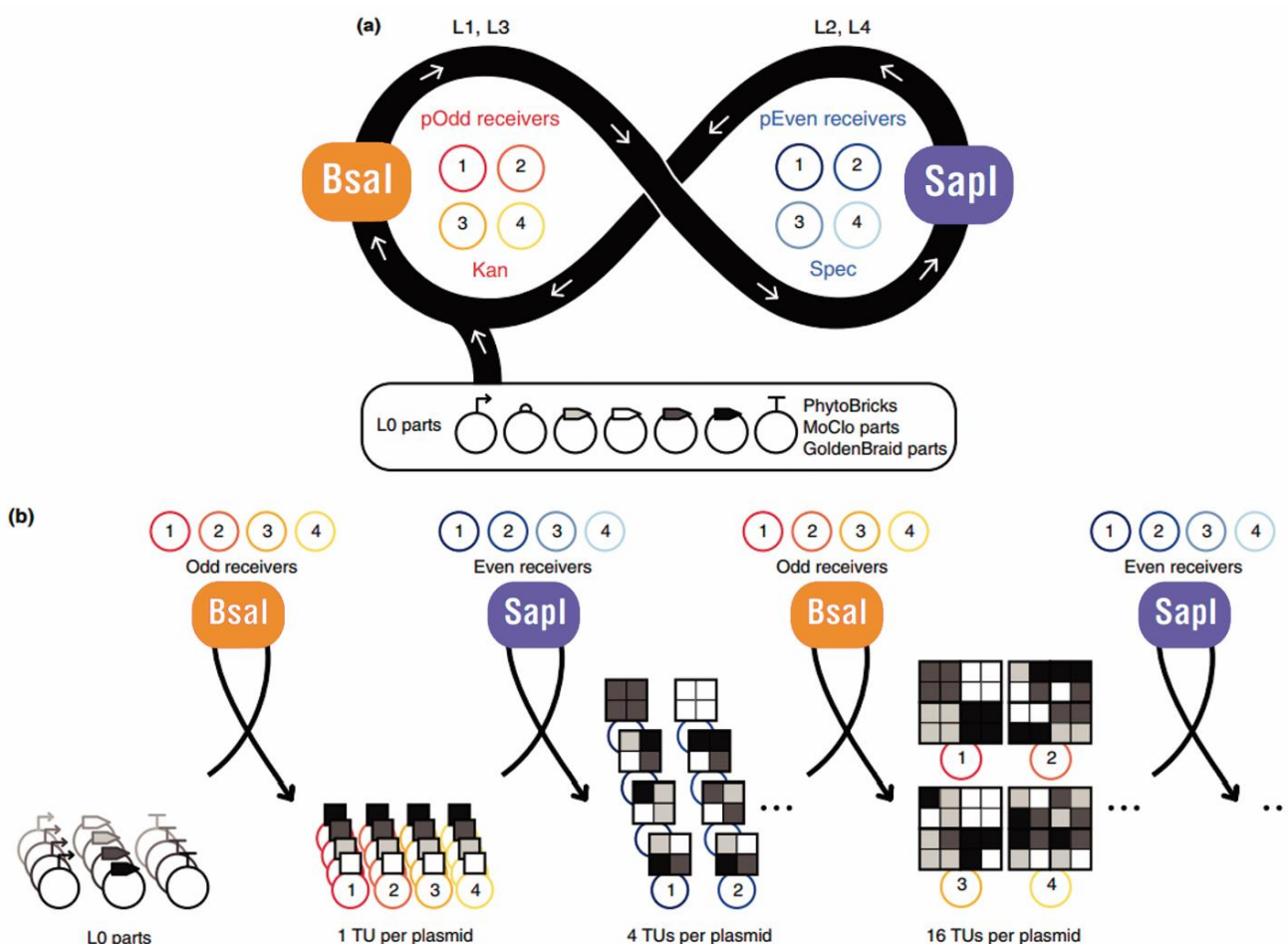


**Figure 1. Loop Assembly Overview.** (a) Recursive procedure in the assembly. Initially, elementary parts (L0 parts) can be assembled in transcriptional units (L1 TUs) into a pOdd receiver through a BsaI-mediated Golden Gate reaction. In turn, L1 TUs can be assembled in multiple transcriptional units (L2 multi-TUs) into a pEven receiver through a SapI-mediated Golden Gate reaction. Loop assembly can be repeated recursively to obtain higher-level arrangements and only requires eight receiver plasmids (four pOdd and four pEven). (b) Increase in TUs number and combinatorial assembly. L0 parts can be assembled into L1 TUs at any of the pOdd receivers. The chosen receiver plasmid will determine the position of the TUs in higher-order assemblies, so both parts and TUs can be easily rearranged into different arrangements. L1 TUs also can be assembled into L2 multi-TUs on any of the pEven plasmids allowing various combinations of the TUs. In each assembly loop, four genetic modules, either parts or TUs, are assembled into a receiver plasmid, generating an increment of TUs assembled described by a geometric series with a common ratio  $r = 4$  (i.e., 1, 4, 16, 64, ...).

Loop plasmids can act as both donors and receivers due to the arrangement of IIS Type RE recognition sites. The pOdd plasmids have a pair of divergent Bsal sites and a pair of convergent SapI sites, while pEven plasmids have these sites in opposite dispositions (**Figure 2a**). The position of the Bsal sites on the pOdd plasmids allows them to be removed during a reaction cycle. In turn, the pair of convergent SapI sites, flanking the Bsal sites, allows the pOdd plasmids to act as donors in the next assembly cycle. In a homologous way, the position of the Bsal and SapI sites in the pEven plasmids allows them to act as donors at the next level of assembly too (i.e. making the product of one assembly the substrate of the next at a higher level). Once the Golden Gate reaction begins with either of the two restriction enzymes depending on the assembly level (Bsal or SapI), the donor plasmids release the DNA fragments that lie between the convergent RE sites. The released fragments have specific overhangs that determine their position and direction in the desired construct (**Figure 2b, c**). Moreover, the receiver plasmids release a fragment with the divergent RE sites, exposing a complementary overhang to the fragments released by the donor plasmids. It is important to mention that the overhangs exposed by Bsal-mediated digestion of the pOdd receivers facilitates the design of TUs from L0 parts repositories that use the PhytoBrick standard (Patron et al., 2015), such as those derived from tools for modular assembly like MoClo (Engler et al., 2014) or GoldenBraid (Vazquez-Vilar et al., 2017). However, the parts must lack SapI and Bsal RE sites to be compatible with Loop assembly (the removal of these sites is widely known as part domestication). Regarding the overhang sequences, Bsal digestion leaves overhangs labeled as A, B, C, D and F, being A and F those that flank the fragment to be assembled in the pOdd receiver plasmids (**Figure 2b**). While SapI digestion leaves overhang sequences labeled as  $\alpha$ ,  $\beta$ ,  $\gamma$ ,  $\epsilon$  and  $\omega$ , being  $\alpha$  and  $\omega$  those that flank the fragment to be assembled in the pEven receiver plasmids (**Figure 2c**).

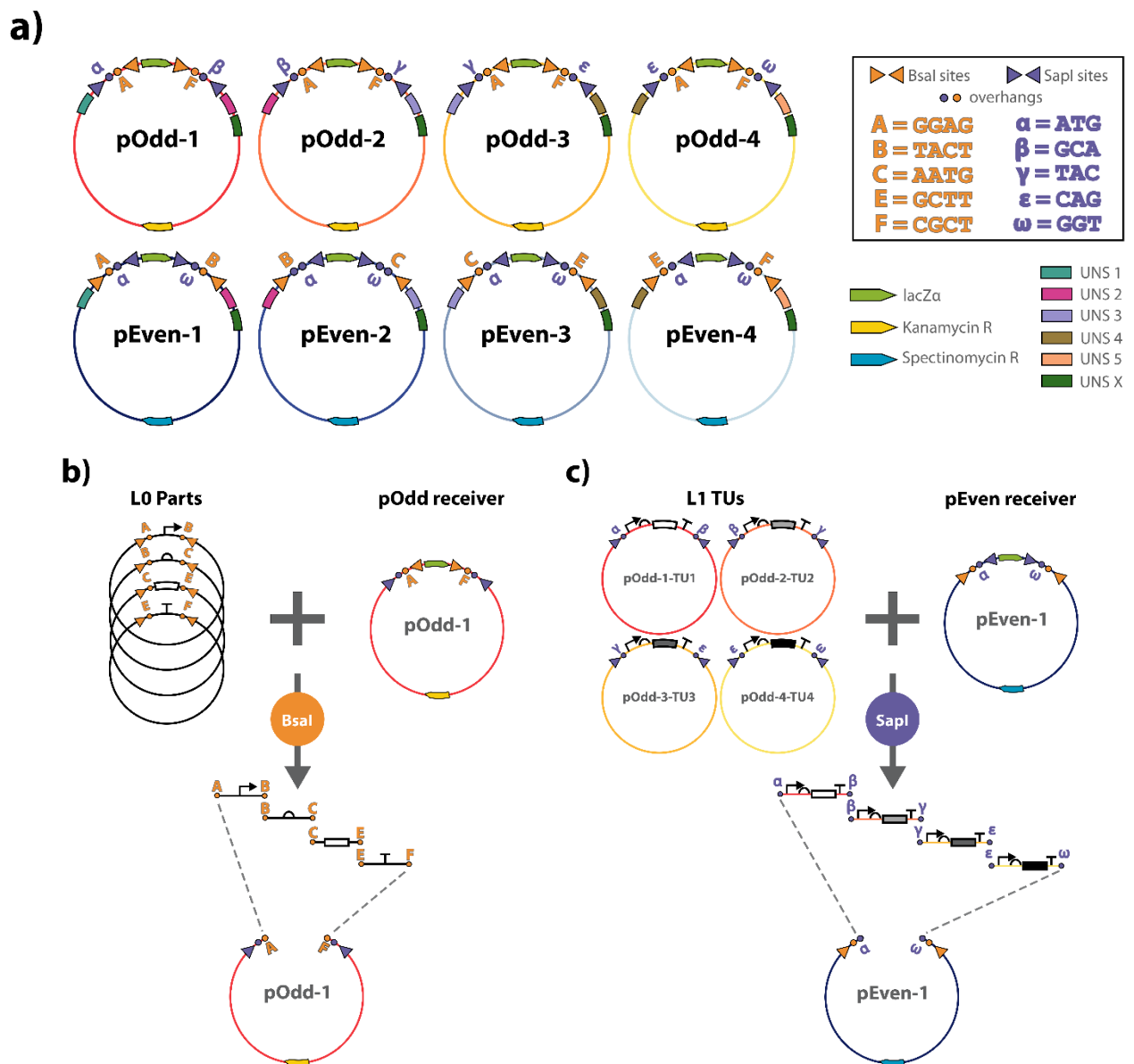


**Figure 2. Components and general procedure of Loop assembly. (a)** Structure of Loop plasmids. Each of the four pOdd and pEven receiver plasmids has SapI and Bsal-specific convergent sites that generate 3 and 4 pair base (bp) overhangs, respectively. The pOdd plasmids have divergent Bsal restriction sites and terminal overhangs that make them compatible for the assembly of L0 parts. In addition, they contain convergent SapI sites that give rise to the necessary overhangs to assemble TUs into even receivers through a Golden Gate reaction. In contrast, pEven plasmids have divergent SapI restriction sites and terminal overhangs to receive fragments derived from pOdd plasmids. For higher-level assemblies, pEven plasmids contain convergent Bsal sites that generate overhangs compatible with pOdd receivers. Additionally, the six unique sequences (UNSe) are shown, flanking restriction sites, which will facilitate precise ordered assembly in receiver plasmids via Gibson assembly. **(b)** Loop odd level assembly. Lv0 parts can be assembled into any pOdd plasmid through the common syntax of terminal overhangs. A Bsal-mediated reaction releases DNA fragments with 4-bp overhangs that are directionally assembled into pOdd plasmids. The fragment assembled from multiple parts (TU in the figure) must have A and F as terminal overhangs to assemble into pOdd receivers. Once cloned, this fragment will be flanked by convergent SapI sites that generate 3-bp overhangs for even-level assemblies. **(c)** Loop even level assembly. Four L1 TUs are assembled into a pEven plasmid, giving rise to an L2 multi-TUs. SapI-mediated digestion releases the TUs from the L1 plasmids, and these are directionally cloned into a pEven receiver by 3-bp overhangs. The fragment assembled from multiple TUs must have  $\alpha$  and  $\omega$  as terminal overhangs to be compatible with pEven receivers. Once cloned, this fragment will be flanked by convergent Bsal sites that generate 4-bp overhangs for odd-level assemblies.

As mentioned above, once an L1 TU is obtained, each Loop assembly reaction requires four donor plasmids to be assembled into a receiver plasmid at the next level. Nonetheless, if less than 4 TUs or multi-TUs arrangements are required, a 200bp universal spacer can replace any of the four modules that a Loop assembly cycle needs. The spacer was designed from random DNA sequences free of BsaI and SapI recognition sites and can be cloned into any Loop receiver vectors. At an even-assembly level, the pOdd-spacer plasmid allows assembling the spacer via the A and F terminal overhangs into a pOdd receiver (**Figure 3a**). Conversely, in an odd-level assembly, the plasmid pEven-spacer allows cloning the spacer into a pOdd plasmid by  $\alpha$  and  $\omega$  terminal overhangs (**Figure 3b**). To illustrate the use of pOdd and pEven plasmids, assemblies involving plasmids L1- and L2-spacer are shown (**Figure 3c and d, respectively**).

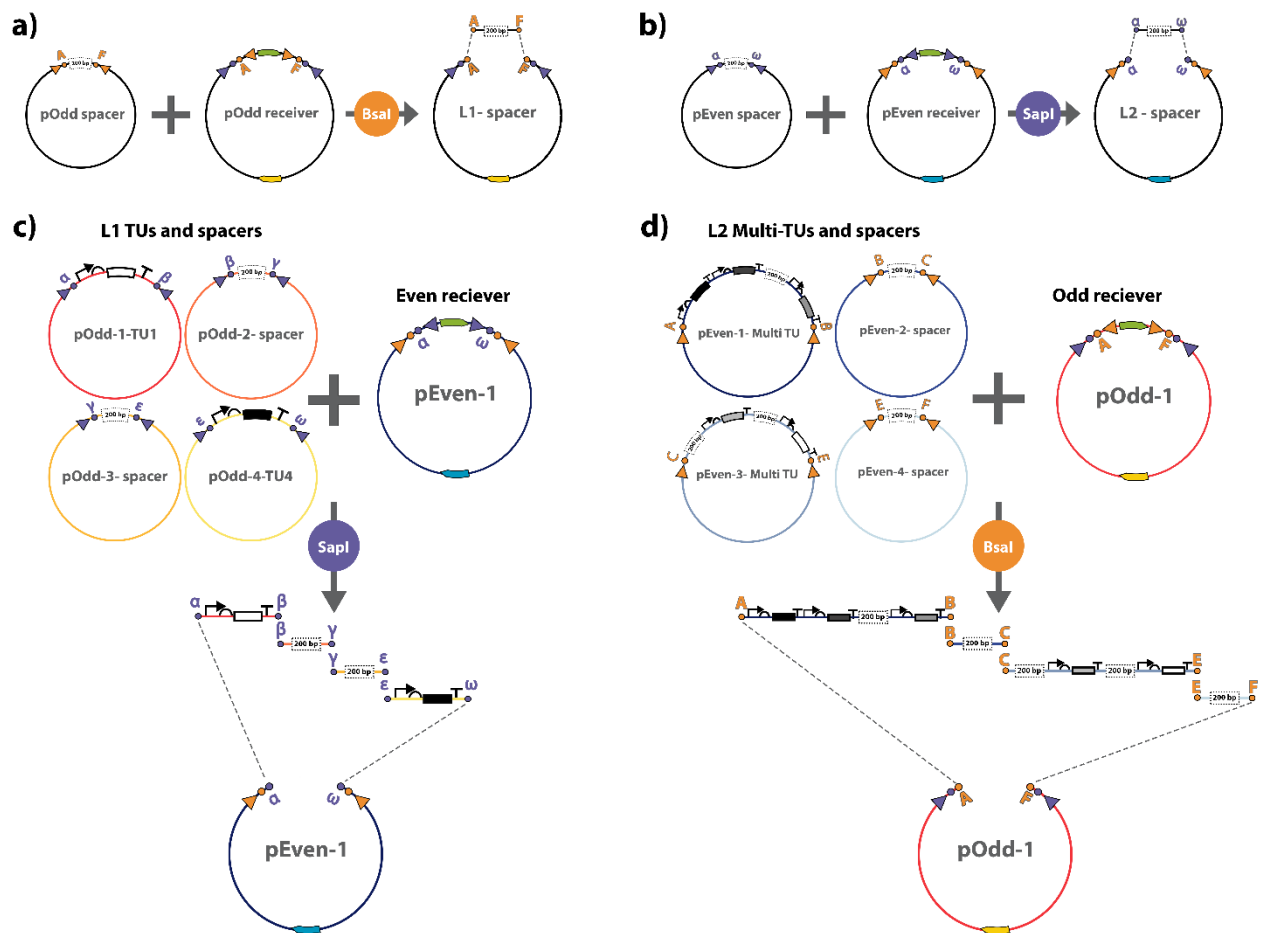


**Figure 3. Use of spacers in Loop assembly.** (a) Assembly of the pOdd-spacer plasmid. Plasmid pOdd-spacer digested with Bsal exposes terminal overhangs A and F compatible with any of the pOdd receivers. (b) Assembly of the pEven-spacer plasmid. Plasmid pEven-spacer SapI-digested leaves terminal overhangs α and ω compatible with the pEven receivers. (c) L2 assembly example using L1 spacers. TUs can be used with L1 spacers to assemble them on pEven receivers. (d) L3 assembly example using L1 and L2 spacers. L2 plasmids with any arrangement of TUs and spacers (derived from the pOdd-spacer plasmid) combined with L2 spacers (derived from the pEven-spacer plasmid) can be assembled into pOdd receivers.

## Construction of synthetic promoters via Loop Assembly

Direct control over gene expression is necessary for synthetic circuits to function as expected. Spatiotemporal regulation of gene expression is highly-regulated through mechanisms such as transcriptional elongation, antisense transcription, and post-transcriptional and translational processes (Cai et al., 2020). Despite this, the simplest way to control and balance the expression of genes in genetic circuits is through transcription since information flow begins with it. (Engstrom and Pflieger, 2017). To achieve this, synthetic promoters that regulate transcription through standardized and characterized regulatory elements are needed. Noteworthy, the recursive nature of Loop assembly also allows the assembly of L0 parts in addition to genetic modules of higher levels. This property permits to design and build, among other things, synthetic promoters with multiple regulatory elements in a predefined order, which is of particular interest for my thesis. **Figure 4** shows the creation of synthetic promoters through recursive assembly. Instead of using traditional L0 parts such as promoters, CDS, or terminators, functional domains comprising transcription factor (TF) recognition sites or minimal promoters are used. L0 functional domains with terminal overhangs A and F (syntax generally reserved for a full TU) can be cloned into pOdd receiver plasmids, and the chosen plasmid will determine which of the four available positions it will occupy in an L2 assembly. As the example shows, up to 7 TF recognition sites are used to assemble a synthetic promoter by cloning the recognition sites in all pOdd receivers and a minimal promoter in pOdd-4 (**Figure 4a**). L1 assembled plasmids can be placed into pEven1 and pEven2, using the last position of L2 assembly ( $\epsilon$  and  $\omega$  terminal overhangs) to clone L1-minimal promoter plasmid into pEven2 plasmid. In this way the seven boxes of regulatory elements can be placed in any order upstream of the minimal promoter, giving rise to many combinatorial

possibilities that would be practically unattainable by other means (e.g., repeats are problematic for DNA synthesis or Gibson-based approaches). Finally, L2 even plasmids with TF binding boxes and the minimal promoter are used together with standardized L0 parts to hybrid assemble into an odd receiver plasmid and create a TU with a customized synthetic promoter (**Figure 4b**). Hybrid assemblies of plasmids of different levels with multiple TUs can be made using the same assembly logic. The only requirement is that they share parity (e.g., L1 and L3 or L2 and L4) and that overhangs are compatible, which allows obtaining different TU numbers in the assemblies than those provided by the geometric progression of each Loop cycle.

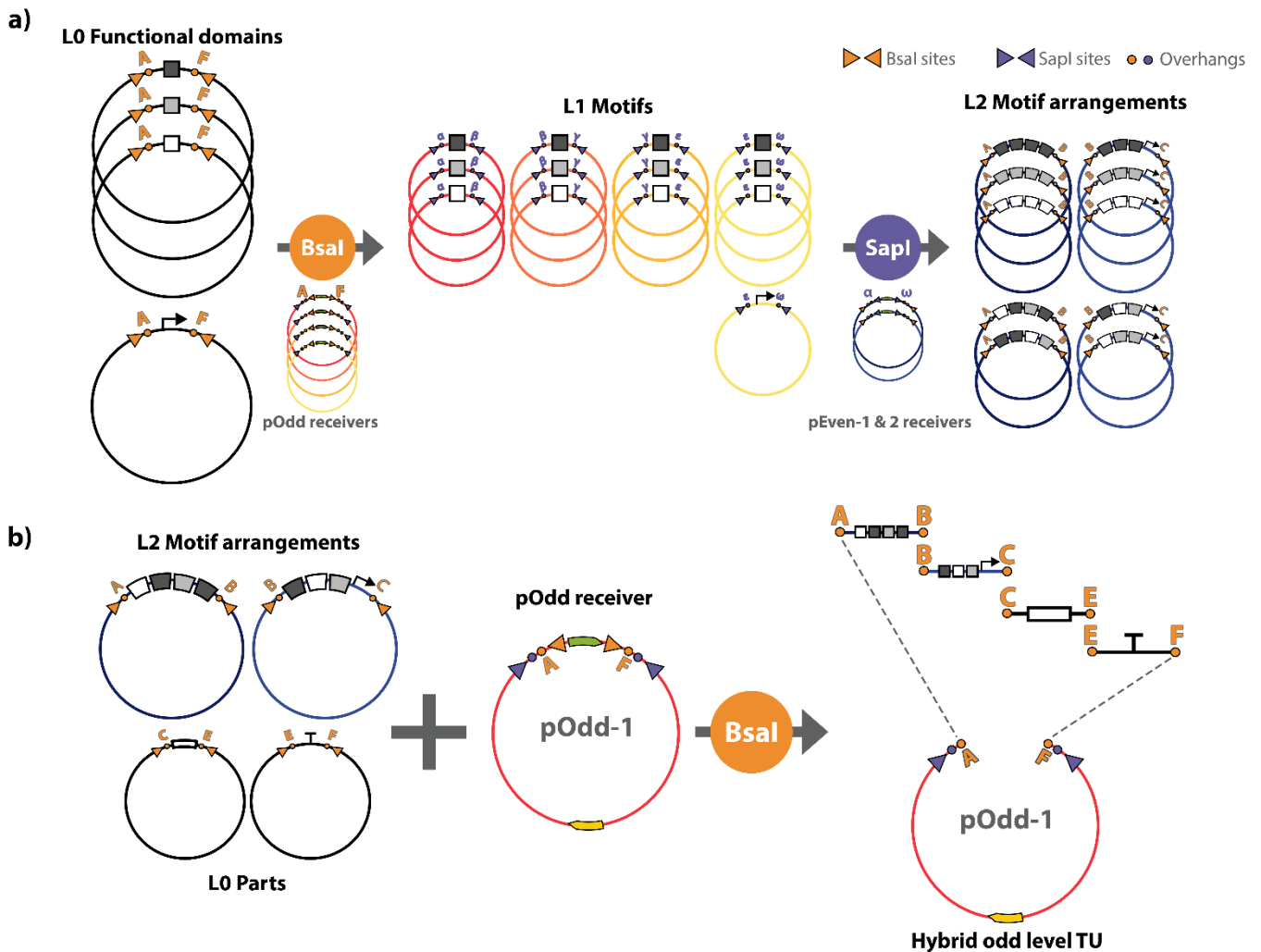


**Figure 4. Design of synthetic promoters through hybrid assembly. (a)** Functional element distribution in pEven receivers. L0 functional domains are assembled directly on pOdd receptors through terminal overhangs A and F. Subsequently, the regulatory elements (L1 motifs) are placed into four-element arrays (L2 motif arrangements) using pEven-1 and pEven-2 receivers, the position of the motifs will be according to the previously chosen pOdd plasmid. Up to 8 boxes of regulatory elements can be mixed, reserving the last position (fourth position of the L2 assembly in pEven-2) for a minimal promoter to provide functionality. **(b)** Hybrid assembly between L2 motif arrangements and L0 parts. L2 motif arrangement, assembled into pEven1 and pEven2 plasmids, can be used in hybrid assemblies with L0 parts to give rise to TUs whose transcription is controlled by regulatory elements (TF binding boxes and minimal promoter) of the synthetic promoter.

## **UNSEs for ordered overlap assembly.**

Loop plasmids are not only able to perform type IIS assembly but were also designed for overlap-based techniques. Loop receivers plasmids contain unique nucleotide sequences (UNSEs) that allow the use of standardized primers to amplify TUs derived from type IIS part repositories (e.g., PhytoBricks, MoClo, and GoldenBraid). This is possible since when the L0 parts are assembled by Bsal-mediated golden gate based on Bsal, the resulting TU is flanked by the UNSEs. Alternatively, TUs can also be assembled into Loop plasmids from DNA synthesis or PCR fragments by overlapping methods, such as Gibson assembly. All Loop plasmids have three UNSEs; two flanking (an adjoining pair numbered between 1 and 5) and a terminal (UNS X). In this way, TUs can be assembled into a destination plasmid containing the terminal UNSEs of the amplified fragments, as shown in the example in **Figure 5**. The figure shows the overlap assembly of four TUs using UNS1 and UNSX as terminal UNSEs at the ends of the amplified fragment of plasmid pEven1. However, fewer TUs can also be assembled by using different pOdd to clone the TUs, and PCR-amplified UNS-compatible fragments of pEven plasmids to receive them by Gibson assembly. UNSEs have been designed to optimize PCR amplification and overlap-mediated assembly, and all considerations regarding their design are mentioned in the Materials and Methods section. UNSEs sequences and the standardized forward and reverse primers for each UNS (first 20 bp in forward and reverse complementary form) are listed in **Table I**, respectively. UNS-flanked TUs can be efficiently isolated by PCR under predefined standard conditions (60 °C and 35 thermal cycles), eliminating the need for gel purification for subsequent assembly, if appropriate on-column purification is performed.

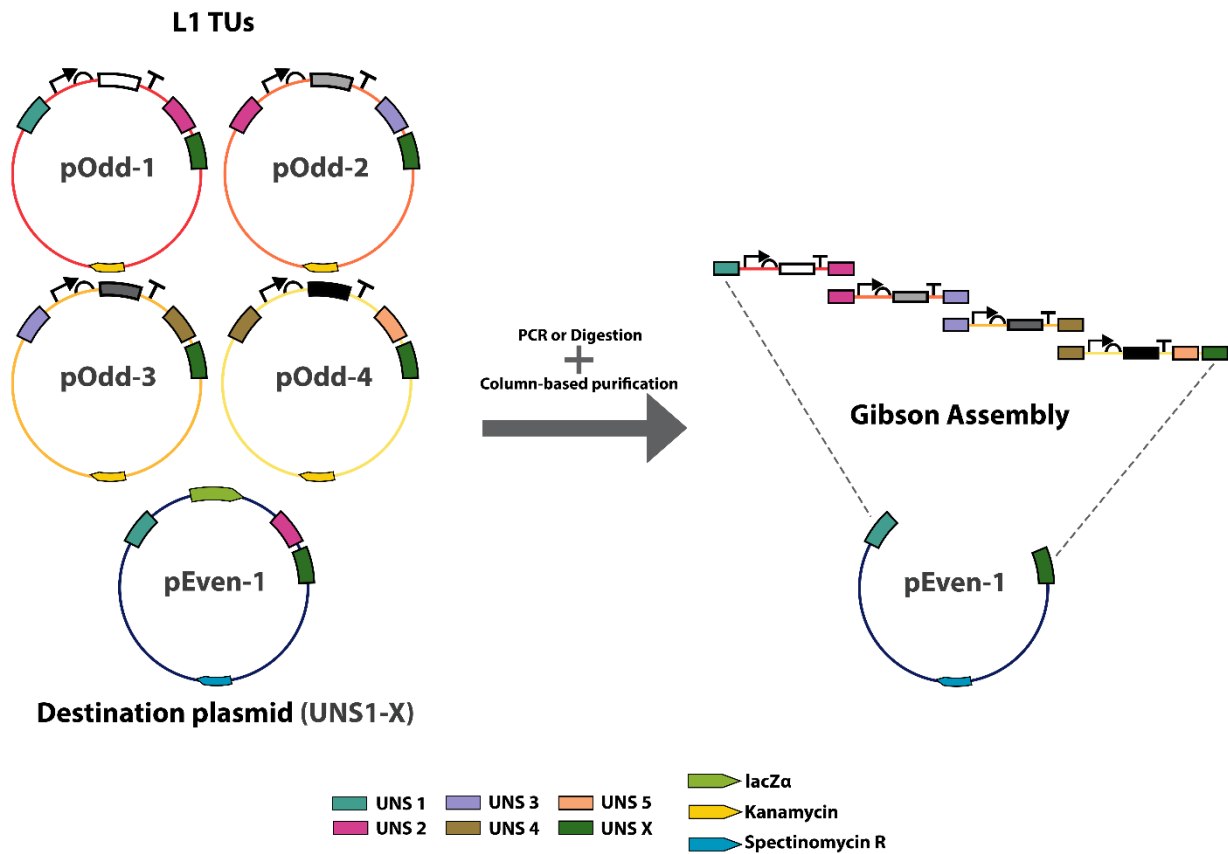


**Figure 5. UNSes-mediated overlapping assembly.** Four previously Golden Gate- or Gibson-assembled TUs are flanked by pairs of contiguous numbered UNSes. PCR of UNS-flanked is performed, including a receiver plasmid fragment compatible with the ends of the amplified TUs (UNS1 and UNS X of pEven-1). TUs can also be obtained from L1 plasmids through digestion by uncommon restriction enzymes. After being purified, the linear UNS-flanked TUs can be assembled into the destination plasmid using overlapping methods such as Gibson assembly.

## Accuracy and *in planta* evaluation of Loop Assembly.

To assess the accuracy of the constructs assembled by Loop assembly, we evaluated plasmids of different complexity generated in two different laboratories (Table II).

**Table II. Loop efficiency in different types of assemblies**

| Level        | Assembled plasmids | Average length (bp) | Overall efficiency* (%) | Average efficiency** (%) |
|--------------|--------------------|---------------------|-------------------------|--------------------------|
| <b>Lab 1</b> |                    |                     |                         |                          |
| L1           | 104                | 6243                | 96                      | 97                       |
| L2           | 79                 | 13519               | 82                      | 88                       |
| L3           | 23                 | 26731               | 81                      | 83                       |
| Hybrid       | 3                  | 5473                | 100                     | 100                      |
| <b>Lab 2</b> |                    |                     |                         |                          |
| L1           | 249                | 5895                | 91                      | 92                       |
| L1***        | 187                | 5610                | 97                      | 99                       |
| L2           | 116                | 10998               | 80                      | 83                       |
| L3           | 17                 | 30588               | 81                      | 85                       |
| Hybrid       | 37                 | 4229                | 91                      | 93                       |
| UNSES        | 14                 | 15456               | 74                      | 76                       |

\* Percentage of samples with the expected digestion pattern among all the samples evaluated.

\*\*Average percentage of samples with the expected digestion pattern among the number of samples analyzed per construct.

\*\*\*Plasmids assembled using Bsal-HFv2 as Type IIS restriction enzyme (optimized for Golden Gate Assembly)

More than 800 plasmids were assembled using Type IIS Loop Assembly for L1, L2, and L3 constructs, obtaining consistent results with an efficiency between 83 and 99%, depending on the construct complexity. In parallel, 40 synthetic promoters were built through hybrid assemblies, obtaining an efficiency between 93 and 100%. On the other hand, 14 plasmids constructed by UNSES-mediated Gibson assembly had an average efficiency of 76%. All constructs underwent restriction endonuclease digestion and were compared with the expected digestion pattern. To corroborate the results obtained with the digestions, we performed Illumina sequencing of 92 assembled constructs (L2 and L3 plasmids), allowing us to observe whether misassembly occurred or mutations were acquired. We found that 95.4% of the constructs were correctly assembled, of which 98.8% had the overhang scars in the

expected positions. Among all the evaluated constructs, 99.8% of the nucleotides were in the assigned positions, and the few inaccurate constructs had some missing regions as a result of misassembly.

Both pOdd and pEven plasmids are derived from the pGreenII binary Ti vector for *Agrobacterium*-mediated plant transformation (Hellens et al., 2000). However, during the adaptation of pGreenII as a backbone for Loop plasmids, the plant selection markers were removed to make them a customizable module during assembly (details in Materials and Methods). Loop plasmids retain all of the elements of pGreenII necessary to promote their propagation in *Agrobacterium tumefaciens* and allow a wide range of transformation procedures for many plant species. To test the transformation of these vectors in plants, we designed L2 constructs composed of TUs with different fluorescent proteins fused to localization tags, whose expression was driven by endogenous promoters allowing us to highlight cellular features and track patterns of gene expression *in planta*. From L0 parts (**Appendix I**), an L2 construct was assembled by Loop Assembly containing 4 TUs composed of; a hygromycin resistance gene cassette, a mTurquoise2-N7 nuclear-localized reporter driven by MpEF1 $\alpha$  (Nagaya et al., 2011; Althoff et al., 2014), a Venus-N7 nuclear-localized reporter driven by an MpTPL tissue-specific promoter (Flores-Sandoval et al., 2015) and an eGFP-Lti6b membrane-localized marker driven by MpEF1 $\alpha$  promoter (**Figure 6a**). The L2 construct was transformed into *Marchantia polymorpha* and regenerated transformants were obtained. Gemmae were collected and examined using confocal microscopy, observing that the three fluorescent proteins were expressed and presented the expected subcellular localizations (**Figure 6b**). In parallel, four L1 TUs constructed by Type IIS Loop assembly were assembled into a pEven-1 destination plasmid using Gibson assembly. This multi-TU plasmid allows us to co-express

transiently a mTagBFP2–Lti6b membrane marker (Subach et al., 2011), mTurquoise2-N7 nuclear reporter, a YPet-Hemme chloroplast reporter (Nguyen and Daugherty, 2005), and untagged mRuby3 marker in *Arabidopsis* mesophyll protoplast (**Figure 6c**). Transfected protoplasts showed the expression of the engineered fluorescent reporters in their expected localizations (**Figure 6d**), providing a fast and efficient system to evaluate the functionality of Loop constructs.

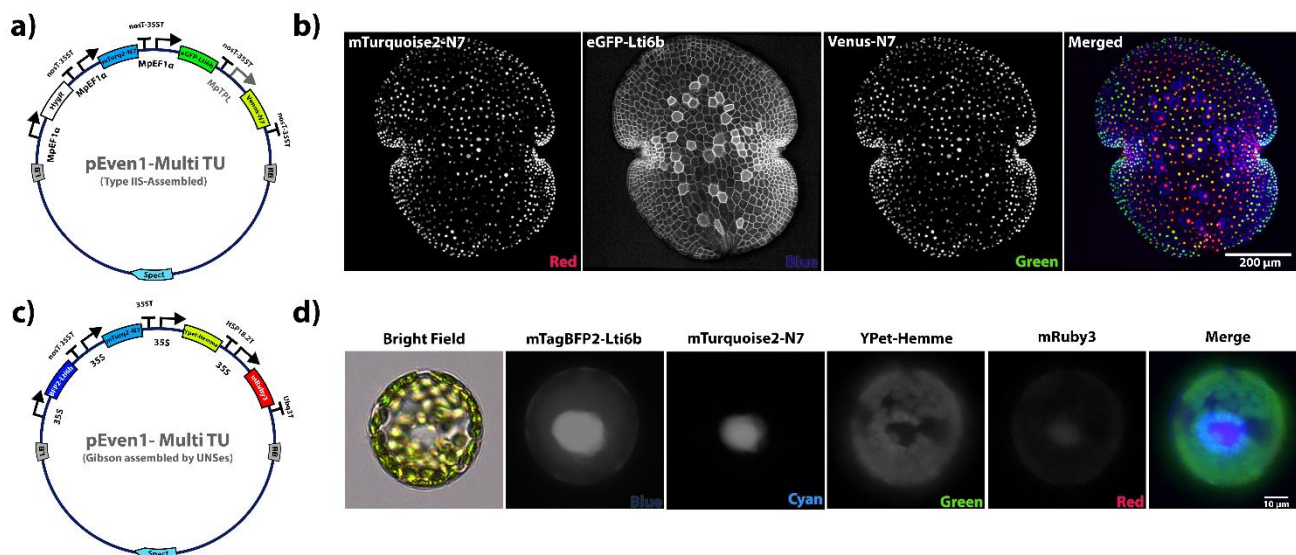


**Figure 6. *In planta* evaluation of Loop-assembled plasmids. (a)** L2 construct constructed using Loop assembly mediated by SapI. This plasmid was obtained from 4 previously assembled TUs: a hygromycin resistance cassette (selection of transformed plants) and three fluorescent reporters with different localization tags (mTurquoise2-N7, Venus-N7, and eGFP-Lti6b). In addition, the left and right borders are shown (LB and RB, respectively). **(b)** Marchantia gemmae transformed with the type-IIS assembled L2 construct. Images were obtained by a Leica SP8 laser scanning confocal microscope. Fluorescent reporters were excited with the appropriate wavelengths, and the fluorescence was obtained in their respective emission range in sequential scanning mode. Images shown are Z-stack maximum intensity projections. Transformation and microscopy images of the construct used in Marchantia were obtained by Bernardo Pollak (University of Cambridge, UK) **(c)** L2 construct assembled using UNSes-guided Gibson assembly. This plasmid was obtained from 4 previously assembled fluorescent reporters with different localization tags (mTagBFP2-Lti6b, mTurquoise2-N7, YPet-Hemme, and mRuby3). **(d)** Transient expression of a multi-TUs L2 construct in Arabidopsis mesophyll protoplasts. Fluorescent protein expression was evaluated through epifluorescence microscopy using a Nikon Ni microscope. The colors used in the merged images are shown at the bottom right border of each image.

## Objective 2

### **Design of the L0 parts for the construction of synthetic circuits in *Marchantia polymorpha*.**

After developing an assembly method suitable for evaluating regulatory functions in plants, we proceeded to design standardized components for the construction of TUs in plants. Independent of the genetic circuit to be built, we decided to create different regulatory functions that would allow us to explore a broad spectrum of design possibilities. In this objective, multiple standardized components were developed for its use in plants, mainly *Arabidopsis thaliana* and *Marchantia polymorpha* (Marchantia). However, after focusing this project mainly on Marchantia, most of the L0 parts have a design approach that favors their functionality in Marchantia (e.g., codon optimization considering codon usage of Marchantia). The parts were designed considering the standard Type IIS syntax for plants described by Patron et al. (2015), which contains 12 Loop-compatible syntax sites to implement the facile assembly of plant TUs and provide functionality. To facilitate its use in Marchantia and easily discriminate the different parts and their location within a TU, we decided to use numbers to describe each of the positions of this plant syntax (**Figure 7**). The TUs in Loop are flanked by A and F terminal overhangs, syntaxes equivalent to the numbers 1 and 11, respectively. As seen in the figure, the TUs were divided into three large modules; promoter (1-6), coding region (6-9), and terminator (9-11). However, if required the coding region (CDS) could be divided into sub-modules to satisfy other design possibilities. For example, instead of using a single CDS (6-9), it could be divided into a DNA-binding domain (6-7B), an activation or repression domain (7B-8), and an induction domain (8-9). On the other hand, CDS can also be fused to C- and N-terminal tags. The C-terminal fusion tags (8-9) require

the use of a CDS without a stop codon (6-8), while the N-terminal fusion tags require a promoter with a different syntax (1-5). The syntaxes that give identity to the DNA parts were added through high-fidelity PCR using primers that add the flanking syntaxes or directly synthesized including those regions (**Figure 7b and c**). In addition to the syntaxes, specific regions were added to allow the assembly of the DNA part at an L0 backbone. Most of the L0 parts were assembled via Gibson assembly, so regions homologous to the L0 backbone (pUPD2) were added to promote the reaction (**Figure 7b**). In case that Gibson assembly did not work, *SapI*-mediated Golden Gate was used alternatively, adding the necessary restriction sites to promote the assembly of the DNA part in the entry vector pLOR-lacZ (**Figure 7c**). As mentioned above, the DNA part sequences must not contain the sites for the enzymes used in the type IIS assembly system to be compatible with it, i.e., *BsaI* and *SapI* sites in Loop Assembly. If the DNA part had these sites, they were removed through site-directed mutagenesis by Gibson assembly or directly synthesizing the part without those sites. For the construction of TUs shown in this work, more than 80 level 0 parts were designed (**Table SI**). The current part repository includes, among others, promoters, reporter genes, terminators, localization peptides, TF binding domains, and activation or repression domains.

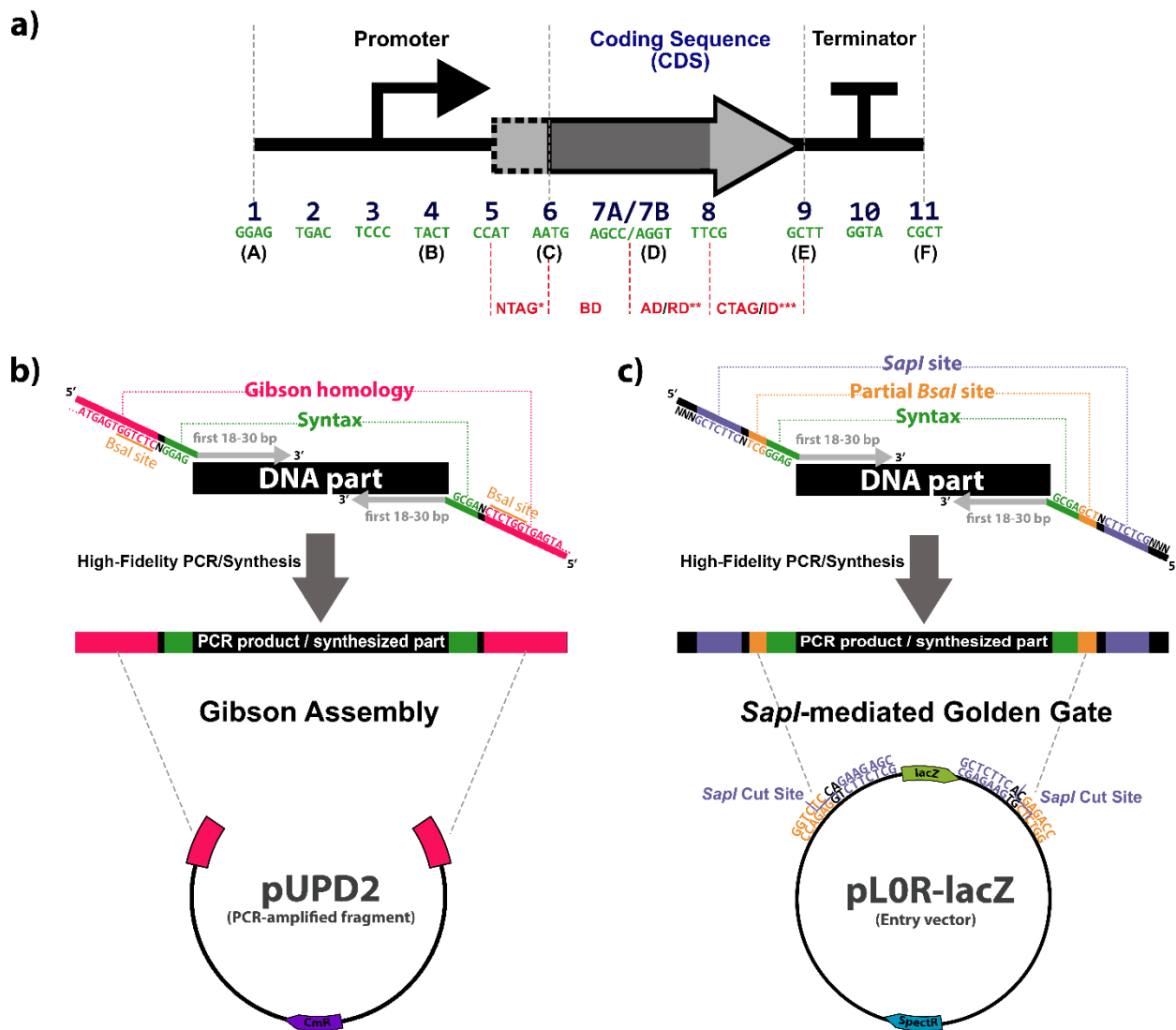


**Figure 7. Design and construction of L0 parts. (a)** Plant common syntax used in L0 DNA parts. The standard used here (Patron et al., 2015) comprises 12 standard fusion sites for Type IIS restriction endonuclease-mediated assembly (4-bp in green). Each site has been renamed with a number to account for the position of the DNA part within a TU (blue numbers). TUs have been divided (gray dashed lines) into three regions: promoter (1-6), coding sequence (6-9) and terminator (9-11). The coding region has been subdivided (red dashed lines) into a DNA binding domain (6-7B), an activation or repression domain (7B-8) and an induction domain (8-9). The CDS can also be fused to C- and T-terminal tags (5-6 and 8-9, respectively). The terminal overhangs used in Loop assembly and their equivalence with the numbered syntax are shown in parentheses. \*If an N-terminal tag is used, a promoter with syntax 1-5 will also be required. \*\*If a C-terminal tag or induction domain is not required, the activation or repression domains can be cloned with syntax 6-9. \*\*\*If a C-terminal tag is used, the CDS must be cloned without a stop codon (6-8). **(b)** Construction of an L0 part using Gibson assembly. The DNA parts need to be flanked by the specific syntax (green) and sequences homologous to the pUPD2 vector (magenta). **(c)** Construction of an L0 part using SapI-mediated Golden Gate. The DNA parts need to be flanked by the specific syntax (green), a partial Bsal site (orange) and a SapI site (purple). Independent of whether **(b)** or **(c)** is used for the L0 assembly, DNA parts can be obtained through synthesis or be amplified by high-fidelity PCR with primers that add the necessary regions for assembly.

## Evaluation of reporter transcriptional units in *Marchantia polymorpha*.

Once the different L0 parts were designed and built, TUs were assembled to be evaluated by stable transformation in *Marchantia polymorpha*. The first TUs to be characterized corresponded to constitutively expressed fluorescent reporters, mainly because versatility for all types of investigations in live-cell imaging studies. Fluorescent proteins not only allow us to visualize whole-plant cellular responses, but also provide us with an easy and non-invasive way to distinguish those plants that have been successfully transformed. Additionally, we decided to determine the success of the transformation in *Marchantia* gemmae, given that their small, flat, quasi-two-dimensional structure is well suited for quantitative imaging techniques. Besides, gemma surface cells allow accessible measurement of growth, gene expression and division of individual cells in the entire plant body (Boehm et al., 2017).

To evaluate reporters in *Marchantia* gemmae, L2 plasmids consisting of a resistance gene cassette and a constitutively expressed fluorescent reporter were constructed (**Figure 8a**). As a constitutive promoter, the endogenous elongation factor 1 $\alpha$  (MpEF1 $\alpha$ ) was chosen since compared to the classic viral 35S cauliflower mosaic virus (CaMV35) presents a more ubiquitous and strong expression in the *Marchantia* thallus and gemmae. Hygromycin phosphotransferase resistance gene was chosen as the selection marker, due to its widely reported use in *Agrobacterium*-mediated transformation methods for *Marchantia* (Ishizaki et al., 2015). Different transformation methods were evaluated using an improved version of the YFP fluorescent reporter called 'Venus' (Nagai et al., 2002), driven by the MpEF1 $\alpha$  promoter and a nosT-35ST double terminator (Pollak et al., 2019). Regardless of whether sporelings (Ishizaki et al., 2008) or regenerating thallus (Kubota et al., 2013) were used, both methods allowed obtaining hygromycin-resistant plants that showed expression of the

fluorescent protein Venus (**Figure 8b**). Although the sporelings transformation has the disadvantage that spore preparation is tedious (induction of reproductive organs, spore maturation, sporangia collection and appropriate dehydration), we decided to use this protocol because in our hands we obtained a higher number of transformed plants. Moreover, most of these plants showed fluorescence evaluated by epifluorescence microscopy and fluorescent plants tested were positive for the presence of the gene encoding for Venus (**Figure 8b, bottom panel**). We also tested the same construct mentioned above but using different terminators instead of nosT-35ST, obtaining similar results in qualitative terms (**Figure 8c**).

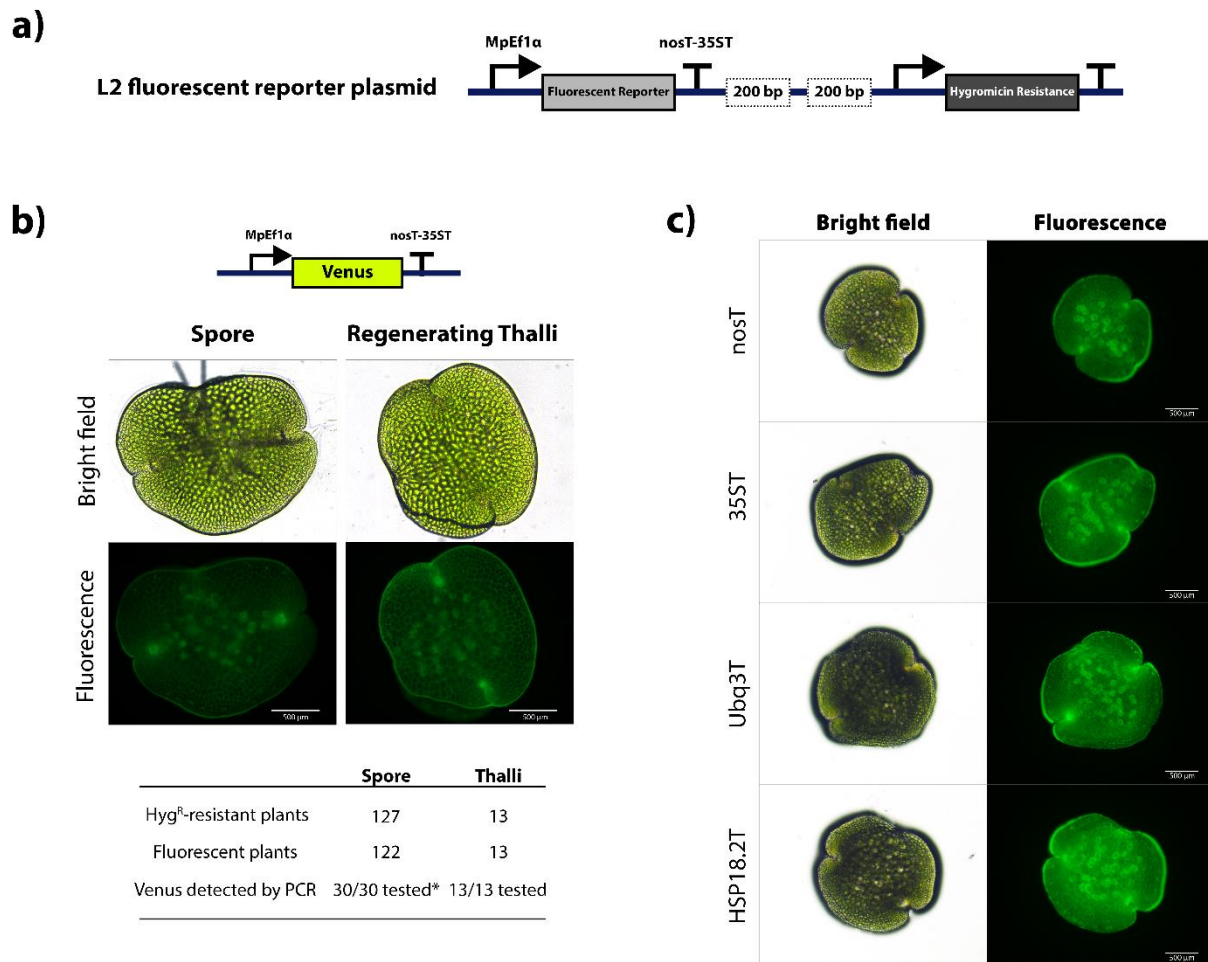


**Figure 8. Transformation of *Marchantia polymorpha* using a fluorescent L2 plasmid. (a)** General scheme of the L2 plasmid used to characterize fluorescent reporters. The construct has a fluorescent reporter driven by a constitutive MpEF1 $\alpha$  promoter and a nosT-35ST double terminator. In addition, a hygromycin resistance cassette is observed at the last position, separated from the reporter by two 200-bp universal spacers. **(b)** Evaluation of different methods of transformation of *Marchantia*. *Marchantia* sporelings and thalli were transformed with a constitutively expressed Venus fluorescent protein. The table below shows the individuals hygromycin-resistant obtained with each method. The numbers of fluorescent plants and PCR-positive transgenic plants are also shown. \*Only plants showing fluorescence were evaluated. **(c)** Representative two-day old gemmae transformed with Venus constitutively expressed but with different terminators. *Marchantia* gemmae transformed with an L2 construct containing the constitutively expressed Venus fluorescent reporter and different terminators. The expression of the fluorescent protein encoded in the construct was assessed in *Marchantia* gemmae by epifluorescence microscopy using a Nikon Ni microscope. Scale bar = 500  $\mu$ m.

Having defined the routine transformation method, we evaluated distinct fluorescent reporters using the same structure depicted in **Figure 8a**. With the aim of finding good reporters for whole plant imaging, these reporters were fused to different localization tags, such as Lti6b (membrane), N7 (nucleus), and Hemme (chloroplast). Fluorescent reporters and localization tags used are described in the L0 parts table (**Table S1**). Sixteen L2 constructs were stably transformed into *Marchantia*, and gemmae of these transgenic lines were observed by epifluorescent microscopy (**Figure 9**). All the transformed lines analyzed showed fluorescence in the center and edges of the gemma, concentrating preferentially in the meristems, coinciding with the MpEF1 $\alpha$  promoter description given by Althoff et al. (2014). Furthermore, all the proteins fused to a localization tag exhibited the expected subcellular localizations (Cutler et al., 2000), being the easiest to identify the nuclear localization since its dotted pattern allowed us to distinguish the nuclei of individual cells (Venus::N7, Citrine::N7, mTagBFP2::N7 and mTurquoise::N7, **Figure 9**). However, the cytosol (fluorescent reporter without localization tag) and membrane localization were difficult to distinguish by epifluorescent microscopy. Mainly because plant cells are highly vacuolated and displace almost all the fluorescent signals to a thin layer at the edges of the cell, making both location tags look similar. It is also relevant to mention that imaging mTagBFP2 ( $\lambda$  ex =399 and  $\lambda$  em = 454 nm) and mTurquoise2 ( $\lambda$  ex =434 and  $\lambda$  em = 474 nm) resulted on high levels of autofluorescence (mTagBFP2::Lti6b, mTagBFP::N7, mTurquoise2, mTurquoise2::Lti6b and mTurquoise2::N7, **Figure 9**) due to the culture medium used to grow *Marchantia* (solid half-strength Gamborg's B5 medium). For this reason, we decided to discard its use since it is essential in live-cell fluorescence imaging to visualize fluorescent signals over the background without negatively impacting fluorophore signal-to-noise (S:N) ratios.

To dispel doubts about subcellular locations of reporters, spectral confocal microscopy was used. **Figure 10a** shows that the localization tags used directed the fusion protein to the corresponding subcellular compartments. It also allows us to determine that Venus::Lti6b and Venus (No tagged) in effect have different locations, being membrane and cytosol, respectively. In addition to that, we wanted to observe the behavior of the absorbing and emitting reporters in the red spectral region (~600 - 700 nm) to determine if we could distinguish them from chlorophylls in the tissue. When evaluating the mRuby3 localization (No tagged,  $\lambda_{ex} = 558$  and  $\lambda_{em} = 592$  nm), it turned out to be cytosolic and different from the chloroplastic localization of the chlorophylls as seen in the upper panel of **Figure 10b**. Finally, we scanned the emission spectrum from 577 to 732 nm, observing that mRuby3 and chlorophylls spectra (Chl-a $\lambda_{em} = 650$  nm and Chl-b $\lambda_{em} = 670$  nm ) are separated and therefore differentiated by confocal microscopy (bottom panel, Figure 10b).

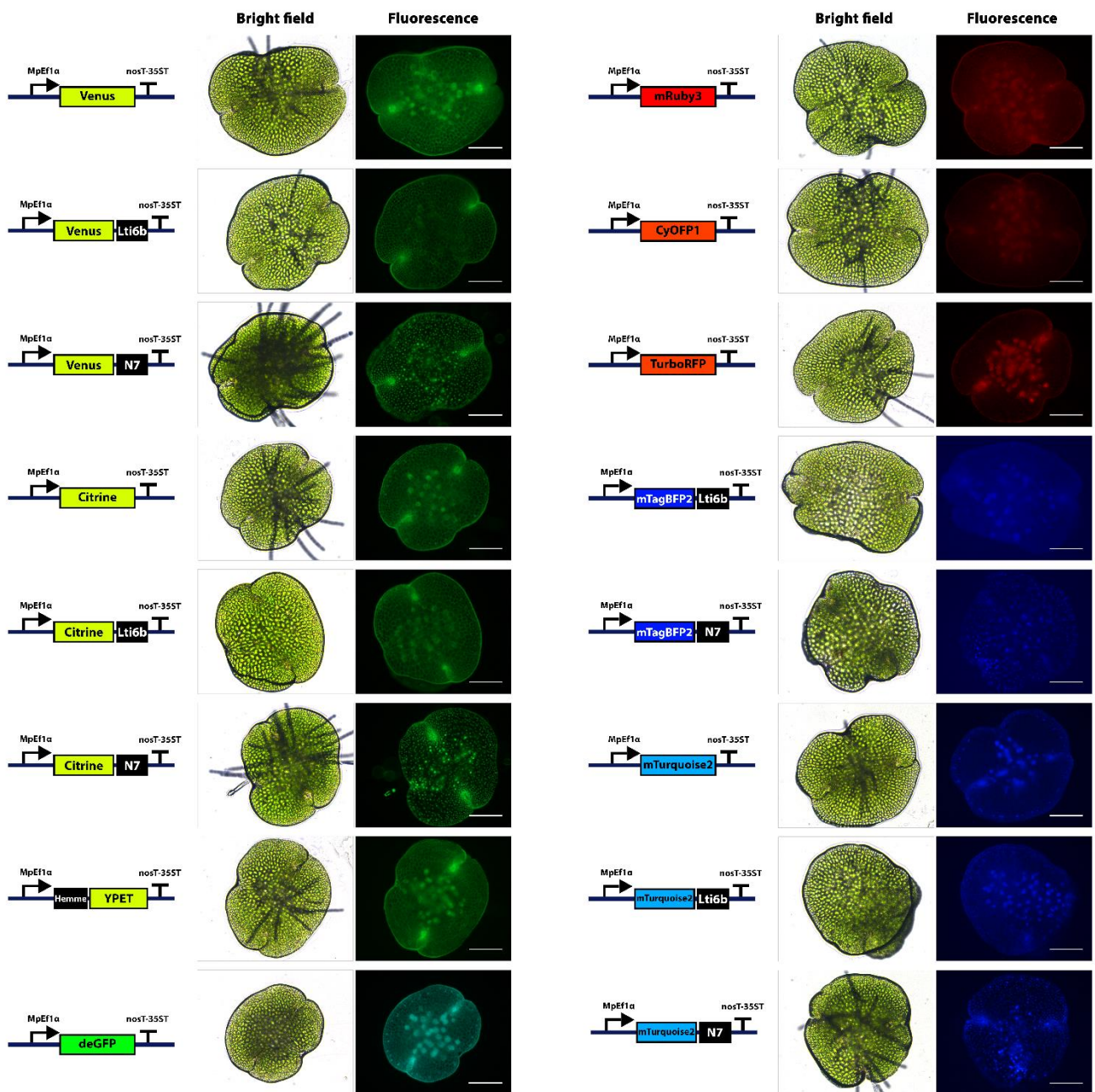


**Figure 9. *Marchantia* gemmae transformed with different reporter TU constructs.** Representative gemmae of lines stably transformed with a fluorescent reporter driven by the constitutive MpEF1 $\alpha$  promoter and nosT-35ST double terminator. It is also indicated if the reporter is fused to any of the location tags (black rectangle); either Lti6b (membrane), N7 (nucleus) or hemme (chloroplast). Images were obtained by epifluorescence microscopy using a Nikon Ni microscope. Scale bar = 500  $\mu$ m.

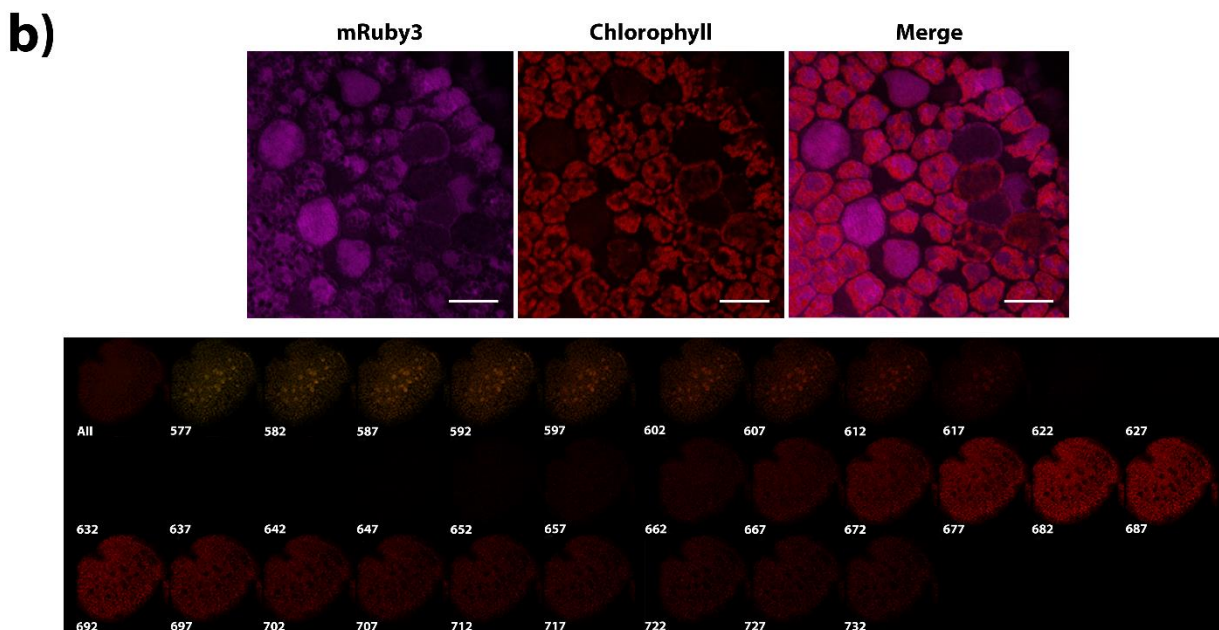
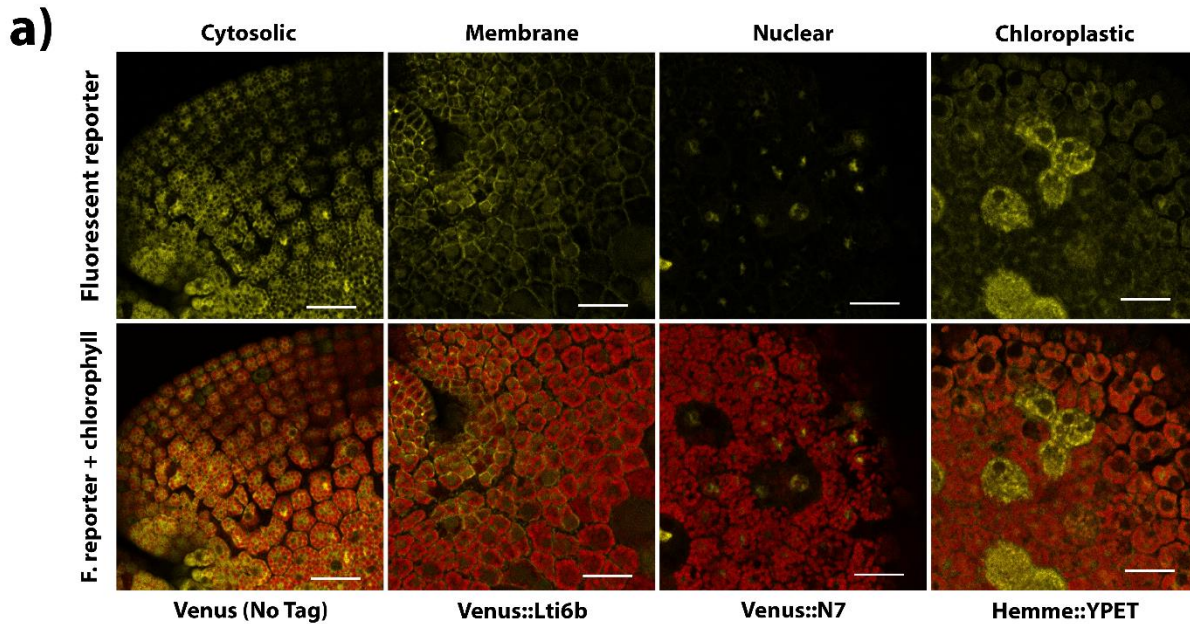


**Figure 10. Subcellular localization of fluorescent reporters in *Marchantia*.** *Marchantia* gemmae transformed with different fluorescent reporters were visualized (z-stack images) by a Nikon Ti-E C2si confocal microscope. (a) Venus (cytosol), Venus::Lti6b (membrane), Venus::N7 (nucleus) and Hemme::YPet (chloroplast) were excited with the corresponding wavelengths. The fluorescence of the reporters merged with the autofluorescence of chlorophyll (chloroplast localization) is also indicated. (b) The upper panel indicates the subcellular localization of mRuby3 (cytosol) and chlorophyll (chloroplast). The merged image shows that they have different locations. The lower panel shows the gemma emission spectrum transformed with the mRuby3 reporter. The scan was performed from 577 to 732 nm, revealing that emission spectra can be differentiated. Fluorescence was captured in their respective emission windows in sequential scanning mode. Scale bar = 50  $\mu$ m.

## Effect of fluorescent reporter TUs on *Marchantia gemma* development

At first glance, the yellow fluorescent reporters (i.e., Venus, Citrine and YPet) stood out for intensity and low autofluorescence of the growth medium among all the reporters evaluated. To corroborate these preliminary observations, we studied the growth and fluorescence intensity in *Marchantia gemmae* stably transformed with Venus ( $\lambda_{ex} = 515$  and  $\lambda_{em} = 528$ , cytosol), Venus::Lti6b (membrane), Venus::N7 (nucleus) and Hemme::YPet (chloroplast) during five days (**Figure 11**). Additionally, the proteins mRuby3 and mTurquoise2 (no localization tags) were added to this evaluation to have reference reporters to normalize the signal through dual-channel fluorescence measurements in the case that was necessary later (Federici et al., 2012; Rudge et al., 2016). In all the reporters evaluated, it was observed that from the fourth day, the flat structure of the gemma lost its quasi-bidimensional characteristic, making it very difficult to perform quantitative measurements by epifluorescent microscopy (day 5, **Figure 11**). All transgenic plants developed structurally similar to the wild type during the five days but had a decrease in size that was particularly evident in those transformed with nuclear-targeted Venus (Venus::N7 in **figure 11**). It is important to mention that almost all the gemmae were obtained from one-month-old plants, while those plants transformed with the reporter Venus::Lti6b were the only ones in which the gemmae were collected on one-and-a-half month plants due to a delay in the formation of gemma cups.

To quantitatively evaluate these observations, we performed an image processing pipeline in python to accurately measure the area and fluorescence intensity of the *Marchantia gemmae* (**Figure 12a**). This python pipeline allowed us to work with several images in an automated way, reducing background noise and eliminating *Marchantia* rhizoids or growth medium imperfections by image

segmentation. Briefly, the blue channel of the original images (best differentiates gemma from the background) is thresholded to create a mask that is processed by a series of steps to remove noise and rhizoids. Then, this mask is used to determine the thalli area and is superimposed on the original image to remove the background and measure fluorescence. Using this code, the area and fluorescence intensity of the thallus of 20 independent transgenic lines were measured for each reporter construct during four days. The average thalli area was smaller when compared to wild-type plants in almost all the reporter constructs, except for Venus::Lti6b and Venus, where no significant differences were observed from the second and fourth day onwards, respectively (**Figure 12b**). Furthermore, the plants transformed with the Venus construct presented higher fluorescence during the four days under similar exposure and light intensity conditions (**Figure 12c**). Conversely, the lowest intensity of fluorescence was obtained in those proteins destined for the nucleus and chloroplast (Venus::N7 and Hemme::YPet, **Figure 12c**). A linear correlation between the thallus area and fluorescence intensity of all reporter constructs was observed (**Figure 12d**) and the ratio between both parameters was relatively constant during the first days of gemma growth (**Figure 12e**). Both observations could facilitate the modeling of fluorescent reporter expression during the first days of *Marchantia* gemma growth in a way similar to a mathematical method used for measuring bacteria gene expression (Klumpp et al., 2009). This finding is relevant because it indicates that the rate of reporter production (assumed from the measured fluorescent signal as a proxy) per unit of tissue would be constant. This steady state production simplifies the mathematical characterization of the modules. Based on this screening, we decided on cytoplasmic Venus as reporter for our future constructions to maximize the amount of fluorescent signal without saturating the image or inducing photobleaching or phototoxicity in the plant.

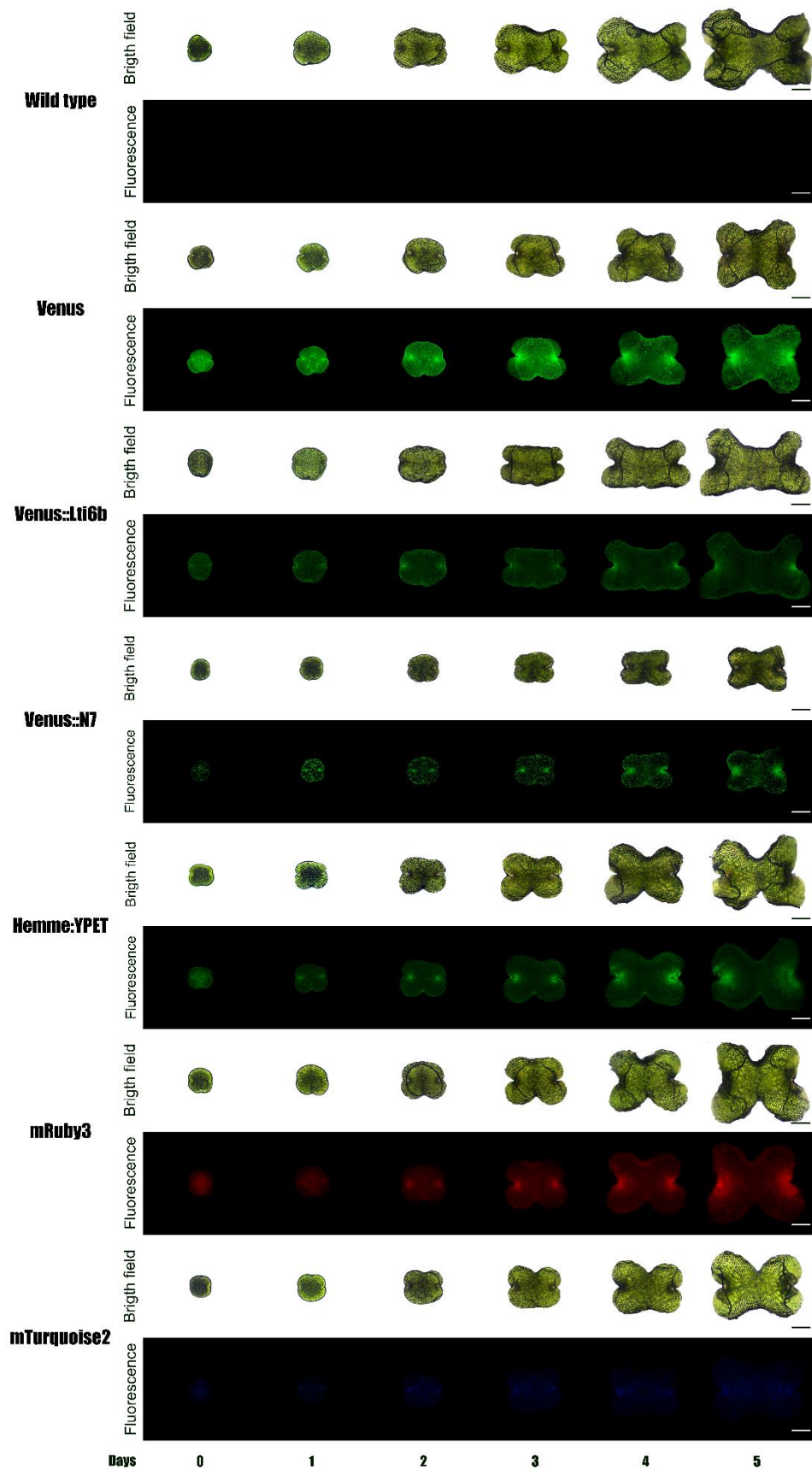


**Figure 11. Growth and fluorescence of *Marchantia gemmae* transformed with fluorescent reporters TUs.** Images were obtained by epifluorescent microscopy (Nikon Ni) during the first five days of growth of a representative transgenic gemma. Venus, (cytosol), Venus::Lti6b (membrane), Venus::N7 (nucleus), Hemme::YPet (chloroplast), mRuby3 (cytosol) and mTurquoise2 (cytosol). Scale bar = 500  $\mu$ m

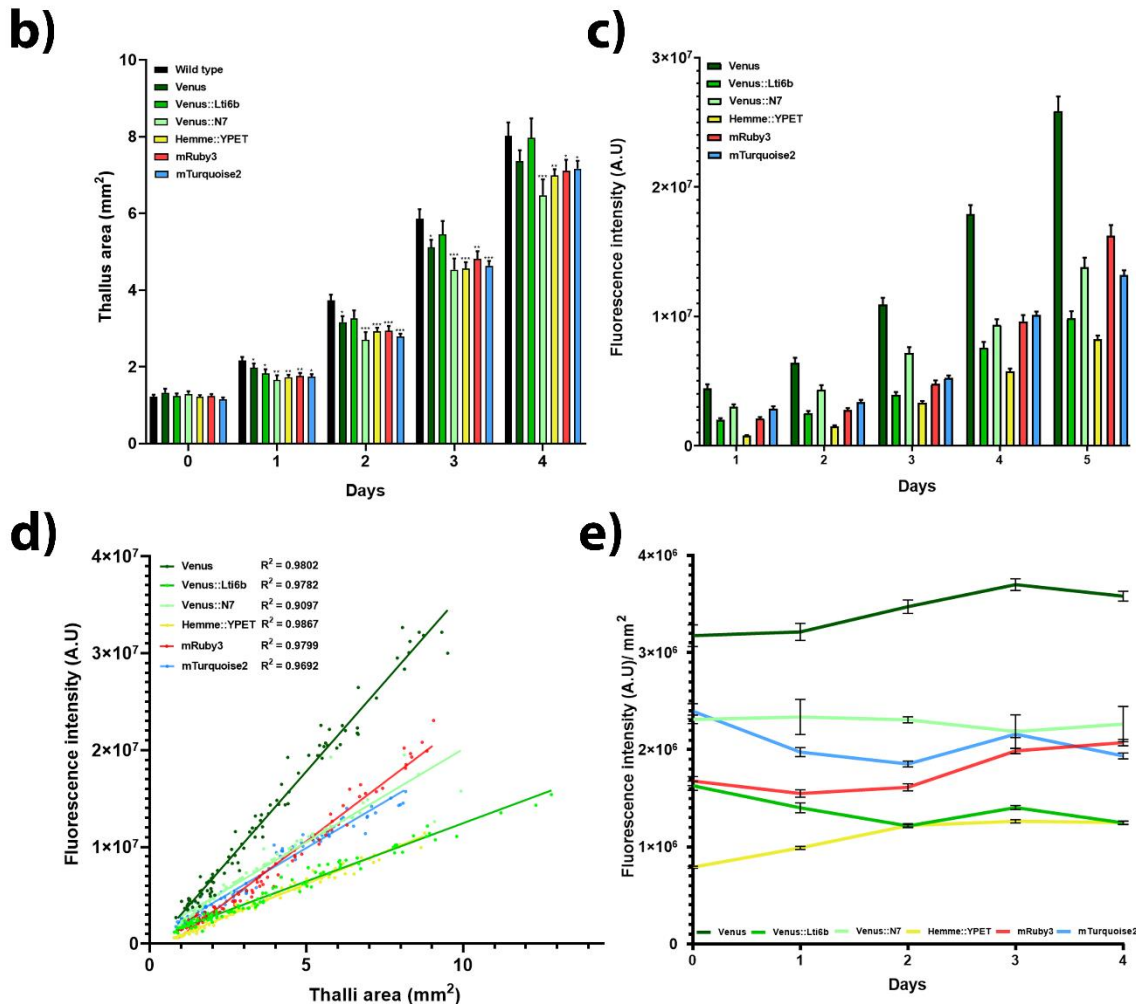
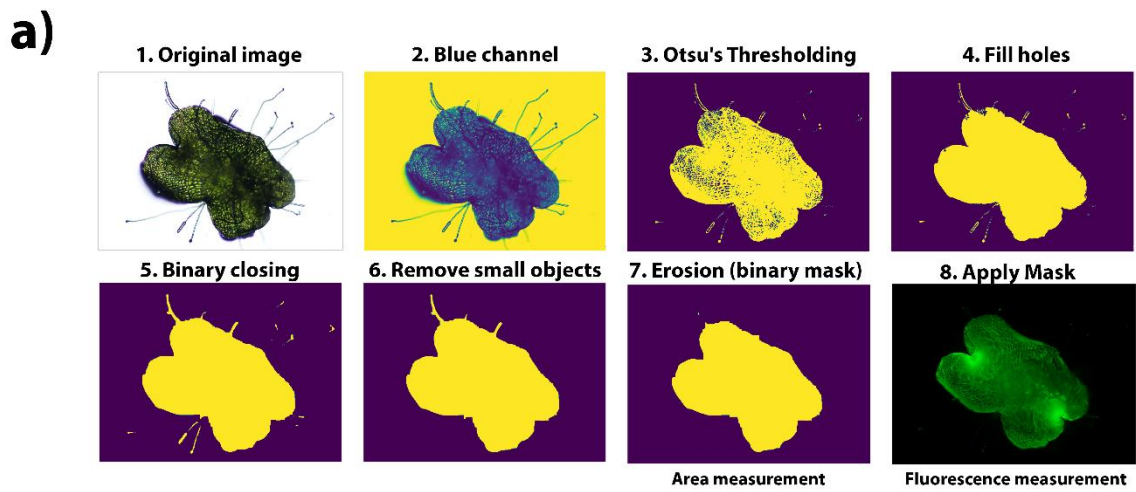


**Figure 12. Thallus area and fluorescence intensity in transformed *Marchantia gemmae*.** The total thallus area (mm<sup>2</sup>) and the fluorescence intensity (A.U.) of all the reporters transformed in *Marchantia* were obtained during four days. Mean and standard error of 20 plants per construct are given. **(a)** General scheme of the image processing pipeline used to obtain data from microscope images. **(b)** Total area of the *Marchantia* thallus during the first 4 days of growth. It is indicated if there are significant differences when compared with wild type plants (\*:  $p < .05$ , \*\*:  $p < .01$ , \*\*\*:  $p < .001$ ). **(c)** Fluorescence intensity of *Marchantia gemmae* during the first 4 days of growth. **(d)** Relation between area and intensity of fluorescence. The line fitted to the data and its respective R<sup>2</sup> are shown. **(e)** Average fluorescence intensity normalized by the thallus area on each of the days observed.

### Objective 3

#### **Activation of a synthetic promoter through a modular transcription factor.**

Once the foundational elements were tested, we evaluated all the gene elements necessary for logic based on synthetic promoters. First, we generated modular DNA elements that allow the construction of hybrid transcription factors (TF) composed of DNA binding domains (BD) and activation domains (AD) or repression domains (RD). This modularity is given by the CDS syntax that we embraced earlier in the design of the L0 parts (**Figure 7a**). We chose the DNA-binding domain of the yeast transcription factor GAL4 (Fields and Song, 1989; Pan and Coleman, 1989) due to its wide use and reported functionality in other plant models (Ma et al., 1988; Aoyama and Chua, 1997; Haseloff, 1999; Moore et al., 2006). A fragment of the DNA-binding domain of yeast HAP1 was also selected (Pfeifer et al., 1989; Hon et al., 1999; Lan et al., 2004). This fragment retains sufficient DNA-binding activity and has been used in transactivation constructs for enhancer-trap systems in plants (Haseloff et al., 2005). As an alternative, the DNA-binding domains of the bacterial transcription factors TetR and SprR were also considered (Stanton et al., 2014). Although these BD have not been evaluated in plants, they were chosen due to their potential orthogonality with plant regulatory systems, a highly-desirable feature in synthetic circuits. The activation domain of the herpes viral protein VP16 (Sadowski et al., 1988) was also cloned so that our hybrid TF could activate genes transcriptionally. This domain has been widely used in conjunction with the GAL4 BD in synthetic transactivation systems in plants (Aoyama and Chua, 1997; Haseloff, 1999; Yang et al., 2000; Engineer et al., 2005). While the EAR-motif will be used as a repression domain, since transcription factors fused to this motif act as strong transcriptional repressors in Arabidopsis and are conserved across diverse plant species (Hiratsu et al., 2003; Kagale and

Rozwadowski, 2010). In addition to the DNA-binding domains, we also constructed L0 parts that contained the binding sequences of these elements. In the case of the GAL4 and HAP1 BDs, we synthesized sequences termed Upstream Activation sequences (UAS<sub>GAL4</sub> and UAS<sub>HAP1</sub>, respectively) that will allow the binding of our modular TFs to synthetic promoters (Guarente et al., 1982; West et al., 1984; Giniger et al., 1985; Zhang and Guarente, 1994). Following the same line of thinking, we also synthesized the DNA operator sequences to which the TetR and SprR BDs bind, named TetR<sub>op</sub> and SprR<sub>op</sub> (Stanton et al., 2014). To ensure that we obtain fluorescent signals at our synthetic promoters in response to TF binding, we generated L0 parts with the response elements duplicated in tandem as well (i.e., 2xUAS<sub>GAL4</sub>, 2xUAS<sub>HAP1</sub>, 2xTetR<sub>op</sub> and 2xSprR<sub>op</sub>). With all these modular DNA elements we built TUs consisting of a transcriptional activator (BD + VP16) driven by the constitutive MpEF1 $\alpha$  promoter and its cognate synthetic promoter driving the expression of the Venus fluorescent reporter (**Figure 13a**). The synthetic promoter consisted of 4 identical transcription factor binding sites (TFBS) separated by 20 bp spacers, specially designed to contain no known Marchantia TF sites (see Materials and Methods for details). In addition, these promoters had a minimal CaMV35S promoter (pMin35S) that requires upstream enhancers to promote Venus transcription (F. Federici and J. Haseloff, unpublished results). Fluorescence was observed in all the constructs we evaluated in gemmae from transgenic Marchantia lines, regardless of whether they contained single or double TFBS (**Figure 13b-m**). Great variability was observed between the fluorescence of the transgenic lines, but those lines with duplicated TFBS promoters generally presented higher fluorescence than those with simple regulatory elements (**Figure 13d, g and m**). This was true for almost all constructs except TetR, where no apparent relationship between single and double TFBS was observed (**Figure j**). This

result demonstrates that the modular DNA elements we designed are functional in a *Marchantia* context and promote transcription at custom-designed promoters.

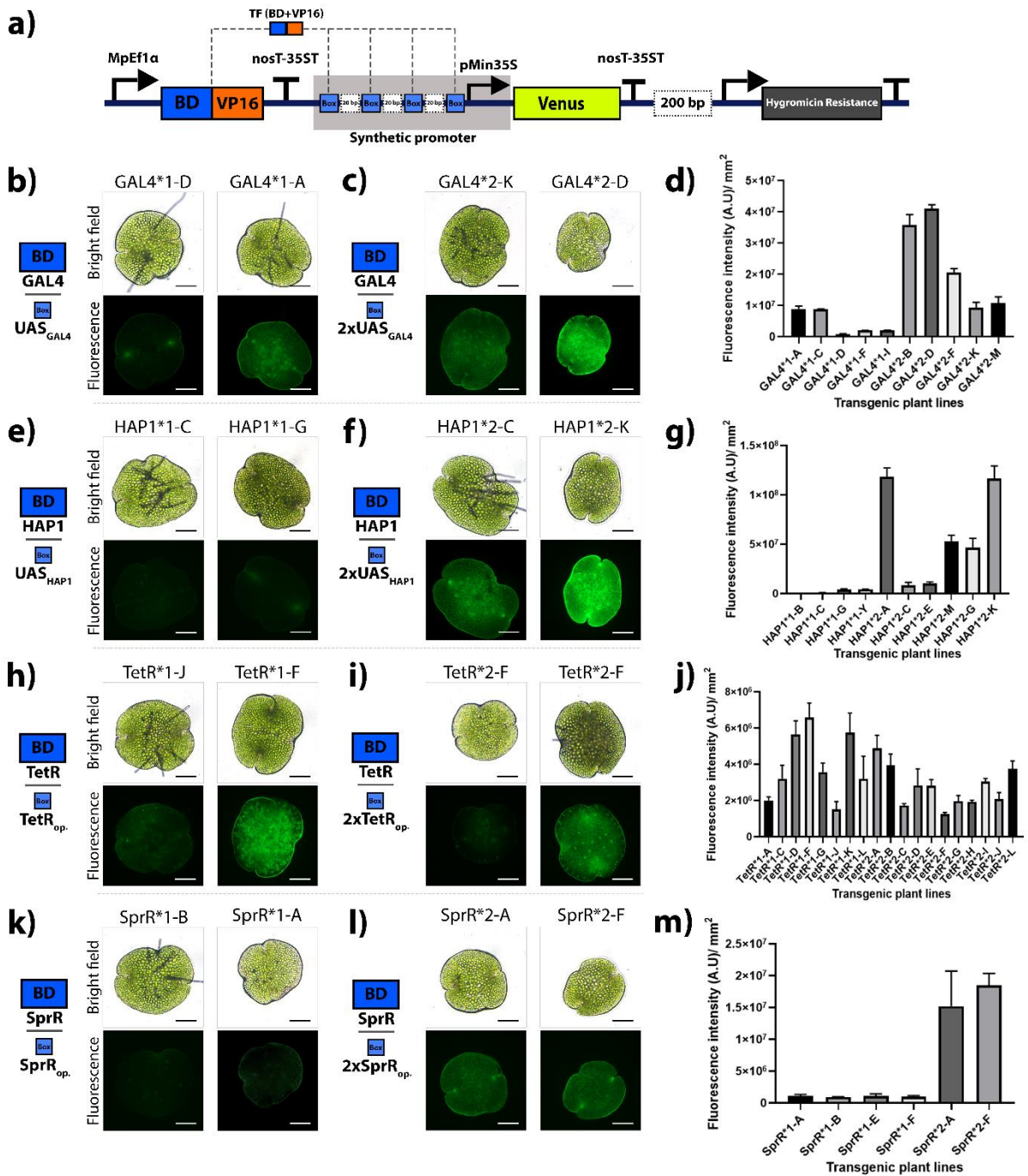


**Figure 13. Fluorescence in *Marchantia* gemmae driven by synthetic promoters activated through modular transcription factors.** (a) Scheme of the construct used to stably transform *Marchantia*. The construct has a modular TF that includes a DNA-binding domain plus the VP16 activation domain and can bind to a synthetic promoter that drives the expression of Venus. The synthetic promoter has an arrangement of 7 cis-elements and the minimal 35S promoter (gray rectangle), these elements correspond to 4 transcription factor binding sites (TFBS) separated by 20 bp spacers. A 200 bp spacer and hygromycin resistance cassette are also indicated. As appropriate, the BD and TFBS used in each set of transgenic lines are indicated, showing for each construct a two-day old gemma of the transgenic line with the lowest and highest fluorescence. GAL4 BD with UAS<sub>GAL4</sub> (b) and 2xUAS<sub>GAL4</sub> (c). HAP1 BD with UAS<sub>HAP1</sub> (e) and 2xUAS<sub>HAP1</sub> (f). TetR BD with TetR<sub>op</sub> (h) and 2xTetR<sub>op</sub> (i). SprR BD with SprR<sub>op</sub> (k) and 2xSprR<sub>op</sub> (l). For each transgenic line obtained, the average fluorescence (20 gems per line) and the standard error are indicated. In each graph, the lines are grouped according to their BD. GAL4 BD (d), HAP1 BD (g), TetR BD (j) and SprR BD (m). Scale bar = 500  $\mu$ m.

## Evaluation of leaky expression in the synthetic constructs

To verify that the fluorescent signal we observed corresponded to the interaction between the modular TF and the synthetic promoter with the corresponding TFBS, we constructed different plasmids to evaluate the leaky expression. First, we wanted to rule out the possibility that the minimal 35S promoter in the presence of the constitutively expressed TFs had a similar basal expression to that observed in the fluorescent *Marchantia* lines indicated in **Figure 13**. For that, we generated plasmids that contained the four TFs (GAL4::VP16, HAP1::VP16, TetR::VP16 and SprR16::VP16) and the pMin35S promoter driving the expression of Venus (**Figure 14a**). We placed seven 20-bp spacers upstream of pMin35S that did not contain known TFBS in *Marchantia*, so in the absence of specific binding sites for TFs, the expression of Venus should be negligible or minimal. No fluorescence was observed in any of the 16 transgenic lines analyzed per construct (3 representative transgenic lines for each construct, **figure 14 b-e**). Furthermore, the average fluorescence of the lines (GAL4/pMin, HAP1/pMin, TetR/pMin and SprR/pMin) was significantly lower in all constructs when compared to the average fluorescence of lines possessing TFBS (single or double) to which TF could bind (**Figure. 14f**). This demonstrates that the pMin35S promoter does not have a significant leaky expression concerning fluorescent transgenic lines. We also measured the average thallus area of the transgenic lines, and differences with wild-type plants were only observed in 2 constructs that possessed the TF and its related promoter with double TFBS (GAL4/2xUAS<sub>GAL4</sub> and SprR/2xSprR<sub>op</sub>, **figure 14g**). To demonstrate that the low expression of the pMin35S promoter is not due to nonspecific binding of endogenous TFs to TFBS, we designed plasmids containing single and double TFBS promoters (4 copies of each response element upstream of the pMin35S promoter) and replaced

the constitutively expressed TF with a 200 bp spacer (**Figure 15a**). These eight different constructs would allow us to assess whether TFBS alone are capable of eliciting transcription from Venus. We evaluated 16 transgenic plants per construct, and in most of the evaluated lines, absence or very low fluorescence was observed (**Figure 15b-i**). For each construct, two representative gemmae of the transgenic lines are shown. However, the third gemma with basal fluorescence was added to highlight this fact. We wanted to emphasize this, because even though most of the lines had an imperceptible level of fluorescence, in all the groups there were lines with levels of fluorescence considerably higher than the rest. This phenomenon did not occur with the lines that possessed the transcription factor driven by the MpEF1 $\alpha$  promoter together with the pMin35S driving the expression of Venus (**Figure 13**). To gather more information in this regard, we generated a construct that only contained the 200-bp spacer followed by the pMin35S promoter with seven empty boxes upstream (20-bp spacers), and we observed the same behavior (**Figure 15j**). Therefore, we think that having replaced the constitutively expressed TF transcriptional unit (~3000-bp by 200-bp) could have generated greater susceptibility of the synthetic promoter to endogenous enhancers at the transgene insertion site. This is seen more clearly in **Figure 15k**, where all the constructs that have a TF preceding the empty synthetic promoter (GAL4/pMin, HAP1/pMin, TetR/pMin and SprR/pMin) tend to have a lower fluorescence intensity than the pMin35S promoter without TF (NoTF/pMin). Conversely, those lines that lack the TF, but have a synthetic promoter with single or double TFBS (NoTF/TFBS and NOTF/2xTFBS lines), generally have higher fluorescence than the plant lines without TF and pMin35S lacking TFBS (lines NoTF/pMin). This difference could be because some endogenous transcription factors can non-specifically bind to synthetic promoters. Regardless of this leaky expression,

all fluorescence levels are significantly lower than the fluorescent transgenic lines that possess the corresponding TF/TFBS pair.

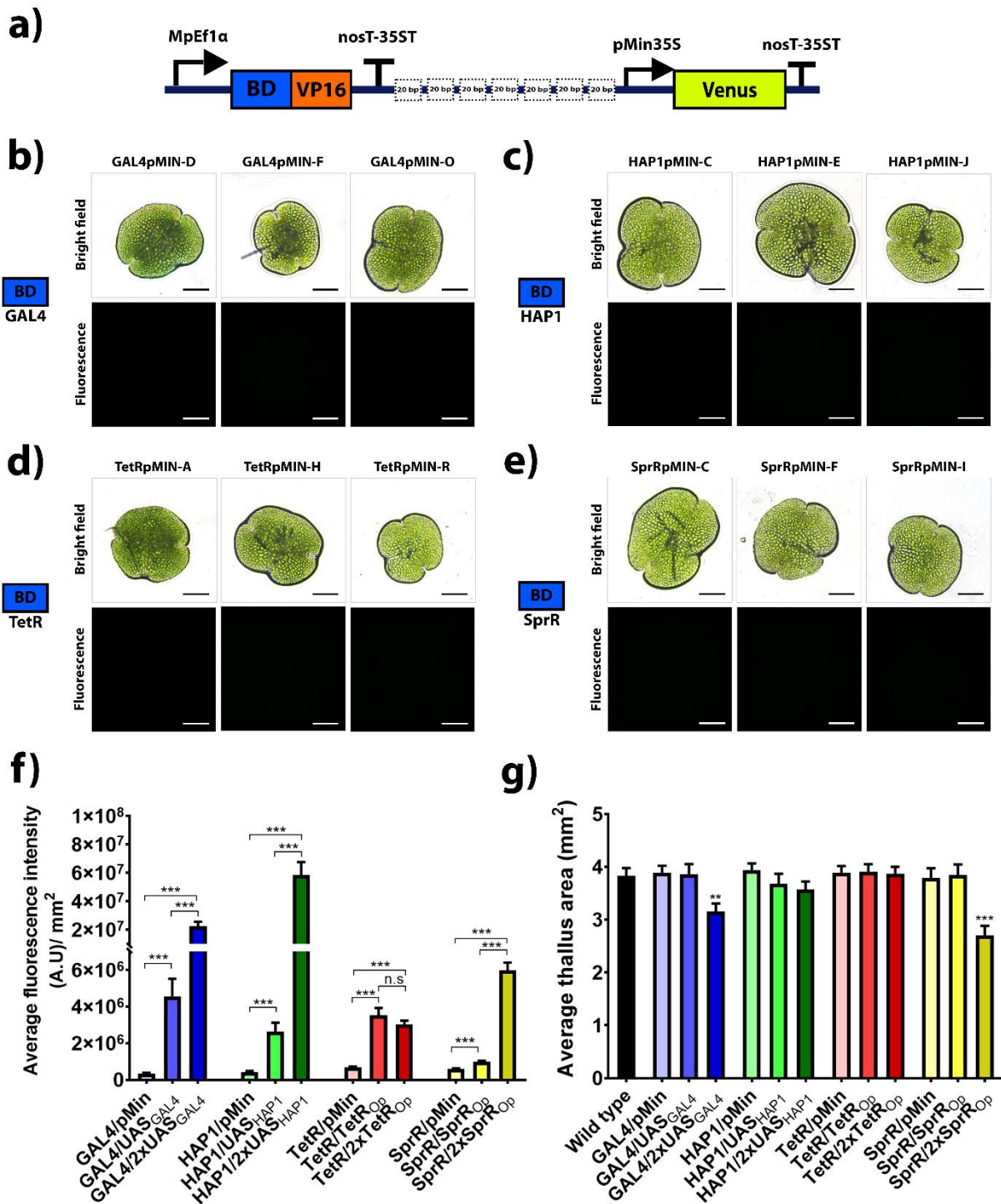


**Figure 14. Analysis of leaky expression in pMin35S promoter.** (a) General diagram of the constructs used to transform *Marchantia*. It indicates a constitutively expressed TF (DNA-binding domain and VP16 activation domain) and the synthetic promoter (seven 20-bp spacers and a pMin35S promoter) driving Venus expression. 20 transgenic lines were transformed with each BD construct and three representative lines per construct are shown: GAL4 (b), HAP1 (c), TetR (d) and SprR (e). (f) Comparison of average fluorescence between constructs. Average fluorescence and the standard error for each group are indicated. The y-axis has been divided into two segments to highlight the difference between the lower fluorescence intensities. (g) Comparison of average thallus area. The average and standard error for each construct are shown, indicating if there is a significant difference compared to wild-type plants. An average of 16 transgenic lines (20 gems per line) was used for the BD/pMin constructs (f and g). \*:  $p < .05$ , \*\*:  $p < .01$ , \*\*\*:  $p < .001$ , n.s = not statistically significant. Scale bar = 500  $\mu\text{m}$ .

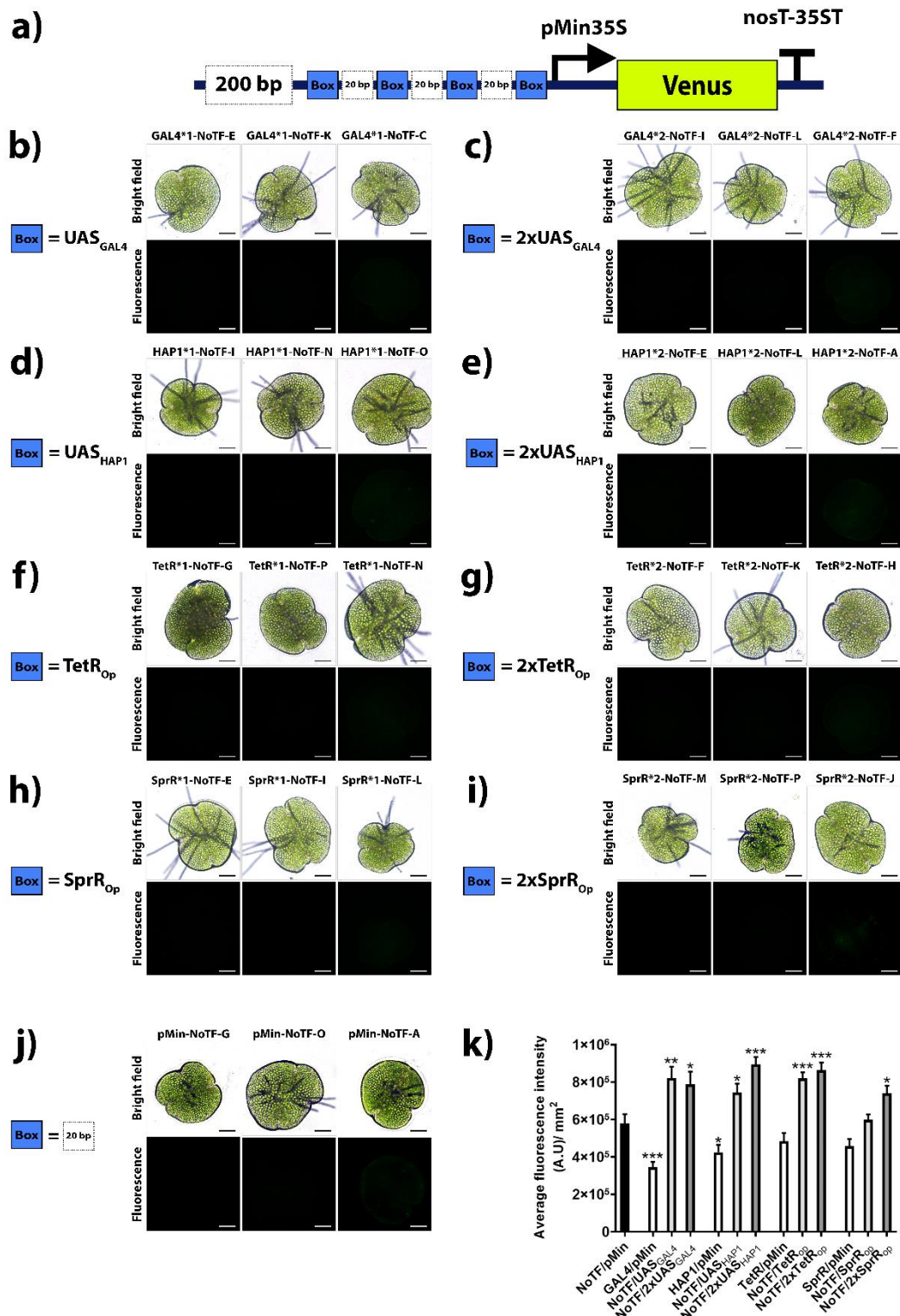


**Figure 15. Testing of synthetic promoters in the absence of constitutively expressed transcription factors.** (a) General structure of the plasmids that were used to evaluate the basal expression of the synthetic promoters. The TF has been replaced by a 200-bp spacer and the synthetic promoter is composed of 4 specific TFBS (separated by 20-bp spacers) upstream of a minimal 35S promoter. Both spacers (20- and 200-bp) contain no known regulatory sequences in *Marchantia*. The regulatory boxes in the synthetic promoter corresponded to 4 identical elements of: UAS<sub>GAL4</sub> (b), 2xUAS<sub>GAL4</sub> (c), UAS<sub>HAP1</sub> (d), 2xUAS<sub>HAP1</sub> (e), TetR<sub>Op</sub> (f), 2xTetR<sub>Op</sub> (g), SprR<sub>Op</sub> (i) and 2xSprR<sub>Op</sub> (i). Representative gemmae of the obtained lines (first two) and a representative gemma of a transgenic line with the basal expression of fluorescence in the absence of TF (third of each group) are indicated in each construct. In addition, a construct was included in which all spaces preceding the pMin35S promoter (7 boxes) correspond to 20-bp spacers (j). Finally, the average fluorescence intensity (16 lines per construct) was compared between the transgenic lines showing leaky expression (k). The average and standard error for each construct are shown, indicating if there is a significant difference compared to the lines containing the pMin35S promoter without TF (NoTF/pMin): \* p < .05, \*\* p < .01, \*\*\* p < .001, n.s. = not statistically significant. Scale bar = 500  $\mu$ m.

## **Induction of transcriptional activation by an external input.**

In order to transcriptionally regulate the expression of Venus using an external inducer, we fused the modular TFs to the ligand-binding domain of the glucocorticoid receptor (GR, Rusconi and Yamamoto, 1987; Picard et al., 1988). In the absence of a steroid hormone such as dexamethasone (DEX), the TF-GR fusion proteins are retained in the cytoplasm, but upon application of DEX, the proteins are released and can enter the nucleus where they exert their effect (Lloyd et al., 1994; Aoyama and Chua, 1997; Padidam, 2003). This domain and the synthetic glucocorticoid DEX have been widely used because of their simplicity and lack of pleiotropic effects in plants (Böhner et al., 1999; Ouwerkerk et al., 2001; Craft et al., 2005; Samalova et al., 2005). Recently, Gateway binary vectors that express a transcriptional regulator fused to the GR domain in *Marchantia* have also been designed (Ishizaki et al., 2015). In our work, we performed a C-terminal fusion of the GR domain to the previously characterized TFs, so that the activity of the TFs could be conditioned to the presence of DEX (**Figure 16**). We then transformed the eight generated constructs (combinations of TFs and synthetic promoters with four copies of single or double TFBS) and evaluated gemmae of the transgenic lines for two days in the presence of the DEX inducer (48 h treatment). We expected that TFs could not promote transcription because they stayed retained in the cytoplasm without the inducer (0h treatment), but there was basal fluorescence in the absence of DEX in most constructs. (**Figure 16b, d and bottom panel of c**). On the other hand, at least three constructs showed considerably low fluorescence levels in the absence of DEX. (**Figure 16e and upper panel of c**). The lines that presented visible fluorescence levels without treatment did not change their behavior after 48 hours of DEX treatment, while those constructs with lower levels (HAP1-GR/UAS<sub>HAP1</sub>, SprR/SprR<sub>Op</sub> and SprR/2xSprR<sub>Op</sub> constructs) significantly

changed the average fluorescence intensity upon treatment (**Figure 16f**). The fusion protein SprR::VP16::GR by means of the GR domain was able to generate two well-demarcated states of "OFF" (0 h of treatment) and "ON" (48 h of treatment) of fluorescence in the synthetic promoters with single or duplicate TFBS (**Figure 16e**). Moreover, there was a higher intensity of fluorescence in those DEX-treated lines that possessed double binding sites (SprR<sub>Op</sub> v/s 2xSprR<sub>Op</sub>, **figure 16f**). In the case of HAP1::VP16::GR the situation was different, since only those lines with simple TFBS achieved this effect of ON/OFF demarcated states (UAS<sub>HAP1</sub> v/s 2xUAS<sub>HAP1</sub>, **figure 16c and f**). Lastly, the thallus area of the transgenic lines was always significantly smaller than the size of the wild type plants, showing that the expression of these TF::GR may be affecting plant growth. There are multiple reasons for these results, but we think that the high expression mediated by the strong and constitutive promoter MpEF1 $\alpha$  could be one of the main causes. This was also reflected in the number of transforming plants when this promoter was used, since compared to those plants without TFs, it was always lower. All these results show that the GR domain can be used to generate inducible TFs in the presence of an external input (DEX) and can be used for the future characterization of transcriptional repressors.

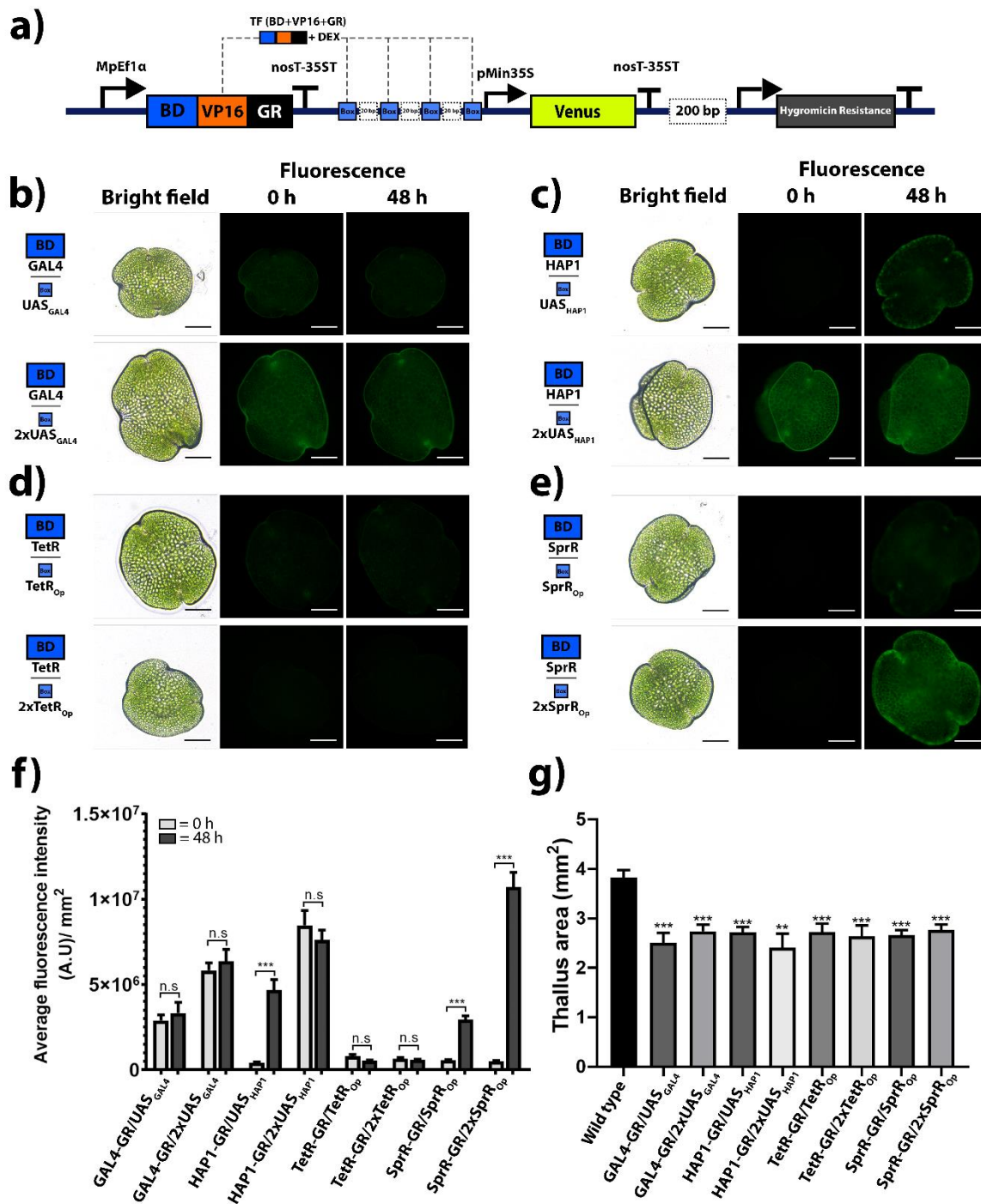


**Figure 16. Characterization of inducible transcriptional activators upon dexamethasone treatments. (a)** Construct used to characterize DEX-inducible TFs. The transcription factor (BD+VP16) has been fused to the GR induction domain (C-terminal fusion). In addition, a synthetic promoter consisting of 4 transcription factor binding sites separated by 20 bp spacers is indicated. **(b-e)** Representative gemmae of plants transformed with the constitutively expressed TF::GR. In each panel the plants with synthetic promoters containing single (top row) or duplicate (bottom row) binding motifs are shown. **(f)** Comparison of the average fluorescence intensity obtained in the 8 constructs before (0 h) and after treatment (48 h) with DEX. **(g)** Comparison of average thallus area. The average and standard error for each construct are shown, indicating if there is a significant difference compared to the wild type plants \*:  $p < .05$ , \*\*:  $p < .01$ , \*\*\*:  $p < .001$ , n.s = not statistically significant. Scale bar = 500  $\mu\text{m}$ .

## Characterization of ligand-induced transcriptional repressors

Finally, we decided to characterize transcriptional repressors using the previously described DNA-binding domains (GAL4, HAP1, TetR and SprR) and exchanging the VP16 activation domain for the EAR repression domain to complete our repertoire of regulatory functions (Hiratsu et al., 2003). The characterization of repressors in our model requires the use of transcriptional activators and an induction domain to make repressor activity conditional. **Figure 17** shows the constructs designed to evaluate the activity of conditional transcriptional repressors in *Marchantia*. In an ON state, plants transformed with these constructs should fluoresce due to the interaction of the transcriptional activator (BD1::VP16) with the TFBS in the synthetic promoter (**Figure 17a**). The use of an activator is necessary to generate a basal-regulated level of fluorescence since the pMin35S promoter needs upstream enhancers to promote Venus transcription. The fluorescence intensity will depend on the promoter used to express the activator (e.g., MpEF1 $\alpha$ ) and the number of TFBS present in the synthetic promoter capable of binding the activator (e.g., 4 TFBS). While in an OFF state, exogenous application of DEX will allow translocation of the repressor (BD2::EAR::GR) from the cytoplasm to the nucleus, where it will bind to the synthetic promoter through repressor-specific TFBS (**Figure 17b**). Although TFs (activator and repressor) will bind to the promoter during treatment, the EAR domain acts as a dominant repressor in *Arabidopsis* and other plant models, even in the presence of redundant endogenous TFs or chimeric TFs containing the VP16 activation domain (Ohta et al., 2001; Hiratsu et al., 2002). Thus, we expect that once the repressor binds during DEX treatment, the ON-state fluorescence is likely to disappear, and its temporal dynamics would depend on the number of available binding sites (e.g., 3 repressors TFBS). An essential requirement to achieve an ON/OFF state transition is

that the binding domains are different (BD1 and BD2, **figure 17**) so that the TFs do not compete for the same sites. The constructs have already been sequenced and only need to be evaluated by stable transformation in *Marchantia*. This experiment would demonstrate that the EAR domain is functional and sufficient to build modular repressors in *Marchantia*. With all the elements characterized so far, it is possible to make plant synthetic circuits with logic based on activators, repressors, induction domains and synthetic promoters with customized TFBS arrangements.

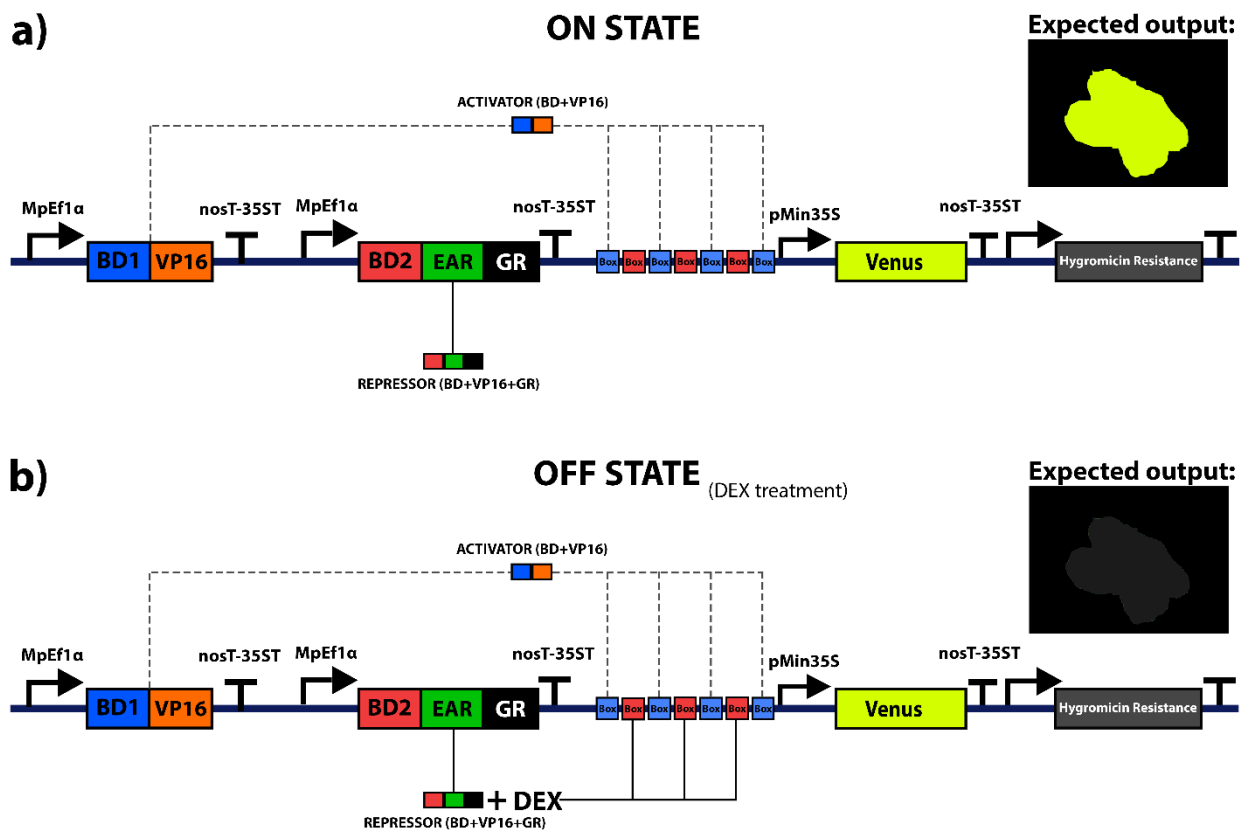


**Figure 17. Design of the constructs required to evaluate the functionality of the repressors.** L2 plasmid showing two states (ON and OFF) during treatment with the DEX external inducer. A constitutively expressed transcriptional activator (BD1::VP16) and repressor (BD1::EAR::GR) are indicated. Also shown are a synthetic promoter constituted of 7 TFBS (4 for activator BD1 and 3 for repressor BD2) driving Venus expression and the hygromycin resistance cassette. **(a)** ON state, before DEX application. During this state, only the activator will be present in the nucleus, so once it binds to its specific sites (blue boxes) it will be able to promote the transcription of the Venus fluorescent protein. The repressor can not bind to the synthetic promoter because it is retained in the cytoplasm via its GR domain. **(b)** OFF state, after at least 48 hours of DEX-treatment. After the external application of DEX, the repressor will be translocated to the nucleus, where it can exert its function. Given the dominant effect of EAR on the VP16 activation domain, we expect that repressor binding (red boxes) will be sufficient to turn off the expression of the Venus fluorescent reporter.

## Objective 4

The tools and DNA elements developed would allow us to design and develop genetic circuits to explore plant pattern formation and make significant progress in establishing the field of morphogenetic engineering in *Marchantia*. The most studied models to generate patterns within a given domain are based on positional information defined by the concentration of an external input (Isalan et al., 2005; Scholes and Isalan, 2017; Santos-Moreno and Schaeerli, 2019). These mechanisms trigger differential expression programs based on each cell's position within the gradient. A wide design of possible stripe-forming networks in a morphogen gradient has been described computationally and synthetically (Schaeerli et al., 2014). However, these networks are burdensome to implement in plants due to the absence of artificial cell-to-cell signals capable of diffusing throughout the tissue by passive diffusion. One solution to this problem is to rely on internal gradients of phytohormones, molecules that control a myriad of aspects related to plant growth and development. As proof of concept, we had planned the design of genetic circuits based on the work of Saka and Smith (2007), in which a simple network with mutual negative feedback can respond to different levels of a diffusible molecule. Circuits with this behavior require a molecule (phytohormone) that induces two TFs that mutually repress each other's transcription (**Figure 18a**). This synthetic network can convert a graded signal into a binary output and exhibit sharp thresholds (**Figure 18b**), which may be biologically relevant to creating boundaries between two cell types. To build these circuits, two transcriptional repressors are needed, which can be built using the EAR repression domain with two previously characterized DNA-binding domains (e.g., HAP1 and SprR). These repressors must be driven by promoters capable of responding to the BDs and the chosen phytohormone. Such promoters can be easily assembled by Loop assembly

using already characterized TFBS and cis-regulatory elements for phytohormone responses. Furthermore, repressors can specifically inhibit fluorescent reporters driven by synthetic promoters with specific binding motifs, thus the transition between the two states can be seen by epifluorescent microscopy. Phytohormones in *Marchantia* are still under study and classic response promoters do not have the same results as in other model organisms such as *Arabidopsis* (Ishizaki et al., 2012). However, some studies describe the possible elements involved in the phytohormone-response and the patterns observed during plant development using reporters such as GUS or fluorescent proteins (Flores-Sandoval et al., 2015; Kato et al., 2015; Eklund et al. al., 2015; Ghosh et al., 2016). Some of these response elements were synthesized to evaluate and characterize their functionality in *Marchantia*. As a test, we generated constructs that possessed seven repeats of these elements upstream of a pMin35S promoter driving Venus expression (**Figure 18c**). Cytokinin response elements (Müller and Sheen, 2008), ABA (Ghosh et al., 2016), and auxin response elements (Hagen et al., 1991; Ishizaki et al., 2012) were included in the assembled promoters. Additionally, the mRuby3 fluorescent protein was added as a reference reporter and aided to insulate our synthetic promoter from the insertion context. As preliminary results, we were able to transform the synthetic promoters with ABA response elements and cytokinins (**Figure 18 d-f**), being the ABA elements those that presented the highest fluorescence intensity in transgenic *Marchantia gemmae* (**Figure 18e and f**).

Aside from the genetic tools and elements, the development of morphogenetic models requires mathematical formalisms that allow us to develop predictive models. The dynamics of the repressors in the network dependent on inducer concentration (in our case phytohormone) have already been described by two time-dependent

ordinary differential equations (Saka and Smith, 2007). However, it is necessary to incorporate equations that predict gene expression based on the regulatory elements of synthetic promoters, an essential fact since with Loop assembly we can generate a highly modular environment (7 customizable boxes) upstream of the minimal promoter. For this reason, we decided to use thermodynamic state ensemble models, which describe the transcription probability of a promoter based on its modular cis-regulatory elements, following a modular design fashion (Sherman and Cohen, 2012). Based on this thermodynamic framework we generate sets of equations that describe: (i) the possible states of the promoter based on the TFs that can bind to it, (ii) the affinity constants of the interactions that occur in each state, and (iii) whether each state allows transcription. The equations and assumptions used to generate these equations are described in **Appendix II** and indicate a cis-regulatory function representing the probability of our synthetic promoter being active. Some of these assumptions have already been evaluated (e.g., expression of the minimal promoter), but testing this set of equations *in planta* still is necessary. If adjustments are needed, the high tunability of the modular elements developed aids this task. Therefore, we believe that all the tools shown here allow the construction and implementation of morphogenetic models in *Marchantia* in a simpler way.

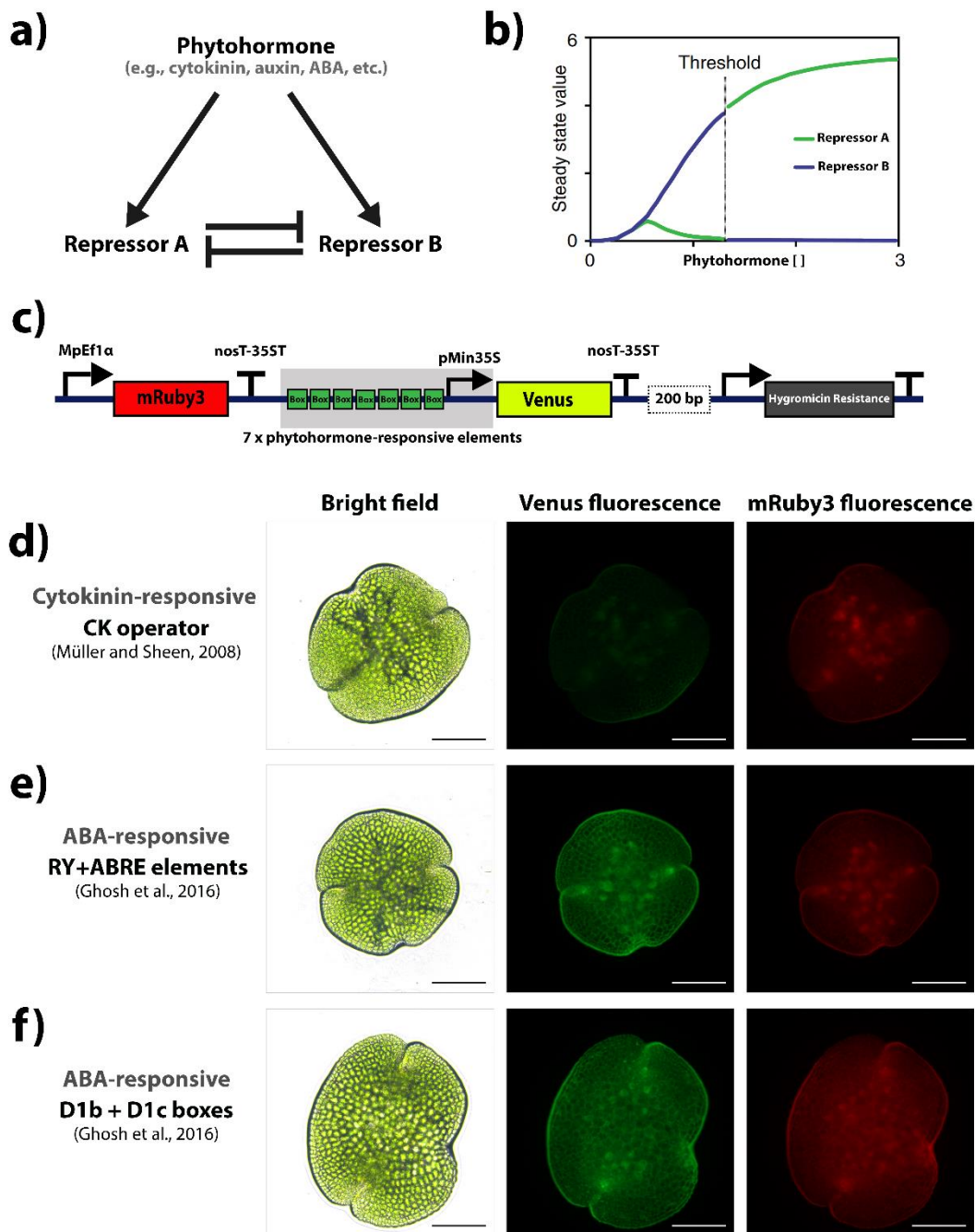


**Figure 18. Bases for the implementation of a morphogenetic model in *Marchantia*.** (a) Abstraction of a network of a phytohormone and two repressors (A and B) in which the hormone induces both and these in turn mutually repress their expression. (b) Steady-state values of repressors A and B plotted against the concentration of a phytohormone (modified from Saka and Smith, 2017). When certain conditions are met, the synthetic system reaches one of two opposite stable states (high concentration of repressor A and low concentration of B, or vice versa) according to the phytohormone concentration. As shown in the figure, the bifurcation of this system occurs within a sharp threshold. (c) Construct used to preliminarily evaluate whether the phytohormone response motifs could respond to the internal signs of *Marchantia*. Plasmids consisted of a constitutively expressed reference reporter (mRuby3) and a Venus reporter driven by a synthetic promoter carrying seven phytohormone-response repeat motifs and the pMin35S promoter. (d-f) *Marchantia* gemmae stably transformed with the constructs with seven repeated response elements. ABA- and cytokinin-responsive motifs were included. Auxin response motifs are not yet tested. Scale bar = 500  $\mu$ m.

## DISCUSSION

### **Loop assembly as a tool for rapid, modular and combinatorial construction of plant gene circuits.**

In recent years, there has been a growing interest in one-step assembly methods due to how well they fit into the growing requirements of synthetic circuit construction such as modular design, standardized functionalities and interoperativity across labs. In fact, the idea and principles of Loop Assembly are highly-inspired by such methods (Gibson Assembly, MoClo and GoldenBraid cloning system) trying to integrate all their benefits in a multipurpose routine DNA assembly system. Loop plasmid design takes advantage of type-IIS enzyme mechanisms to create a simple, recursive assembly platform based on head-to-head configuration by eliminating the requirement for end-linkers (as used in MoClo). The orientation and identity of the restriction sites within the receiver plasmids allow the assembly of up to four transcriptional units simultaneously, so larger constructs can be generated and rapidly scale in complexity (**Figure 2**). The requirement of using four plasmids at each level allowed us to systematize the assemblies without increasing the complexity of our method through completely standardized reactions, assisted by L0 parts and their overhangs. An exclusive feature of the Loop design is that it allows the generation of L0 modular part libraries from lower levels (i.e., -L1, -L2, etc), as is the case with the combinatorial assembly of synthetic promoters (**Figure 4**). For instance, to put the combinatorial capacity of Loop in numbers, with only 7 L0 parts of regulatory elements and a minimal promoter, more than 800,000 different synthetic promoters could be built without the need to synthesize anything else. Furthermore, the recursive feature of Loop Assembly reduced the number of plasmids used in our method without losing versatility. Another example of Loop's versatility is the possibility of performing overlapping assembly methods (e.g., Gibson) through standardized UNSes flanking

type-IIS restriction sites (**Figure 5**) and allowing reuse of UNS-specific primers to assemble multiple TUs (and even assemble fewer TUs without spacer-requirement). The possibility of using overlap or type-IIS assembly also provides flexibility in situations that require altering the native sequence (e.g., promoters that, when domesticated, affect some TF-responsive element) or when the assembly fails using one of the pathways. The large number of constructs with different TUs generated in this thesis demonstrates the effectiveness and efficiency of Loop Assembly, most of them with L0 parts also designed and built during this work (**Appendix I**). The functionality of the assembled plasmids was also demonstrated through their activity in both *Arabidopsis thaliana* protoplast and *Marchantia polymorpha* gemmae (**Figure 6**). The integration of overlap and type-IIS (e.g., Golden Gate) assemblies encourages community development around the use of modular DNA elements, which, in turn, promotes the growth of repositories of standardized L0 parts, TUs or more complex combinations. Moreover, the compatibility of Loop with other assembly systems, such as MoClo, SEVA and Goldenbraid, facilitates the constant updating and improvement of DNA element repositories, granting and guaranteeing better collaboration and cross-validation.

It is important to highlight that in order to facilitate easier exchange and transfer of DNA modules between different laboratories, Loop assembly is provided under an Open Material Transfer Agreement license (OpenMTA) for unrestricted sharing and open access. The OpenMTA provides a simple, standardized legal tool that enables individuals or organizations to share their materials to effectively place them in the public domain (Kahl et al., 2018). This formal tool is a collaborative effort between the BioBricks Foundation and the OpenPlant initiative, with the help of researchers, technology transfer professionals, lawyers, social scientists, and other collaborators.

Although the cost of DNA synthesis is declining and has dropped by nearly three orders of magnitude (Carlson, 2009; Kosuri and Church, 2014), synthetic biology will still require the ability for rapid, high-throughput combinatorial assembly. The best representation of this in our work is the combinatorial assembly of synthetic promoters (**Figure 4**), in which the characterization and troubleshooting of small DNA parts and more complex constructs is fundamental. Doing this by hand is too labor-intensive, but Loop can also easily be prone to being part of automation pipelines. Assembly systems that can take advantage of the opportunities of automation technologies will benefit from each other in the future. Platforms that automate the synthesis of synthetic circuits are becoming more prevalent, as they enable larger constructs using less research time and considerably increasing design space (Kanigowska et al., 2016; Goyal et al., 2020; Storch et al., 2020).

### **Foundational DNA elements and regulatory functions characterized in *Marchantia*.**

The use and characterization of L0 parts in *Marchantia* was possible due to the robustness and reliability of Loop, independent of the level of assembly and the part type. Using these L0 parts allowed us to generate more complex constructs that varied in size, composition, and TUs number. One of the main challenges in our work was to choose genetic elements that could be consistently reused in different contexts, allowing the exploration and construction of diverse synthetic circuits and ideally the entire design space. Thus, we create a compact set composed of different DNA-binding domains (GAL4, HAP1, TetR and SprR), the VP16 activation domain, the EAR repression domain, and the GR induction domain. These modular elements were easily tested due to the selected syntax (**Figure 7**), the previously characterized

foundational elements (**Figure 8 and 9**), and the benefits of using *Marchantia* as a model. *Marchantia* provided us with an excellent prototyping tool due to its genetic advantages that allowed us, among other things, to have a large number of individuals through sporeling transformation (Ishisaki et al., 2008). Besides, *Marchantia* transgenic lines were propagated through gemma, allowing us to obtain an isogenic haploid tissue, highly accessible for epifluorescent microscopy on the same plate.

During the characterization of the foundational elements, a series of fluorescent reporters and localization peptides for multispectral imaging were evaluated (**Figure 9 and 10**) to reduce noise (e.g., autofluorescence) without impacting the fluorophore signal, a key challenge in live-cell fluorescence imaging. Furthermore, we compared the area of the transgenic thalli with the wild type, as a quick way to assess the effect of reporter expression in *Marchantia*, because there were reports that GFP fluorescent reporter has a toxic effect in *Marchantia* (Ishizaki et al., 2016). Bearing these considerations in mind, we chose cytoplasmic Venus as the reporter for our constructs instead of some that had a lower fluorescence intensity (nuclear tag N7), high autofluorescence in solid media (mTagBFP2 and mTurquoise2) or affected the growth and development of *Marchantia* (membrane Lti6b tag). Although Venus allowed us to test all the elements shown in this work, there were some constructs in which the transgenic line number was affected. The reasons can be varied, and it is difficult to address them in plant models where the effects of cellular burden and evolutionary failure have been poorly studied. For example, when modular TFs were constitutively expressed (**Figure 13, 14 and 16**), there was a reduction in the number of transgenic plants obtained, and some lines had a decrease in their growth and total area (**Figure 14g and 16g**). There were also transgenic lines in which we did not observe functionality of the modular TFs (e.g., TetR::VP16::GR, **figure 16d**) or reduced

fluorescence was reported (e.g., some lines of HAP1::VP16, **figure 13g**), leading to suspect gene silencing. High expression levels triggered by the MpEf1a promoter can be the answer to this problem since several cases of slower and deformed growth and higher frequency of gene silencing in plants have been described when using MpEF1 $\alpha$  to drive fluorescent protein expression (Sauret-Güeto et al., 2020). The identification of tissue- and cell-specific promoters in Marchantia concerns not only synthetic biology but also metabolic engineering and developmental biology. Promoters that are expressed throughout the whole gemma and achieve a trade-off between low toxicity and high expression are required in Marchantia. Recently, Sauret-Güeto et al. (2020), through transcriptome data and in planta analysis, discovered that the ubiquitin-conjugating enzyme E2 promoter (MpUBE2) drives the constitutive expression of transgenes in gemmae, so this promoter might be a candidate to consider. While this problem did not impede us from functionally testing modular DNA elements, it is important to consider it as synthetic circuits keep growing in size and complexity. Another point to consider is that even though the transformation of spores ensured us to obtain a large number of plants per construct, Marchantia thallus transformation remains a plausible alternative if one wants to work with isogenic backgrounds and not depend on the tedious spore preparation (Kubota et al., 2013). This is relevant considering that the sporelings are heterogeneous due to the parental crossing of male (Cam1) and female (Cam2) lines with different genetic backgrounds, affecting the consistency between the resulting transgenic plants.

Finally, the insertional effects became apparent in different lines. That was most evident in those constructs whose synthetic promoter was exposed to inappropriate enhancer-promoter interactions and chromosomal positional effects (**Figure 15**), often resulting in high variability between independent transgenic lines or transgene

silencing (Singer et al., 2012). In some cases, it is sufficient to insert an additional nucleotide space between the possible enhancers and the promoter (as was the case when we added a 200 bp spacer or a TU) but using insulators could be more appropriate to separate the enhancing effect and decrease interactions with the insertion site (Bilas et al., 2016). Insulators neutralize the positional effect and the influence of adjacent sequences on gene expression (Papadakis et al., 2004; Singer et al., 2012). Therefore, its application in multigene constructs may be beneficial to guarantee the autonomy of synthetic circuits from the insertional context in plants. The identity of these elements is not the focus of this work, but there are several insulators in plants that have been recently described and can be used for these purposes (Bilas et al., 2016; Kurbidaeva and Purugganan, 2021).

### **Paving the way to morphogenetic engineering in plants.**

Unlike electronics, biological circuits can function in a diffusive environment instead of being deeply wired and isolated. Therefore, it is necessary to be constantly concerned about the effect of the constructs within the chassis organism, inciting orthogonality to avoid molecular crosstalk. This, for example, was the incentive to demonstrate the functionality of parts such as the TetR and SprR DNA-binding domains of bacterial origin in *Marchantia* in our work. However, many of these circuits seek precisely to affect the structure and form of the host organism in the long term. Plants are an attractive platform to study how genetic circuits can regulate development and morphogenesis through artificial mechanisms of pattern formation. The use of *Marchantia* to test our constructs showed that it is an appropriate model chassis for morphogenetic engineering. *Marchantia* offers a simple model whose life cycle can be observed continuously under the microscope directly on a plate, enabling

molecular relationships within growing tissues to be readily visualized, quantified, or altered by stable transformation (**Figure 11 and 12**). One of the things that is delaying our understanding of plant morphogenesis is the limited ability to control gene expression in space and time. First efforts consisted in transcriptional fusion to promoters of known (and desired) expression patterns (e.g., the root apical meristem promoter pRCH1, Casamitjana-Martinez et al., 2003). Later enhancer traps were developed as a way to detect regulatory sequences in plants and get a better understanding of gene expression control (Sundaresan et al., 1995; Campisi et al., 1999; Haseloff, 1999; Wu et al., 2003). Laser induction has also been developed for precise control (Swarup et al., 2005). Synthetic biology, on the other hand, permits the elaboration of synthetic gene networks (SGNs) that are able to self-organize into more complex designs, clearing the path to the next wave of gene regulation in plants (e.g., domain of artificial cell states). We proposed to follow the model of Saka and Smith (2007) because it proposes a simple mechanism by which small differences in a morphogen concentration can create a boundary between two different cell types. The first step in the design of these SGNs is the creation of promoters that can integrate activation and repression inputs. In our work, we demonstrate that by giving the identity of TUs (1-11 syntax) to the regulatory element boxes, we can build synthetic promoters consisting of 7 regulatory elements and a minimal promoter. Customizing the identity and spacing of these elements allowed us to test for modular transcription factors in *Marchantia* (Figure 13a, 14a, 15a and 16a). To achieve this, we built promoters with 4 copies of TFBS (single and double sites: UAS<sub>GAL4</sub>, UAS<sub>HAP1</sub>, TetR<sub>op</sub> and SprR<sub>op</sub>), elements that were spaced by 20-bp sequences to reduce steric effects between TFs bound to DNA. In principle, we design 20-bp and 40-bp spacers (**Appendix I**), but the modularity of the elements involved allows more rigorous studies on the appropriate

helical orientation to space TFBS. At the same time, it must be taken into account that the use of repetitive cis-elements with identical core-sequences can monopolize the TFs and reduce endogenous gene expression (Bhullar et al., 2003; Venter et al., 2007). Regardless of this, the combined and well-designed use of modular TFs and synthetic promoters is a valuable approximation to parameterize the genetic parts, using constructs in which the TFs can be induced by an external input (DEX) through the GR induction domain and whose promoters can adjust their dynamic range by rearranging their elements (**Figure 17**).

All these opportunities led us to propose a morphogenetic model that integrates the synthetic circuit and phytohormones' internal signals (**Figure 18**). Integration can be easily mediated by synthetic promoters, for that we tested preliminary whether some phytohormone response elements were capable of responding to endogenous signals (**Figure 18d-f**). Synthetic promoters and modular TFs provide enormous advantages over their natural counterparts with regards to transgene expression strength and specificity. Nevertheless, the design of these parts can be in vain without mathematical formalisms that help parameterize various aspects of the circuits. Recently Brophy et al. (2022) showed that robust circuits can be built and tuned in *Arabidopsis* through quantitative transient expression assays. Once characterized, these constructs can be transformed into whole plants to control the spatial patterns of root gene expression and predictably modify the plant's body plan. This work shows the possibilities of reprogramming plant growth through synthetic circuits using modular elements similar to those we evaluated in *Marchantia* (i.e., activation domains, repression domains and synthetic promoters with a specific arrangement of TFBS). However, it lacks the systematic building of synthetic promoters that Loop assembly offers. The modular assembly of promoters allowed us to apply

thermodynamic state ensemble models and express the probability of transcription of our synthetic promoter with equations with strong physical bases (**Appendix II**). These formalisms could help us predict gene expression based on regulatory cis-elements from DNA sequence and biologically-based assumptions. Sooner than later, we believe that the modular elements and tools shown here will bring the field of morphogenetic engineering even closer to plant models.

## CONCLUSIONS

- We develop Loop assembly, a versatile, straightforward, and efficient DNA assembly method based on a recursive approach and test foundational elements for the characterization of synthetic circuits in *Marchantia*.
- Loop-mediated assembly of DNA elements allowed the creation of fully-functional modular regulatory functions composed of DNA-binding domains, activation/repression domains, and induction domains in *Marchantia polymorpha*.
- Regulatory functions can be customized both at the modular TF level and by rearranging the cis-elements of a synthetic promoter, generating a wide combinatorial design space of both level 0 components and transcriptional units.
- The possibilities created by this work led us to propose a morphogenetic model based on internal gradients and whose characterization can be done through thermodynamic state ensemble models applied to synthetic promoters with phytohormones-responsive elements.

## BIBLIOGRAPHY

- Althoff, F., Kopischke, S., Zobell, O., Ide, K., Ishizaki, K., Kohchi, T., & Zachgo, S.** (2014). Comparison of the MpEF1 $\alpha$  and CaMV35 promoters for application in *Marchantia polymorpha* overexpression studies. *Transgenic research*, 23(2), 235–244.
- Alvarez-Buylla, E. R., Azpeitia, E., Barrio, R., Benítez, M., & Padilla-Longoria, P.** (2010). From ABC genes to regulatory networks, epigenetic landscapes and flower morphogenesis: making biological sense of theoretical approaches. *Seminars in cell & developmental biology*, 21(1), 108–117.
- Annaluru, N., Muller, H., Mitchell, L. A., Ramalingam, S., Stracquadanio, G., Richardson, S. M., Dymond, J. S., Kuang, Z., Scheifele, L. Z., Cooper, E. M., Cai, Y., Zeller, K., Agmon, N., Han, J. S., Hadjithomas, M., Tullman, J., Caravelli, K., Cirelli, K., Guo, Z., London, V., ... Chandrasegaran, S.** (2014). Total synthesis of a functional designer eukaryotic chromosome. *Science (New York, N.Y.)*, 344(6179), 55–58.
- Aoyama, T., & Chua, N. H.** (1997). A glucocorticoid-mediated transcriptional induction system in transgenic plants. *The Plant journal : for cell and molecular biology*, 11(3), 605–612.
- Arce, A., Guzman Chavez, F., Gandini, C., Puig, J., Matute, T., Haseloff, J., Dalchau, N., Molloy, J., Pardee, K., & Federici, F.** (2021). Decentralizing Cell-Free RNA Sensing With the Use of Low-Cost Cell Extracts. *Frontiers in bioengineering and biotechnology*, 9, 727584.
- Ausländer, S., Ausländer, D., Müller, M., Wieland, M., & Fussenegger, M.** (2012). Programmable single-cell mammalian biocomputers. *Nature*, 487(7405), 123–127.
- Baskin T. I.** (2005). Anisotropic expansion of the plant cell wall. *Annual review of cell and developmental biology*, 21, 203–222.
- Basu, S., Mehreja, R., Thiberge, S., Chen, M. T., & Weiss, R.** (2004). Spatiotemporal control of gene expression with pulse-generating networks. *Proceedings of the National Academy of Sciences of the United States of America*, 101(17), 6355–6360.
- Basu, S., Gerchman, Y., Collins, C. H., Arnold, F. H., & Weiss, R.** (2005). A synthetic multicellular system for programmed pattern formation. *Nature*, 434(7037), 1130–1134.
- Bhullar, S., Chakravarthy, S., Advani, S., Datta, S., Pental, D., & Burma, P. K.** (2003). Strategies for development of functionally equivalent promoters with minimum

sequence homology for transgene expression in plants: cis-elements in a novel DNA context versus domain swapping. *Plant Physiology*, 132(2), 988-998.

**Biłas, R., Szafran, K., Hnatuszko-Konka, K., & Kononowicz, A. K.** (2016). Cis-regulatory elements used to control gene expression in plants. *Plant Cell, Tissue and Organ Culture (PCTOC)*, 127(2), 269-287.

**Blain, J. C., & Szostak, J. W.** (2014). Progress toward synthetic cells. *Annual review of biochemistry*, 83, 615–640.

**Boehm, C. R., Pollak, B., Purswani, N., Patron, N., & Haseloff, J.** (2017). Synthetic Botany. *Cold Spring Harbor perspectives in biology*, 9(7), a023887.

**Böhner, S., Lenk, I., Rieping, M., Herold, M., & Gatz, C.** (1999). Transcriptional activator TGV mediates dexamethasone-inducible and tetracycline-inactivatable gene expression. *The Plant Journal*, 19(1), 87-95.

**Bonnet, J., Subsoontorn, P., & Endy, D.** (2012). Rewritable digital data storage in live cells via engineered control of recombination directionality. *Proceedings of the National Academy of Sciences of the United States of America*, 109(23), 8884–8889.

**Bowman, J. L., Kohchi, T., Yamato, K. T., Jenkins, J., Shu, S., Ishizaki, K., Yamaoka, S., Nishihama, R., Nakamura, Y., Berger, F., Adam, C., Aki, S. S., Althoff, F., Araki, T., Arteaga-Vazquez, M. A., Balasubramanian, S., Barry, K., Bauer, D., Boehm, C. R., Briginshaw, L., ... Schmutz, J.** (2017). Insights into Land Plant Evolution Garnered from the *Marchantia polymorpha* Genome. *Cell*, 171(2), 287–304.e15.

**Brophy, J. A., Magallon, K. J., Kniazev, K., & Dinneny, J. R.** (2022). Synthetic genetic circuits enable reprogramming of plant roots. *bioRxiv*.

**Cachat, E., Liu, W., Martin, K. C., Yuan, X., Yin, H., Hohenstein, P., & Davies, J. A.** (2016). 2- and 3-dimensional synthetic large-scale de novo patterning by mammalian cells through phase separation. *Scientific reports*, 6, 20664.

**Cai, Y. M., Kallam, K., Tidd, H., Gendarini, G., Salzman, A., & Patron, N. J.** (2020). Rational design of minimal synthetic promoters for plants. *Nucleic acids research*, 48(21), 11845–11856.

**Cameron, D. E., Bashor, C. J., & Collins, J. J.** (2014). A brief history of synthetic biology. *Nature reviews. Microbiology*, 12(5), 381–390.

**Campisi, L., Yang, Y., Yi, Y., Heilig, E., Herman, B., Cassista, A. J., ... & Jack, T.** (1999). Generation of enhancer trap lines in Arabidopsis and characterization of expression patterns in the inflorescence. *The Plant Journal*, 17(6), 699-707.

**Carlson, R.** (2009). The changing economics of DNA synthesis. *Nature biotechnology*, 27(12), 1091-1094.

**Casamitjana-Martinez, E., Hofhuis, H. F., Xu, J., Liu, C. M., Heidstra, R., & Scheres, B.** (2003). Root-specific CLE19 overexpression and the sol1/2 suppressors implicate a CLV-like pathway in the control of Arabidopsis root meristem maintenance. *Current Biology*, 13(16), 1435-1441.

**Chen, Z., & Elowitz, M. B.** (2021). Programmable protein circuit design. *Cell*, 184(9), 2284–2301.

**Craft, J., Samalova, M., Baroux, C., Townley, H., Martinez, A., Jepson, I., ... & Moore, I.** (2005). New pOp/LhG4 vectors for stringent glucocorticoid-dependent transgene expression in Arabidopsis. *The Plant Journal*, 41(6), 899-918.

**Cutler, S. R., Ehrhardt, D. W., Griffitts, J. S., & Somerville, C. R.** (2000). Random GFP:: cDNA fusions enable visualization of subcellular structures in cells of Arabidopsis at a high frequency. *Proceedings of the National Academy of Sciences*, 97(7), 3718-3723.

**Daniel, R., Rubens, J. R., Sarpeshkar, R., & Lu, T. K.** (2013). Synthetic analog computation in living cells. *Nature*, 497(7451), 619–623.

**Dobrin, A., Saxena, P., & Fussenegger, M.** (2016). Synthetic biology: applying biological circuits beyond novel therapies. *Integrative biology : quantitative biosciences from nano to macro*, 8(4), 409–430.

**Doursat, R., Sayama, H. & Michel, O.** (2013) A review of Morphogenetic Engineering. "Frontiers of Natural Computing" (FNC 2012) Special Issue. M. Lones, A. Tyrrell, S. Stepney & L. Caves, eds. *Natural Computing* 12(2): 517-535.

**Eklund, D. M., Ishizaki, K., Flores-Sandoval, E., Kikuchi, S., Takebayashi, Y., Tsukamoto, S., ... & Bowman, J. L.** (2015). Auxin produced by the indole-3-pyruvic acid pathway regulates development and gemmae dormancy in the liverwort *Marchantia polymorpha*. *The Plant Cell*, 27(6), 1650-1669.

**Elowitz, M. B., & Leibler, S.** (2000). A synthetic oscillatory network of transcriptional regulators. *Nature*, 403(6767), 335–338.

**Endy D.** (2005). Foundations for engineering biology. *Nature*, 438(7067), 449–453.

- Engineer, C. B., Fitzsimmons, K. C., Schmuke, J. J., Dotson, S. B., & Kranz, R. G.** (2005). Development and evaluation of a Gal4-mediated LUC/GFP/GUS enhancer trap system in *Arabidopsis*. *BMC plant biology*, 5, 9.
- Engler, C., Kandzia, R., & Marillonnet, S.** (2008). A one pot, one step, precision cloning method with high throughput capability. *PLoS one*, 3(11), e3647.
- Engler, C., Gruetzner, R., Kandzia, R., & Marillonnet, S.** (2009). Golden gate shuffling: a one-pot DNA shuffling method based on type II restriction enzymes. *PLoS one*, 4(5), e5553.
- Engler, C., Youles, M., Gruetzner, R., Ehnert, T. M., Werner, S., Jones, J. D., Patron, N. J., & Marillonnet, S.** (2014). A golden gate modular cloning toolbox for plants. *ACS synthetic biology*, 3(11), 839–843.
- Engstrom, M. D., & Pfleger, B. F.** (2017). Transcription control engineering and applications in synthetic biology. *Synthetic and systems biotechnology*, 2(3), 176–191.
- Farzadfard, F., & Lu, T. K.** (2014). Synthetic biology. Genomically encoded analog memory with precise in vivo DNA writing in living cell populations. *Science (New York, N.Y.)*, 346(6211), 1256272.
- Federici, F., Dupuy, L., Laplaze, L., Heisler, M., & Haseloff, J.** (2012). Integrated genetic and computation methods for in planta cytometry. *Nature methods*, 9(5), 483–485.
- Federici, F., Rudge, T. J., Pollak, B., Haseloff, J., & Gutiérrez, R. A.** (2013). Synthetic Biology: opportunities for Chilean bioindustry and education. *Biological research*, 46(4), 383–393.
- Fields, S., & Song, O.** (1989). A novel genetic system to detect protein-protein interactions. *Nature*, 340(6230), 245–246.
- Flores-Sandoval, E., Eklund, D. M., & Bowman, J. L.** (2015). A Simple Auxin Transcriptional Response System Regulates Multiple Morphogenetic Processes in the Liverwort *Marchantia polymorpha*. *PLoS genetics*, 11(5), e1005207.
- Friedland, A. E., Lu, T. K., Wang, X., Shi, D., Church, G., & Collins, J. J.** (2009). Synthetic gene networks that count. *Science (New York, N.Y.)*, 324(5931), 1199–1202.

**Gander, M. W., Vrana, J. D., Voje, W. E., Carothers, J. M., & Klavins, E.** (2017). Digital logic circuits in yeast with CRISPR-dCas9 NOR gates. *Nature communications*, 8, 15459.

**Gardner, T. S., Cantor, C. R., & Collins, J. J.** (2000). Construction of a genetic toggle switch in *Escherichia coli*. *Nature*, 403(6767), 339–342.

**Ghosh, T. K., Kaneko, M., Akter, K., Murai, S., Komatsu, K., Ishizaki, K., ... & Takezawa, D.** (2016). Abscisic acid-induced gene expression in the liverwort *Marchantia polymorpha* is mediated by evolutionarily conserved promoter elements. *Physiologia plantarum*, 156(4), 407-420.

**Gibson, D. G., Young, L., Chuang, R. Y., Venter, J. C., Hutchison, C. A., 3rd, & Smith, H. O.** (2009). Enzymatic assembly of DNA molecules up to several hundred kilobases. *Nature methods*, 6(5), 343–345.

**Gibson, D. G., Glass, J. I., Lartigue, C., Noskov, V. N., Chuang, R. Y., Algire, M. A., Benders, G. A., Montague, M. G., Ma, L., Moodie, M. M., Merryman, C., Vashee, S., Krishnakumar, R., Assad-Garcia, N., Andrews-Pfannkoch, C., Denisova, E. A., Young, L., Qi, Z. Q., Segall-Shapiro, T. H., Calvey, C. H., ... Venter, J. C.** (2010). Creation of a bacterial cell controlled by a chemically synthesized genome. *Science (New York, N.Y.)*, 329(5987), 52–56.

**Gilbert, C., & Ellis, T.** (2019). Biological Engineered Living Materials: Growing Functional Materials with Genetically Programmable Properties. *ACS synthetic biology*, 8(1), 1–15.

**Giniger, E., Varnum, S. M., & Ptashne, M.** (1985). Specific DNA binding of GAL4, a positive regulatory protein of yeast. *Cell*, 40(4), 767–774. 8

**Glass, D. S., & Riedel-Kruse, I. H.** (2018). A Synthetic Bacterial Cell-Cell Adhesion Toolbox for Programming Multicellular Morphologies and Patterns. *Cell*, 174(3), 649–658.e16.

**Göpfrich, K., Platzman, I., & Spatz, J. P.** (2018). Mastering Complexity: Towards Bottom-up Construction of Multifunctional Eukaryotic Synthetic Cells. *Trends in biotechnology*, 36(9), 938–951.

**Goyal, G., Elsbree, N., Fero, M., Hillson, N. J., & Linshiz, G.** (2020). Repurposing a microfluidic formulation device for automated DNA construction. *PloS one*, 15(11), e0242157.

**Grant, P. K., Dalchau, N., Brown, J. R., Federici, F., Rudge, T. J., Yordanov, B., Patange, O., Phillips, A., & Haseloff, J.** (2016). Orthogonal intercellular signaling for programmed spatial behavior. *Molecular systems biology*, 12(1), 849.

**Grant, P. K., Szep, G., Patange, O., Halatek, J., Coppard, V., Csikász-Nagy, A., Haseloff, J., Locke, J., Dalchau, N., & Phillips, A.** (2020). Interpretation of morphogen gradients by a synthetic bistable circuit. *Nature communications*, 11(1), 5545.

**Greber, D., & Fussenegger, M.** (2010). An engineered mammalian band-pass network. *Nucleic acids research*, 38(18), e174.

**Guarente, L., Yocum, R. R., & Gifford, P.** (1982). A GAL10-CYC1 hybrid yeast promoter identifies the GAL4 regulatory region as an upstream site. *Proceedings of the National Academy of Sciences*, 79(23), 7410-7414.

**Haellman, V., & Fussenegger, M.** (2016). Synthetic Biology--Toward Therapeutic Solutions. *Journal of molecular biology*, 428(5 Pt B), 945–962.

**Hagen, G., Martin, G., Li, Y., & Guilfoyle, T. J.** (1991). Auxin-induced expression of the soybean GH3 promoter in transgenic tobacco plants. *Plant molecular biology*, 17(3), 567-579.

**Hamant, O., Heisler, M. G., Jönsson, H., Krupinski, P., Uyttewaal, M., Bokov, P., Corson, F., Sahlin, P., Boudaoud, A., Meyerowitz, E. M., Couder, Y., & Traas, J.** (2008). Developmental patterning by mechanical signals in Arabidopsis. *Science (New York, N. Y.)*, 322(5908), 1650–1655.

**Haseloff J.** (1999). GFP variants for multispectral imaging of living cells. *Methods in cell biology*, 58, 139–151.

**Haseloff, J., Bauch, M., Boissard-Lorig, C., Hodge, S., Laplace, L., Runions, J., & Kurup, S.** (2005). Patent, United States of America Patent No US 8,034.915 B2.

**Hatch, M. D.** (1987). C4 photosynthesis: a unique blend of modified biochemistry, anatomy and ultrastructure. *Biochimica et Biophysica Acta (BBA) - Reviews on Bioenergetics*. Vol. 895(2):81-106.

**Hellens, R. P., Edwards, E. A., Leyland, N. R., Bean, S., & Mullineaux, P. M.** (2000). pGreen: a versatile and flexible binary Ti vector for Agrobacterium-mediated plant transformation. *Plant molecular biology*, 42(6), 819–832.

**Hiratsu, K., Matsui, K., Koyama, T., & Ohme-Takagi, M.** (2003). Dominant repression of target genes by chimeric repressors that include the EAR motif, a

repression domain, in Arabidopsis. *The Plant journal : for cell and molecular biology*, 34(5), 733–739.

**Hon, T., Hach, A., Tamalis, D., Zhu, Y., & Zhang, L.** (1999). The yeast heme-responsive transcriptional activator Hap1 is a preexisting dimer in the absence of heme. *The Journal of biological chemistry*, 274(32), 22770–22774.

**Isalan, M., Lemerle, C., & Serrano, L.** (2005). Engineering gene networks to emulate Drosophila embryonic pattern formation. *PLoS biology*, 3(3), e64.

**Ishizaki, K., Chiyoda, S., Yamato, K. T., & Kohchi, T.** (2008). Agrobacterium-mediated transformation of the haploid liverwort *Marchantia polymorpha* L., an emerging model for plant biology. *Plant & cell physiology*, 49(7), 1084–1091.

**Ishizaki, K., Nonomura, M., Kato, H., Yamato, K. T., & Kohchi, T.** (2012). Visualization of auxin-mediated transcriptional activation using a common auxin-responsive reporter system in the liverwort *Marchantia polymorpha*. *Journal of plant research*, 125(5), 643-651.

**Ishizaki, K., Nishihama, R., Ueda, M., Inoue, K., Ishida, S., Nishimura, Y., ... & Kohchi, T.** (2015). Development of gateway binary vector series with four different selection markers for the liverwort *Marchantia polymorpha*. *PloS one*, 10(9), e0138876.

**Ishizaki, K., Nishihama, R., Yamato, K. T., & Kohchi, T.** (2016). Molecular Genetic Tools and Techniques for *Marchantia polymorpha* Research. *Plant & cell physiology*, 57(2), 262–270.

**Johnson, M. B., March, A. R., & Morsut, L.** (2017). Engineering multicellular systems: using synthetic biology to control tissue self-organization. *Current opinion in biomedical engineering*, 4, 163–173.

**Kagale, S., & Rozwadowski, K.** (2011). EAR motif-mediated transcriptional repression in plants: an underlying mechanism for epigenetic regulation of gene expression. *Epigenetics*, 6(2), 141-146.

**Kahl, L., Molloy, J., Patron, N., Matthewman, C., Haseloff, J., Grewal, D., ... & Endy, D.** (2018). Opening options for material transfer. *Nature biotechnology*, 36(10), 923-927.

**Kanigowska, P., Shen, Y., Zheng, Y., Rosser, S., & Cai, Y.** (2016). Smart DNA fabrication using sound waves: applying acoustic dispensing technologies to synthetic biology. *Journal of laboratory automation*, 21(1), 49-56

- Karig, D., Martini, K. M., Lu, T., DeLateur, N. A., Goldenfeld, N., & Weiss, R.** (2018). Stochastic Turing patterns in a synthetic bacterial population. *Proceedings of the National Academy of Sciences of the United States of America*, 115(26), 6572–6577.
- Kato, H., Ishizaki, K., Kouno, M., Shirakawa, M., Bowman, J. L., Nishihama, R., & Kohchi, T.** (2015). Auxin-mediated transcriptional system with a minimal set of components is critical for morphogenesis through the life cycle in *Marchantia polymorpha*. *PLoS genetics*, 11(5), e1005084.
- Khalil, A. S., & Collins, J. J.** (2010). Synthetic biology: applications come of age. *Nature reviews. Genetics*, 11(5), 367–379.
- Kitada, T., DiAndreth, B., Teague, B., & Weiss, R.** (2018). Programming gene and engineered-cell therapies with synthetic biology. *Science (New York, N. Y.)*, 359(6376), eaad1067.
- Klumpp, S., Zhang, Z., & Hwa, T.** (2009). Growth rate-dependent global effects on gene expression in bacteria. *Cell*, 139(7), 1366–1375.
- Knight T. F.** (2003). Idempotent vector design for standard assembly of BioBricks. Technical Report. MIT Synthetic Biology Working Group Technical Reports.
- Kosuri, S., & Church, G. M.** (2014). Large-scale de novo DNA synthesis: technologies and applications. *Nature methods*, 11(5), 499-507.
- Kubota, A., Ishizaki, K., Hosaka, M., & Kohchi, T.** (2013). Efficient Agrobacterium-mediated transformation of the liverwort *Marchantia polymorpha* using regenerating thalli. *Bioscience, biotechnology, and biochemistry*, 77(1), 167–172.
- Kurbidaeva, A., & Purugganan, M.** (2021). Insulators in plants: progress and open questions. *Genes*, 12(9), 1422.
- Kwok R.** (2010). Five hard truths for synthetic biology. *Nature*, 463(7279), 288–290.
- Lan, C., Lee, H. C., Tang, S., & Zhang, L.** (2004). A novel mode of chaperone action: heme activation of Hap1 by enhanced association of Hsp90 with the repressed Hsp70-Hap1 complex. *The Journal of biological chemistry*, 279(26), 27607–27612.
- Lienert, F., Lohmueller, J. J., Garg, A., & Silver, P. A.** (2014). Synthetic biology in mammalian cells: next generation research tools and therapeutics. *Nature reviews. Molecular cell biology*, 15(2), 95–107.
- Liu, W., & Stewart, C. N., Jr** (2015). Plant synthetic biology. *Trends in plant science*, 20(5), 309–317.

- Lloyd, A. M., Schena, M., Walbot, V., & Davis, R. W.** (1994). Epidermal cell fate determination in Arabidopsis: patterns defined by a steroid-inducible regulator. *Science*, 266(5184), 436-439.
- Ma, J., Przibilla, E., Hu, J., Bogorad, L., & Ptashne, M.** (1988). Yeast activators stimulate plant gene expression. *Nature*, 334(6183), 631–633.
- Mathur, M., Xiang, J. S., & Smolke, C. D.** (2017). Mammalian synthetic biology for studying the cell. *The Journal of cell biology*, 216(1), 73–82.
- Miller, M. W.** (1964). A technique for isolating and culturing gemmae of *Marchantia polymorpha* L. under aseptic conditions. *Bryologist*, 317-320.
- Miyamoto, T., Razavi, S., DeRose, R., & Inoue, T.** (2013). Synthesizing biomolecule-based Boolean logic gates. *ACS synthetic biology*, 2(2), 72–82.
- Moon, T. S., Lou, C., Tamsir, A., Stanton, B. C., & Voigt, C. A.** (2012). Genetic programs constructed from layered logic gates in single cells. *Nature*, 491(7423), 249–253.
- Moore, I., Samalova, M., & Kurup, S.** (2006). Transactivated and chemically inducible gene expression in plants. *The Plant Journal*, 45(4), 651-683.
- Müller, B., & Sheen, J.** (2008). Cytokinin and auxin interaction in root stem-cell specification during early embryogenesis. *Nature*, 453(7198), 1094-1097.
- Nagai, T., Iyata, K., Park, E. S., Kubota, M., Mikoshiba, K., & Miyawaki, A.** (2002). A variant of yellow fluorescent protein with fast and efficient maturation for cell-biological applications. *Nature biotechnology*, 20(1), 87–90.
- Nagaya, S., Takemura, M., & Ohyama, K.** (2011). Endogenous promoter, 5'-UTR and transcriptional terminator enhance transient gene expression in a liverwort, *Marchantia polymorpha* L. *Plant Biotechnology*, 1112260060-1112260060.
- Nakayama, N., Smith, R. S., Mandel, T., Robinson, S., Kimura, S., Boudaoud, A., & Kuhlemeier, C.** (2012). Mechanical regulation of auxin-mediated growth. *Current biology : CB*, 22(16), 1468–1476.
- Nakazato, T., Kadota, A., & Wada, M.** (1999). Photoinduction of spore germination in *Marchantia polymorpha* L. is mediated by photosynthesis. *Plant and cell physiology*, 40(10), 1014-1020.

**Nguyen, A. W., & Daugherty, P. S.** (2005). Evolutionary optimization of fluorescent proteins for intracellular FRET. *Nature biotechnology*, 23(3), 355–360.

**Nielsen, A. A., Der, B. S., Shin, J., Vaidyanathan, P., Paralanov, V., Strychalski, E. A., Ross, D., Densmore, D., & Voigt, C. A.** (2016). Genetic circuit design automation. *Science (New York, N.Y.)*, 352(6281), aac7341.

**Niklas, K. J., Wayne, R., Benítez, M., & Newman, S. A.** (2019). Polarity, planes of cell division, and the evolution of plant multicellularity. *Protoplasma*, 256(3), 585–599.

**Núñez, I. N., Matute, T. F., Del Valle, I. D., Kan, A., Choksi, A., Endy, D., Haseloff, J., Rudge, T. J., & Federici, F.** (2017). Artificial Symmetry-Breaking for Morphogenetic Engineering Bacterial Colonies. *ACS synthetic biology*, 6(2), 256–265.

**O'Hanlon ME** (1926) Germination of the spores and early stages in the development of the gametophyte of *Marchantia polymorpha*. *Bot Gaz* 82:215–222.

**Ohta, M., Matsui, K., Hiratsu, K., Shinshi, H., & Ohme-Takagi, M.** (2001). Repression domains of class II ERF transcriptional repressors share an essential motif for active repression. *The plant cell*, 13(8), 1959-1968.

**Ouwerkerk, P. B., de Kam, R. J., Hoge, H. J., & Meijer, A. H.** (2001). Glucocorticoid-inducible gene expression in rice. *Planta*, 213(3), 370-378.

**Padidam M.** (2003). Chemically regulated gene expression in plants. *Current opinion in plant biology*, 6(2), 169–177.

**Pan, T., & Coleman, J. E.** (1989). Structure and function of the Zn (II) binding site within the DNA-binding domain of the GAL4 transcription factor. *Proceedings of the National Academy of Sciences*, 86(9), 3145-3149.

**Papadakis, E. D., Nicklin, S. A., Baker, A. H., & White, S. J.** (2004). Promoters and control elements: designing expression cassettes for gene therapy. *Current gene therapy*, 4(1), 89-113.

**Patron, N. J., Orzaez, D., Marillonnet, S., Warzecha, H., Matthewman, C., Youles, M., Raitskin, O., Leveau, A., Farré, G., Rogers, C., Smith, A., Hibberd, J., Webb, A. A., Locke, J., Schornack, S., Ajioka, J., Baulcombe, D. C., Zipfel, C., Kamoun, S., Jones, J. D., ... Haseloff, J.** (2015). Standards for plant synthetic biology: a common syntax for exchange of DNA parts. *The New phytologist*, 208(1), 13–19.

**Patron, N. J.** (2016). DNA assembly for plant biology. *Current Protocols in Plant Biology*, 1(4), 604-616.

**Patron N. J.** (2020). Beyond natural: synthetic expansions of botanical form and function. *The New phytologist*, 227(2), 295–310.

**Perez, J. G., Stark, J. C., & Jewett, M. C.** (2016). Cell-Free Synthetic Biology: Engineering Beyond the Cell. *Cold Spring Harbor perspectives in biology*, 8(12), a023853.

**Pfeifer, K., Kim, K. S., Kogan, S., & Guarente, L.** (1989). Functional dissection and sequence of yeast HAP1 activator. *Cell*, 56(2), 291–301.

**Picard, D., Salser, S. J., & Yamamoto, K. R.** (1988). A movable and regulable inactivation function within the steroid binding domain of the glucocorticoid receptor. *Cell*, 54(7), 1073-1080.

**Pollak, B., Cerda, A., Delmans, M., Álamos, S., Moyano, T., West, A., ... & Haseloff, J.** (2019). Loop assembly: a simple and open system for recursive fabrication of DNA circuits. *New Phytologist*, 222(1), 628-640.

**Purnick, P. E., & Weiss, R.** (2009). The second wave of synthetic biology: from modules to systems. *Nature reviews. Molecular cell biology*, 10(6), 410–422.

**Rudge, T. J., Federici, F., Steiner, P. J., Kan, A., & Haseloff, J.** (2013). Cell polarity-driven instability generates self-organized, fractal patterning of cell layers. *ACS synthetic biology*, 2(12), 705–714.

**Rudge, T. J., Brown, J. R., Federici, F., Dalchau, N., Phillips, A., Ajioka, J. W., & Haseloff, J.** (2016). Characterization of intrinsic properties of promoters. *ACS synthetic biology*, 5(1), 89-98.

**Rusconi, S., & Yamamoto, K. R.** (1987). Functional dissection of the hormone and DNA binding activities of the glucocorticoid receptor. *The EMBO Journal*, 6(5), 1309-1315.

**Sadowski, I., Ma, J., Triezenberg, S., & Ptashne, M.** (1988). GAL4-VP16 is an unusually potent transcriptional activator. *Nature*, 335(6190), 563–564.

**Sage R. F.** (2004). The evolution of C<sub>4</sub> photosynthesis. *The New phytologist*, 161(2), 341–370.

**Saka, Y., & Smith, J. C.** (2007). A mechanism for the sharp transition of morphogen gradient interpretation in *Xenopus*. *BMC developmental biology*, 7, 47.

**Samalova, M., Brzobohaty, B., & Moore, I.** (2005). pOp6/LhGR: a stringently regulated and highly responsive dexamethasone-inducible gene expression system for tobacco. *The Plant Journal*, *41*(6), 919-935.

**Sampathkumar, A., Yan, A., Krupinski, P., & Meyerowitz, E. M.** (2014). Physical forces regulate plant development and morphogenesis. *Current biology : CB*, *24*(10), R475–R483.

**Santos-Moreno, J., & Schaerli, Y.** (2019). Using Synthetic Biology to Engineer Spatial Patterns. *Advanced biosystems*, *3*(4), e1800280.

**Sarrion-Perdigones, A., Falconi, E. E., Zandalinas, S. I., Juárez, P., Fernández-del-Carmen, A., Granell, A., & Orzaez, D.** (2011). GoldenBraid: an iterative cloning system for standardized assembly of reusable genetic modules. *PLoS one*, *6*(7), e21622.

**Sarrion-Perdigones, A., Vazquez-Vilar, M., Palací, J., Castelijns, B., Forment, J., Ziarsolo, P., Blanca, J., Granell, A., & Orzaez, D.** (2013). GoldenBraid 2.0: a comprehensive DNA assembly framework for plant synthetic biology. *Plant physiology*, *162*(3), 1618–1631.

**Sauret-Güeto, S., Frangedakis, E., Silvestri, L., Rebmann, M., Tomaselli, M., Markel, K., ... & Haseloff, J.** (2020). Systematic tools for reprogramming plant gene expression in a simple model, *Marchantia polymorpha*. *ACS Synthetic Biology*, *9*(4), 864-882.

**Schaerli, Y., Munteanu, A., Gili, M., Cotterell, J., Sharpe, J., & Isalan, M.** (2014). A unified design space of synthetic stripe-forming networks. *Nature communications*, *5*, 4905.

**Schaerli, Y., Gili, M., & Isalan, M.** (2014). A split intein T7 RNA polymerase for transcriptional AND-logic. *Nucleic acids research*, *42*(19), 12322–12328.

**Schaller, G. E., Bishopp, A., & Kieber, J. J.** (2015). The yin-yang of hormones: cytokinin and auxin interactions in plant development. *The Plant cell*, *27*(1), 44–63.

**Scholes, N. S., & Isalan, M.** (2017). A three-step framework for programming pattern formation. *Current opinion in chemical biology*, *40*, 1–7.

**Sekine, R., Shibata, T., & Ebisuya, M.** (2018). Synthetic mammalian pattern formation driven by differential diffusivity of Nodal and Lefty. *Nature communications*, *9*(1), 5456.

- Sherman, M. S., & Cohen, B. A.** (2012). Thermodynamic state ensemble models of cis-regulation. *PLoS computational biology*, *8*(3), e1002407.
- Sheth, R. U., Yim, S. S., Wu, F. L., & Wang, H. H.** (2017). Multiplex recording of cellular events over time on CRISPR biological tape. *Science (New York, N.Y.)*, *358*(6369), 1457–1461.
- Shetty, R. P., Endy, D., & Knight, T. F., Jr** (2008). Engineering BioBrick vectors from BioBrick parts. *Journal of biological engineering*, *2*, 5.
- Shipman, S. L., Nivala, J., Macklis, J. D., & Church, G. M.** (2017). CRISPR-Cas encoding of a digital movie into the genomes of a population of living bacteria. *Nature*, *547*(7663), 345–349.
- Shis, D. L., & Bennett, M. R.** (2013). Library of synthetic transcriptional AND gates built with split T7 RNA polymerase mutants. *Proceedings of the National Academy of Sciences of the United States of America*, *110*(13), 5028–5033.
- Singer, S. D., Liu, Z., & Cox, K. D.** (2012). Minimizing the unpredictability of transgene expression in plants: the role of genetic insulators. *Plant cell reports*, *31*(1), 13-25.
- Siuti, P., Yazbek, J., & Lu, T. K.** (2013). Synthetic circuits integrating logic and memory in living cells. *Nature biotechnology*, *31*(5), 448–452.
- Slomovic, S., Pardee, K., & Collins, J. J.** (2015). Synthetic biology devices for in vitro and in vivo diagnostics. *Proceedings of the National Academy of Sciences of the United States of America*, *112*(47), 14429–14435.
- Smith, W. P., Davit, Y., Osborne, J. M., Kim, W., Foster, K. R., & Pitt-Francis, J. M.** (2017). Cell morphology drives spatial patterning in microbial communities. *Proceedings of the National Academy of Sciences of the United States of America*, *114*(3), E280–E286.
- Sohka, T., Heins, R. A., Phelan, R. M., Greisler, J. M., Townsend, C. A., & Ostermeier, M.** (2009). An externally tunable bacterial band-pass filter. *Proceedings of the National Academy of Sciences of the United States of America*, *106*(25), 10135–10140.
- Somerville, C., Bauer, S., Brininstool, G., Facette, M., Hamann, T., Milne, J., Osborne, E., Paredes, A., Persson, S., Raab, T., Vorwerk, S., & Youngs, H.** (2004). Toward a systems approach to understanding plant cell walls. *Science (New York, N.Y.)*, *306*(5705), 2206–2211.

- Stanton, B. C., Nielsen, A. A., Tamsir, A., Clancy, K., Peterson, T., & Voigt, C. A.** (2014). Genomic mining of prokaryotic repressors for orthogonal logic gates. *Nature chemical biology*, 10(2), 99–105.
- Storch, M., Haines, M. C., & Baldwin, G. S.** (2020). DNA-BOT: a low-cost, automated DNA assembly platform for synthetic biology. *Synthetic Biology*, 5(1), ysaa010.
- Subach, O. M., Cranfill, P. J., Davidson, M. W., & Verkhusha, V. V.** (2011). An enhanced monomeric blue fluorescent protein with the high chemical stability of the chromophore. *PloS one*, 6(12), e28674.
- Sundaresan, V., Springer, P., Volpe, T., Haward, S., Jones, J. D., Dean, C., ... & Martienssen, R.** (1995). Patterns of gene action in plant development revealed by enhancer trap and gene trap transposable elements. *Genes & development*, 9(14), 1797-1810.
- Swarup, R., Kramer, E. M., Perry, P., Knox, K., Leyser, H. M., Haseloff, J., ... & Bennett, M. J.** (2005). Root gravitropism requires lateral root cap and epidermal cells for transport and response to a mobile auxin signal. *Nature cell biology*, 7(11), 1057-1065.
- Takenaka, M., Yamaoka, S., Hanajiri, T., Shimizu-Ueda, Y., Yamato, K. T., Fukuzawa, H., & Ohyama, K.** (2000). Direct transformation and plant regeneration of the haploid liverwort *Marchantia polymorpha* L. *Transgenic research*, 9(3), 179-185
- Tanaka, D., Ishizaki, K., Kohchi, T., & Yamato, K. T.** (2016). Cryopreservation of Gemmae from the Liverwort *Marchantia polymorpha* L. *Plant & cell physiology*, 57(2), 300–306.
- Teague, B. P., Guye, P., & Weiss, R.** (2016). Synthetic Morphogenesis. *Cold Spring Harbor perspectives in biology*, 8(9), a023929.
- Tinafar, A., Jaenes, K., & Pardee, K.** (2019). Synthetic Biology Goes Cell-Free. *BMC biology*, 17(1), 64.
- Toda, S., Blauch, L. R., Tang, S., Morsut, L., & Lim, W. A.** (2018). Programming self-organizing multicellular structures with synthetic cell-cell signaling. *Science (New York, N. Y.)*, 361(6398), 156–162.
- Toda, S., McKeithan, W. L., Hakkinen, T. J., Lopez, P., Klein, O. D., & Lim, W. A.** (2020). Engineering synthetic morphogen systems that can program multicellular patterning. *Science (New York, N. Y.)*, 370(6514), 327–331.

**Todhunter, M. E., Jee, N. Y., Hughes, A. J., Coyle, M. C., Cerchiari, A., Farlow, J., Garbe, J. C., LaBarge, M. A., Desai, T. A., & Gartner, Z. J.** (2015). Programmed synthesis of three-dimensional tissues. *Nature methods*, *12*(10), 975–981.

**Torella, J. P., Boehm, C. R., Lienert, F., Chen, J. H., Way, J. C., & Silver, P. A.** (2014). Rapid construction of insulated genetic circuits via synthetic sequence-guided isothermal assembly. *Nucleic acids research*, *42*(1), 681–689.

**Tsukaya H.** (2003). Organ shape and size: a lesson from studies of leaf morphogenesis. *Current opinion in plant biology*, *6*(1), 57–62.

**van der Walt, S., Schönberger, J. L., Nunez-Iglesias, J., Boulogne, F., Warner, J. D., Yager, N., Guillard, E., Yu, T., & scikit-image contributors** (2014). scikit-image: image processing in Python. *PeerJ*, *2*, e453.

**Vazquez-Vilar, M., Quijano-Rubio, A., Fernandez-Del-Carmen, A., Sarrion-Perdigones, A., Ochoa-Fernandez, R., Ziarsolo, P., Blanca, J., Granell, A., & Orzaez, D.** (2017). GB3.0: a platform for plant bio-design that connects functional DNA elements with associated biological data. *Nucleic acids research*, *45*(4), 2196–2209.

**Venter, M.** (2007). Synthetic promoters: genetic control through cis engineering. *Trends in plant science*, *12*(3), 118-124.

**Virtanen, P., Gommers, R., Oliphant, T. E., Haberland, M., Reddy, T., Cournapeau, D., Burovski, E., Peterson, P., Weckesser, W., Bright, J., van der Walt, S. J., Brett, M., Wilson, J., Millman, K. J., Mayorov, N., Nelson, A., Jones, E., Kern, R., Larson, E., Carey, C. J., ... SciPy 1.0 Contributors** (2020). SciPy 1.0: fundamental algorithms for scientific computing in Python. *Nature methods*, *17*(3), 261–272.

**Wang, B., Kitney, R. I., Joly, N., & Buck, M.** (2011). Engineering modular and orthogonal genetic logic gates for robust digital-like synthetic biology. *Nature communications*, *2*, 508.

**Weber, E., Engler, C., Gruetzner, R., Werner, S., & Marillonnet, S.** (2011). A modular cloning system for standardized assembly of multigene constructs. *PloS one*, *6*(2), e16765.

**Weiss, M., Frohnmayer, J. P., Benk, L. T., Haller, B., Janiesch, J. W., Heitkamp, T., Börsch, M., Lira, R. B., Dimova, R., Lipowsky, R., Bodenschatz, E., Baret, J. C., Vidakovic-Koch, T., Sundmacher, K., Platzman, I., & Spatz, J. P.** (2018). Sequential bottom-up assembly of mechanically stabilized synthetic cells by microfluidics. *Nature materials*, *17*(1), 89–96.

**West Jr, R. W., Yocum, R. R., & Ptashne, M.** (1984). *Saccharomyces cerevisiae* GAL1-GAL10 divergent promoter region: location and function of the upstream activating sequence UASG. *Molecular and cellular biology*, 4(11), 2467-2478.

**Wroblewska, L., Kitada, T., Endo, K., Siciliano, V., Stillo, B., Saito, H., & Weiss, R.** (2015). Mammalian synthetic circuits with RNA binding proteins for RNA-only delivery. *Nature biotechnology*, 33(8), 839–841.

**Wu, C., Li, X., Yuan, W., Chen, G., Kilian, A., Li, J., ... & Zhang, Q.** (2003). Development of enhancer trap lines for functional analysis of the rice genome. *The plant journal*, 35(3), 418-427.

**Xie, Z., Wroblewska, L., Prochazka, L., Weiss, R., & Benenson, Y.** (2011). Multi-input RNAi-based logic circuit for identification of specific cancer cells. *Science (New York, N.Y.)*, 333(6047), 1307–1311.

**Yang, Y., Li, R., & Qi, M.** (2000). In vivo analysis of plant promoters and transcription factors by agroinfiltration of tobacco leaves. *The Plant journal : for cell and molecular biology*, 22(6), 543–551.

**You, M., & Jaffrey, S. R.** (2015). Designing optogenetically controlled RNA for regulating biological systems. *Annals of the New York Academy of Sciences*, 1352(1), 13–19.

**Zhang, L., & Guarente, L.** (1994). Evidence that TUP1/SSN6 has a positive effect on the activity of the yeast activator HAP1. *Genetics*, 136(3), 813–817.

## Appendix I: Plasmids

All the vectors used in this thesis can also be obtained at the following link: [Part Repository](#)

**Table SI. Loop plasmids and assembly utilities**

| Name                     | Sequence  | Syntax (Donor)    | Syntax (Acceptor) | UNSEs               |
|--------------------------|---|-------------------|-------------------|---------------------|
| Lv0 - Backbone (pUPD2)   | <a href="https://benchling.com/s/seq-Uo28gYIzBP1cmALBI0hI">https://benchling.com/s/seq-Uo28gYIzBP1cmALBI0hI</a> | Does not apply    | Does not apply    | Does not apply      |
| Lv0-Backbone (pLOR-lacZ) | <a href="https://benchling.com/s/seq-2P0AZaMybsUdbcvw73AQ">https://benchling.com/s/seq-2P0AZaMybsUdbcvw73AQ</a> | Does not apply    | Does not apply    | UNS 1, UNS X        |
| LK1 - pOdd 1             | <a href="https://benchling.com/s/seq-x4hCy0BIWcLT7OobSlym">https://benchling.com/s/seq-x4hCy0BIWcLT7OobSlym</a> | Alpha and Beta    | 1 and 11          | UNS 1, UNS 2, UNS X |
| LK2 - pOdd 2             | <a href="https://benchling.com/s/seq-R2DhdClqXVkc7vNYs7n">https://benchling.com/s/seq-R2DhdClqXVkc7vNYs7n</a>   | Beta and Gamma    | 1 and 11          | UNS 2, UNS 3, UNS X |
| LK3 - pOdd 3             | <a href="https://benchling.com/s/seq-uyQJdf8AYxUyvP7zvmC4">https://benchling.com/s/seq-uyQJdf8AYxUyvP7zvmC4</a> | Gamma and Epsilon | 1 and 11          | UNS 3, UNS 4, UNS X |
| LK4 - pOdd 4             | <a href="https://benchling.com/s/seq-9HHsRzbpYvk7QkyUR6ly">https://benchling.com/s/seq-9HHsRzbpYvk7QkyUR6ly</a> | Epsilon and Omega | 1 and 11          | UNS 4, UNS 5, UNS X |
| LS1 - pEven 1            | <a href="https://benchling.com/s/seq-zqyj6KssoLTj58mVz7Dh">https://benchling.com/s/seq-zqyj6KssoLTj58mVz7Dh</a> | 1 and 4           | Alpha and Omega   | UNS 1, UNS 2, UNS X |
| LS2 - pEven 2            | <a href="https://benchling.com/s/seq-zwXG6MkqJec6h8VpZmZ6">https://benchling.com/s/seq-zwXG6MkqJec6h8VpZmZ6</a> | 4 and 6           | Alpha and Omega   | UNS 2, UNS 3, UNS X |
| LS3 - pEven 3            | <a href="https://benchling.com/s/seq-Spt1ANx6EKxwiALFgNb0">https://benchling.com/s/seq-Spt1ANx6EKxwiALFgNb0</a> | 6 and 9           | Alpha and Omega   | UNS 3, UNS 4, UNS X |
| LS4 - pEven 4            | <a href="https://benchling.com/s/seq-NYalYU2Ewu997pl0JZj0">https://benchling.com/s/seq-NYalYU2Ewu997pl0JZj0</a> | 9 and 11          | Alpha and Omega   | UNS 4, UNS 5, UNS X |
| Lv0 - pOdd_Spacer        | <a href="https://benchling.com/s/seq-kLIWCYNX1fa42GAWYZiR">https://benchling.com/s/seq-kLIWCYNX1fa42GAWYZiR</a> | 1 and 11          | Does not apply    | Does not apply      |
| Lv1 - pEven_Spacer       | <a href="https://benchling.com/s/seq-glOU2F75KsrPRQJyJFI">https://benchling.com/s/seq-glOU2F75KsrPRQJyJFI</a>   | Alpha and Omega   | Does not apply    | UNS 1, UNS 2, UNS X |
| LK1 - 200 bp spacer      | <a href="https://benchling.com/s/seq-glRbaTwOvQdNLOZnJmr9">https://benchling.com/s/seq-glRbaTwOvQdNLOZnJmr9</a> | Alpha and Beta    | Does not apply    | UNS 1, UNS 2, UNS X |
| LK2 - 200 bp spacer      | <a href="https://benchling.com/s/seq-3ofV0GuiuWViF4CV6wdD">https://benchling.com/s/seq-3ofV0GuiuWViF4CV6wdD</a> | Beta and Gamma    | Does not apply    | UNS 2, UNS 3, UNS X |

|                     |   |                   |                |                     |
|---------------------|---|-------------------|----------------|---------------------|
| LK3 - 200 bp spacer | <a href="https://benchling.com/s/seq-ZVLdxgOxQdTxAfHCiMXI">https://benchling.com/s/seq-ZVLdxgOxQdTxAfHCiMXI</a> | Gamma and Epsilon | Does not apply | UNS 3, UNS 4, UNS X |
| LK4 - 200 bp spacer | <a href="https://benchling.com/s/seq-beVa3WyoFbWAlbKClAZy">https://benchling.com/s/seq-beVa3WyoFbWAlbKClAZy</a> | Epsilon and Omega | Does not apply | UNS 4, UNS 5, UNS X |
| LS1 - 200 bp spacer | <a href="https://benchling.com/s/seq-1HErtWHqMYHxiDn8ZrCF">https://benchling.com/s/seq-1HErtWHqMYHxiDn8ZrCF</a> | 1 and 4           | Does not apply | UNS 1, UNS 2, UNS X |
| LS2 - 200 bp spacer | <a href="https://benchling.com/s/seq-wQojmIWjKH4ntBt3iGYo">https://benchling.com/s/seq-wQojmIWjKH4ntBt3iGYo</a> | 4 and 6           | Does not apply | UNS 2, UNS 3, UNS X |
| LS3 -200 bp spacer  | <a href="https://benchling.com/s/seq-38fVKXQFEfkIDFSm3KsY">https://benchling.com/s/seq-38fVKXQFEfkIDFSm3KsY</a> | 6 and 9           | Does not apply | UNS 3, UNS 4, UNS X |
| LS4 - 200 bp spacer | <a href="https://benchling.com/s/seq-l8R7quN784N1nVN2FgHp">https://benchling.com/s/seq-l8R7quN784N1nVN2FgHp</a> | 9 and 11          | Does not apply | UNS 4, UNS 5, UNS X |
| Lv0 - Spacer20A     | <a href="https://benchling.com/s/seq-ux8hmiPoeAmumXIX1aRS">https://benchling.com/s/seq-ux8hmiPoeAmumXIX1aRS</a> | 1 and 11          | Does not apply | Does not apply      |
| Lv0 - Spacer20B     | <a href="https://benchling.com/s/seq-hynB1GRe4iD0j5ux97ns">https://benchling.com/s/seq-hynB1GRe4iD0j5ux97ns</a> | 1 and 11          | Does not apply | Does not apply      |
| Lv0 - Spacer40A     | <a href="https://benchling.com/s/seq-Qw4Jn7ZcvlC3fmu296E7">https://benchling.com/s/seq-Qw4Jn7ZcvlC3fmu296E7</a> | 1 and 11          | Does not apply | Does not apply      |
| Lv0 - Spacer40B     | <a href="https://benchling.com/s/seq-n3RevKvPPVV0zaA3x1Uz">https://benchling.com/s/seq-n3RevKvPPVV0zaA3x1Uz</a> | 1 and 11          | Does not apply | Does not apply      |
| LK1 - Spacer20A     | <a href="https://benchling.com/s/seq-dH4he4YJ4gOyD5JndLe2">https://benchling.com/s/seq-dH4he4YJ4gOyD5JndLe2</a> | Alpha and Beta    | Does not apply | UNS 1, UNS 2, UNS X |
| LK2 - Spacer20A     | <a href="https://benchling.com/s/seq-nmxtkascalXbyh2Qzf6V">https://benchling.com/s/seq-nmxtkascalXbyh2Qzf6V</a> | Beta and Gamma    | Does not apply | UNS 2, UNS 3, UNS X |
| LK3 - Spacer20A     | <a href="https://benchling.com/s/seq-LHM1Si2ke3fS43qa6jhE">https://benchling.com/s/seq-LHM1Si2ke3fS43qa6jhE</a> | Gamma and Epsilon | Does not apply | UNS 3, UNS 4, UNS X |
| LK4 - Spacer20A     | <a href="https://benchling.com/s/seq-B7a4AKQNV6mVIqr2URGj">https://benchling.com/s/seq-B7a4AKQNV6mVIqr2URGj</a> | Epsilon and Omega | Does not apply | UNS 4, UNS 5, UNS X |
| LK1 - Spacer20B     | <a href="https://benchling.com/s/seq-OPZqcuw3bUMXxcxqrG8f">https://benchling.com/s/seq-OPZqcuw3bUMXxcxqrG8f</a> | Alpha and Beta    | Does not apply | UNS 1, UNS 2, UNS X |
| LK2 - Spacer20B     | <a href="https://benchling.com/s/seq-p8lbjPHhbczBEvrVb00g">https://benchling.com/s/seq-p8lbjPHhbczBEvrVb00g</a> | Beta and Gamma    | Does not apply | UNS 2, UNS 3, UNS X |
| LK3 - Spacer20B     | <a href="https://benchling.com/s/seq-Utv5mPcZB7kgGkPKdkqw">https://benchling.com/s/seq-Utv5mPcZB7kgGkPKdkqw</a> | Gamma and Epsilon | Does not apply | UNS 3, UNS 4, UNS X |
| LK4 - Spacer20B     | <a href="https://benchling.com/s/seq-cMxDgdnnz9qTkfs0V11w">https://benchling.com/s/seq-cMxDgdnnz9qTkfs0V11w</a> | Epsilon and Omega | Does not apply | UNS 4, UNS 5, UNS X |
| LK2 - Spacer40A     | <a href="https://benchling.com/s/seq-m1tC6i2abYCcaU2DRhOx">https://benchling.com/s/seq-m1tC6i2abYCcaU2DRhOx</a> | Beta and Gamma    | Does not apply | UNS 2, UNS 3, UNS X |

|                           |   |                   |                |                     |
|---------------------------|---|-------------------|----------------|---------------------|
| LK4 - Spacer40A           | <a href="https://benchling.com/s/seq-oREyjiOuYdOcUx90LjTb">https://benchling.com/s/seq-oREyjiOuYdOcUx90LjTb</a> | Epsilon and Omega | Does not apply | UNS 4, UNS 5, UNS X |
| LK2 - Spacer40B           | <a href="https://benchling.com/s/seq-Ge4RIUGkVEygp3so6yY7">https://benchling.com/s/seq-Ge4RIUGkVEygp3so6yY7</a> | Beta and Gamma    | Does not apply | UNS 2, UNS 3, UNS X |
| LK4 - Spacer40B           | <a href="https://benchling.com/s/seq-W6roqlsGvRfgMWYPamP0">https://benchling.com/s/seq-W6roqlsGvRfgMWYPamP0</a> | Epsilon and Omega | Does not apply | UNS 4, UNS 5, UNS X |
| LK1_Cassette Hygro        | <a href="https://benchling.com/s/seq-1Y7nMWdbRMDccBiXkDR6">https://benchling.com/s/seq-1Y7nMWdbRMDccBiXkDR6</a> | Alpha and Beta    | Does not apply | UNS 1, UNS 2, UNS X |
| LK2_Cassette Hygro        | <a href="https://benchling.com/s/seq-VT84lxJnFOFaDrBZ5nnz">https://benchling.com/s/seq-VT84lxJnFOFaDrBZ5nnz</a> | Beta and Gamma    | Does not apply | UNS 2, UNS 3, UNS X |
| LK3_Cassette Hygro        | <a href="https://benchling.com/s/seq-7yIWbVp9Jd8Dm1D5HFkW">https://benchling.com/s/seq-7yIWbVp9Jd8Dm1D5HFkW</a> | Gamma and Epsilon | Does not apply | UNS 3, UNS 4, UNS X |
| LK4_Cassette Hygro        | <a href="https://benchling.com/s/seq-69zpUThZbSNkcAoVldN0">https://benchling.com/s/seq-69zpUThZbSNkcAoVldN0</a> | Epsilon and Omega | Does not apply | UNS 4, UNS 5, UNS X |
| LK3 - 35S*2 - Higo - NosT | <a href="https://benchling.com/s/seq-baPSGMFv19Z1dyW4QcF1">https://benchling.com/s/seq-baPSGMFv19Z1dyW4QcF1</a> | Gamma and Epsilon | Does not apply | UNS 3, UNS 4, UNS X |
| LK3 - pNoS - Hygro - NosT | <a href="https://benchling.com/s/seq-TiJBGK9tO3r6QUE7qcD">https://benchling.com/s/seq-TiJBGK9tO3r6QUE7qcD</a>   | Gamma and Epsilon | Does not apply | UNS 3, UNS 4, UNS X |
| LK4 - pNoS - Hygro - NosT | <a href="https://benchling.com/s/seq-kiGU5E3q51FFppLdjub2">https://benchling.com/s/seq-kiGU5E3q51FFppLdjub2</a> | Epsilon and Omega | Does not apply | UNS 4, UNS 5, UNS X |
| LK3 - Cassette Bar        | <a href="https://benchling.com/s/seq-DSprvJax9AatU51t3rnl">https://benchling.com/s/seq-DSprvJax9AatU51t3rnl</a> | Gamma and Epsilon | Does not apply | UNS 3, UNS 4, UNS X |
| LK3 - pNos - Kan - NosT   | <a href="https://benchling.com/s/seq-M3UO1Kg6bO5kuEIZt7Or">https://benchling.com/s/seq-M3UO1Kg6bO5kuEIZt7Or</a> | Gamma and Epsilon | Does not apply | UNS 3, UNS 4, UNS X |
| LK4 - pNos - Kan - NosT   | <a href="https://benchling.com/s/seq-gkvSKBUYehwpwQAYkwh">https://benchling.com/s/seq-gkvSKBUYehwpwQAYkwh</a>   | Epsilon and Omega | Does not apply | UNS 4, UNS 5, UNS X |
| LK4 - Cassette Kan        | <a href="https://benchling.com/s/seq-ET4kbVcfyb7DI8I3AIL9">https://benchling.com/s/seq-ET4kbVcfyb7DI8I3AIL9</a> | Epsilon and Omega | Does not apply | UNS 4, UNS 5, UNS X |

**Table SII. L0 DNA Parts**

| <b>Name</b>               | <b>Description</b>                                       | <b>Sequence</b>   | <b>Syntax</b> | <b>Source, Reference</b>               |
|---------------------------|--|---|---------------|--|
| Lv0_mTagBFP2 (No stop)    | mTagBFP2 without stop codon                              | <a href="https://benchling.com/s/VoKPh0cz">https://benchling.com/s/VoKPh0cz</a>                                 | 6 and 8       | Synthesis, Subach et al., 2011         |
| Lv0_mTurquoise2 (No stop) | mTurquoise2 without stop codon                           | <a href="https://benchling.com/s/rtQRaQ71">https://benchling.com/s/rtQRaQ71</a>                                 | 6 and 8       | Synthesis, Goedhart et al., 2012       |
| Lv0_Venus (No stop)       | Venus without stop codon                                 | <a href="https://benchling.com/s/seq-g3bmydKrpPikMurH53xJ">https://benchling.com/s/seq-g3bmydKrpPikMurH53xJ</a> | 6 and 8       | Synthesis, Nagai et al., 2002          |
| Lv0 - Hemme – Ypet        | YPet fused to Hemme<br>(Chloroplast localization)        | <a href="https://benchling.com/s/JN9DLtzB">https://benchling.com/s/JN9DLtzB</a>                                 | 6 and 9       | Synthesis, Nguyen and Daugherty, 2005  |
| Lv0_mRuby3                | mRuby3   | <a href="https://benchling.com/s/HPhF7XZD">https://benchling.com/s/HPhF7XZD</a>                                 | 6 and 9       | Synthesis, Bajar et al., 2016          |
| Lv0_N7 C-Tag              | N7 C-Tag (Nuclear localization)                          | <a href="https://benchling.com/s/jzvcPp3r">https://benchling.com/s/jzvcPp3r</a>                                 | 8 and 9       | Synthesis, Cutler et al., 2000         |
| Lv0_Lti6b C-Tag           | Lti6b C-Tag (Membrane localization)                      | <a href="https://benchling.com/s/ixVdAgdK">https://benchling.com/s/ixVdAgdK</a>                                 | 8 and 9       | Synthesis, Cutler et al., 2000         |
| Lv0_Hemme N-Tag           | Hemme N-Tag<br>(Chloroplast localization)                | <a href="https://benchling.com/s/seq-GgCqUIqDQfv491Dghu3H">https://benchling.com/s/seq-GgCqUIqDQfv491Dghu3H</a> | 5 and 6       | Synthesis, Boehm, unpublished results  |
| Lv0_p35S                  | CaMV 35S Promoter  | <a href="https://benchling.com/s/PWbznj3t">https://benchling.com/s/PWbznj3t</a>                                 | 1 and 6       | Synthesis, Boisnard-Logig et al., 2001 |
| Lv0 - HT2B - mRFP1        | mRFP1 fused to histone H2B<br>(Nuclear localization)     | <a href="https://benchling.com/s/xHNeIh5t">https://benchling.com/s/xHNeIh5t</a>                                 | 6 and 9       | Synthesis, Campbell et al., 2002       |
| Lv0 - Hemme - mTurquoise2 | mTurquoise2 fused to Hemme<br>(Chloroplast localization) | <a href="https://benchling.com/s/02Et5Vv1">https://benchling.com/s/02Et5Vv1</a>                                 | 6 and 9       | Synthesis, Goedhart et al., 2012       |
| Lv0 - mTagBFP2-N7         | mTagBFP2 fused to N7<br>(Nuclear localization)           | <a href="https://benchling.com/s/7wunHfYT">https://benchling.com/s/7wunHfYT</a>                                 | 6 and 9       | Synthesis, Subach et al., 2011         |
| Lv0_mTagBFP2 - Lti6b      | mTagBFP2 fused to Lti6b<br>(Membrane localization)       | <a href="https://benchling.com/s/l5NA7g7z">https://benchling.com/s/l5NA7g7z</a>                                 | 6 and 9       | Synthesis, Subach et al., 2011         |

|                            |   |   |          |                                   |
|----------------------------|---|---|----------|-----------------------------------|
| Lv0_TagRFP-T-Lti6b(C.O)    | TagRFP-T fused to Lti6b codon optimized (Membrane localization) | <a href="https://benchling.com/s/Rsv6QfPp">https://benchling.com/s/Rsv6QfPp</a>                                 | 6 and 9  | Synthesis, Shaner et al., 2008    |
| Lv0_mRuby3 (No stop)       | mRuby3 without stop codon                                       | <a href="https://benchling.com/s/seq-9ozCioG0bmXzTKVFjEai">https://benchling.com/s/seq-9ozCioG0bmXzTKVFjEai</a> | 6 and 8  | Synthesis, Bajar et al., 2016     |
| Lv0_Venus N-Tag            | Venus N-Tag   | <a href="https://benchling.com/s/seq-8gfFyeFN1hNxoicMW3bl">https://benchling.com/s/seq-8gfFyeFN1hNxoicMW3bl</a> | 5 and 6  | Synthesis, Nagai et al., 2002     |
| Lv0_Venus                  | Venus   | <a href="https://benchling.com/s/seq-sX10fHtXw3Kc0F4UJggb">https://benchling.com/s/seq-sX10fHtXw3Kc0F4UJggb</a> | 6 and 9  | Synthesis, Nagai et al., 2002     |
| Lv0_mTurquoise2            | mTurquoise2   | <a href="https://benchling.com/s/seq-1h0Y5DvIL7tuXAi1LZp5">https://benchling.com/s/seq-1h0Y5DvIL7tuXAi1LZp5</a> | 6 and 9  | Synthesis, Goedhart et al., 2012  |
| Lv0_deGFP (6 and 7B)       | deGFP   | <a href="https://benchling.com/s/seq-0mQrQ9VJLy1KcdBSY0FS">https://benchling.com/s/seq-0mQrQ9VJLy1KcdBSY0FS</a> | 6 and 7B | Synthesis, Hanson et al., 2002    |
| Lv0_mBeRFP (6 and 7B)      | mBeRFP  | <a href="https://benchling.com/s/seq-hy1wOSkYQWEjclxSTpj">https://benchling.com/s/seq-hy1wOSkYQWEjclxSTpj</a>   | 6 and 7B | Synthesis, Yang et al., 2013      |
| Lv0_CyOFFP1 (6 and 7B)     | CyOFFP1   | <a href="https://benchling.com/s/seq-r9WQK5rh5cgBaWwkHutW">https://benchling.com/s/seq-r9WQK5rh5cgBaWwkHutW</a> | 6 and 7B | Synthesis, Chu et al., 2016       |
| Lv0_Citrine (No stop)      | Citrine without stop codon                                      | <a href="https://benchling.com/s/seq-w9whDquKBehjwYSEj5uQ">https://benchling.com/s/seq-w9whDquKBehjwYSEj5uQ</a> | 6 and 8  | Synthesis, Griesbeck et al., 2001 |
| Lv0_Citrine                | Citrine   | <a href="https://benchling.com/s/seq-ILicwLBrSPnSKCPpm0Ba">https://benchling.com/s/seq-ILicwLBrSPnSKCPpm0Ba</a> | 6 and 9  | doi: 10.1074/jbc.m102815200       |
| Lv0_Venus (7 and 8)        | Venus (7 and 8 Syntax)  | <a href="https://benchling.com/s/seq-TbjN4I3qW7dSODs67tua">https://benchling.com/s/seq-TbjN4I3qW7dSODs67tua</a> | 7B and 8 | Synthesis, Nagai et al., 2002     |
| Lv0_mTagBFP2 - Lti6b (C.O) | mTagBFP2 fused to Lti6b codon optimized (Membrane localization) | <a href="https://benchling.com/s/seq-zY6MACrSt6WVgKIzHI35">https://benchling.com/s/seq-zY6MACrSt6WVgKIzHI35</a> | 6 and 9  | Synthesis, Subach et al., 2011    |
| Lv0_pMpEF1a                | MpEF1a Promoter   | <a href="https://benchling.com/s/seq-cYsQWrM3C2DXeRL0RsR7">https://benchling.com/s/seq-cYsQWrM3C2DXeRL0RsR7</a> | 1 and 6  | gDNA, Nagaya et al., 2011         |
| Lv0_pMpEF1a (1 and 5)      | MpEF1a Promoter (1 and 5 Syntax)                                | <a href="https://benchling.com/s/seq-Kw7uf6r0gFxaJObAH8Zx">https://benchling.com/s/seq-Kw7uf6r0gFxaJObAH8Zx</a> | 1 and 5  | gDNA, Nagaya et al., 2011         |
| Lv0_pUbp10                 | Ubp10 Promoter  | <a href="https://benchling.com/s/seq-Va3eltX9NgWFWFilyGAq">https://benchling.com/s/seq-Va3eltX9NgWFWFilyGAq</a> | 1 and 6  | Synthesis, (Grefen et al, 2010)   |
| Lv0_pUbp10 (1 and 5)       | Ubp10 Promoter (1 and 5 Syntax)                                 | <a href="https://benchling.com/s/seq-8XU8KGdWD2LZzg5HoEUA">https://benchling.com/s/seq-8XU8KGdWD2LZzg5HoEUA</a> | 1 and 5  | Synthesis, (Grefen et al, 2010)   |

|   |  |   |           |   |
|---|--|---|-----------|---|
| Lv0_Double CaMV 35S Enhanced                | Double CaMV 35S enhanced                                       | <a href="https://benchling.com/s/seq-FQlc0U1KAbI5OrEPXIKh">https://benchling.com/s/seq-FQlc0U1KAbI5OrEPXIKh</a> | 1 and 6   | Plasmid, Ishizaki et al., 2015              |
| Lv0_pUASGAL4x5-min35S                       | 5 UASGAL4 + min35S Promoter                                    | <a href="https://benchling.com/s/seq-xRVMCIKmtUXYsK038b84">https://benchling.com/s/seq-xRVMCIKmtUXYsK038b84</a> | 1 and 6   | Synthesis, This work                        |
| Lv0_pUASHAP1x5-min35S                       | 5 UASHAP1 + min35S Promoter                                    | <a href="https://benchling.com/s/seq-gTCXu2d7IASYmulPsNkA">https://benchling.com/s/seq-gTCXu2d7IASYmulPsNkA</a> | 1 and 6   | Synthesis, This work                        |
| Lv0_p35S (1 and 5)                          | p35S (1 and 5 Syntax)  | <a href="https://benchling.com/s/seq-7WtGHVgSTLPGEdc4KCq6">https://benchling.com/s/seq-7WtGHVgSTLPGEdc4KCq6</a> | 1 and 5   | Synthesis, Boissard-Logig et al., 2001      |
| Lv0_35S_T                                   | 35S Terminator   | <a href="https://benchling.com/s/cFSKejNw">https://benchling.com/s/cFSKejNw</a>                                 | 9 and 11  | Plasmid, Pietrzark et al., 1986             |
| Lv0_Ubq3_T                                  | Polyubiquitin3 Terminator                                      | <a href="https://benchling.com/s/47noTosM">https://benchling.com/s/47noTosM</a>                                 | 9 and 11  | Plasmid, Callis et al., 1995                |
| Lv0_NosT (pICH41421)                        | 3'UTR, Polyadenylation signal/terminator, nos (A. tumefaciens) | <a href="https://benchling.com/s/Q8C5809O">https://benchling.com/s/Q8C5809O</a>                                 | 9 and 11  | MoClo kit, Engler et al., 2014              |
| Lv0_Hsp18.2_T (GB0035)                      | Hsp18.2 Terminator   | <a href="https://benchling.com/s/xntuz66Q">https://benchling.com/s/xntuz66Q</a>                                 | 9 and 11  | GB 2.0 Kit, Sarrion-Perdigones et al., 2013 |
| Lv0_Nos_T + 35S_T                           | Nos Terminator + 35S Terminator                                | <a href="https://benchling.com/s/E4naFnyM">https://benchling.com/s/E4naFnyM</a>                                 | 9 and 11  | PCR, This work                              |
| Lv0_Nos_T + 35S_T (Bacteria CDS Compatible) | Nos Terminator + 35S Terminator (Bacteria CDS Compatible)      | <a href="https://benchling.com/s/seq-E5FfSD9ol8Z6ZPZvRASI">https://benchling.com/s/seq-E5FfSD9ol8Z6ZPZvRASI</a> | 7B and 11 | Plasmid, This work                          |
| Lv0_35S_T (Bacteria CDS Compatible)         | 35S Terminator (Bacteria CDS Compatible)                       | <a href="https://benchling.com/s/seq-Cp2nVs0AQLaDHQWsWH8A">https://benchling.com/s/seq-Cp2nVs0AQLaDHQWsWH8A</a> | 7B and 11 | Plasmid, Pietrzark et al., 1986             |
| Lv0_Ubq3_T (Bacteria CDS Compatible)        | Ubiquitin3 Terminator (Bacteria CDS Compatible)                | <a href="https://benchling.com/s/seq-sbjxhz2toqkBtNtKRf2E">https://benchling.com/s/seq-sbjxhz2toqkBtNtKRf2E</a> | 7B and 11 | Plasmid, Callis et al., 1995                |
| Lv0_Hsp18.2_T (Bacteria CDS Compatible)     | Hsp18.2 Terminator (Bacteria CDS Compatible)                   | <a href="https://benchling.com/s/seq-iEyzQ1gHX0mpt8QVAjm0">https://benchling.com/s/seq-iEyzQ1gHX0mpt8QVAjm0</a> | 7B and 11 | Plasmid, Sarrion-Perdigones et al., 2013    |

|                             |  |   |          |                                  |
|-----------------------------|--|---|----------|----------------------------------|
| Lv0_pICSL80036 (617)        | Coding sequence for hygromycin phosphotransferase II with an intron (Escherichia coli) | <a href="https://benchling.com/s/7m9cHrpa">https://benchling.com/s/7m9cHrpa</a>                                 | 6 and 9  | Lawrenson et al., 2015           |
| Lv0_pICSL80037 (618)        | Coding sequence for neomycin phosphotransferase II (Escherichia coli)                  | <a href="https://benchling.com/s/fan1FiJw">https://benchling.com/s/fan1FiJw</a>                                 | 6 and 9  | Lawrenson et al., 2015           |
| Lv0_MpHygromycin Cassette   | MpHygromycin Cassette  | <a href="https://benchling.com/s/seq-VXePWcVxAacflF33lr5D">https://benchling.com/s/seq-VXePWcVxAacflF33lr5D</a> | 1 and 11 | Plasmid, Ishizaki et al., 2015   |
| Lv0_MpGUS                   | Beta-glucuronidase (GUS) gene  | <a href="https://benchling.com/s/seq-U3UHaCvVzWgCWgY6WDlp">https://benchling.com/s/seq-U3UHaCvVzWgCWgY6WDlp</a> | 6 and 9  | Plasmid, Ishizaki et al., 2015   |
| Lv0_SYNZIP17                | SYNZIP17 Heterospecific Coiled-Coil Interaction Domain                                 | <a href="https://benchling.com/s/seq-01Q711hqzLXNY0v1VsMo">https://benchling.com/s/seq-01Q711hqzLXNY0v1VsMo</a> | 7 and 9  | Synthesis, Thompson et al., 2012 |
| Lv0_SYNZIP18                | SYNZIP18 Heterospecific Coiled-Coil Interaction Domain                                 | <a href="https://benchling.com/s/seq-Wu4ullwe1Av9ZuHePjPY">https://benchling.com/s/seq-Wu4ullwe1Av9ZuHePjPY</a> | 6 and 7B | Synthesis, Thompson et al., 2012 |
| Lv0_GAL4_BD                 | Gal4 Binding Domain (~438pb)   | <a href="https://benchling.com/s/seq-prMpmpZx5NMxWtecj8S4">https://benchling.com/s/seq-prMpmpZx5NMxWtecj8S4</a> | 6 and 7B | Synthesis, Fields and Song, 1989 |
| Lv0_GAL4 (short version BD) | Short Version of binding domain of Gal4 (74 aa only)                                   | <a href="https://benchling.com/s/seq-ibQsCSqO4OiWV4aF0WRt">https://benchling.com/s/seq-ibQsCSqO4OiWV4aF0WRt</a> | 6 and 7B | Synthesis, Fields and Song, 1989 |
| Lv0_HAP1_BD                 | Hap1 Binding Domain  | <a href="https://benchling.com/s/seq-stVXFjn9dOCetmFpwH97">https://benchling.com/s/seq-stVXFjn9dOCetmFpwH97</a> | 6 and 7B | Synthesis, Pfeifer et al., 1989  |
| Lv0_SprR_BD                 | SprR Binding Domain  | <a href="https://benchling.com/s/seq-7OedcuKuQW5nEHeqM0II">https://benchling.com/s/seq-7OedcuKuQW5nEHeqM0II</a> | 6 and 7B | Synthesis, Stanton et al., 2013  |
| Lv0_TetR_BD                 | TetR Binding Domain  | <a href="https://benchling.com/s/seq-pq7kH6ZCN9ZTxTRwj8s5">https://benchling.com/s/seq-pq7kH6ZCN9ZTxTRwj8s5</a> | 6 and 7B | Synthesis, Stanton et al., 2013  |
| Lv0_VP16_AD                 | VP16 Activation Domain   | <a href="https://benchling.com/s/seq-u22RgvezPmPPq2FjU4nz">https://benchling.com/s/seq-u22RgvezPmPPq2FjU4nz</a> | 7B and 9 | Synthesis, Sadowski et al., 1988 |
| Lv0_VP16_AD (No stop)       | VP16 Activation Domain without stop codon  | <a href="https://benchling.com/s/seq-5RKc1mhse15iFbo4LNEj">https://benchling.com/s/seq-5RKc1mhse15iFbo4LNEj</a> | 7B and 8 | Synthesis, Sadowski et al., 1988 |
| Lv0_EAR_RD (No stop)        | EAR Repression Domain without stop codon   | <a href="https://benchling.com/s/seq-sPPtt73gzZG3rIQd4KIK">https://benchling.com/s/seq-sPPtt73gzZG3rIQd4KIK</a> | 7B and 8 | Synthesis, Hiratsu et al., 2003  |

|                              |   |   |               |   |
|------------------------------|---|---|---------------|---|
| Lv0_EAR_RD                   | EAR Repression Domain   | <a href="https://benchling.com/s/seq-eYbUw5qe5vN6mZxJZ8w8">https://benchling.com/s/seq-eYbUw5qe5vN6mZxJZ8w8</a> | 7B and 9      | Synthesis, Hiratsu et al., 2003                     |
| Lv0-NLS_Nucleoplasmina C-Tag | NLS_Nucleoplasmina C-Tag (Nuclear localization)               | <a href="https://benchling.com/s/seq-UyVSBqrXx7keKC6jXKXk">https://benchling.com/s/seq-UyVSBqrXx7keKC6jXKXk</a> | 8 and 9       | Synthesis, Stanton et al., 2013                     |
| Lv0_GR                       | Glucocorticoid Receptor (Dexamethasone induction)             | <a href="https://benchling.com/s/seq-gM8wtdVd37R3GLKL2PWy">https://benchling.com/s/seq-gM8wtdVd37R3GLKL2PWy</a> | 8 and 9       | Synthesis, Picard et al., 1988                      |
| Lv0_GR (No NLS)              | Glucocorticoid Receptor (Dexamethasone induction) without NLS | <a href="https://benchling.com/s/seq-2Otqh8GDJyi1gJQsOWAN">https://benchling.com/s/seq-2Otqh8GDJyi1gJQsOWAN</a> | 8 and 9       | Synthesis, Picard et al., 1988                      |
| Lv0_SprR_BD (No NLS)         | SprR Binding Domain without NLS                               | <a href="https://benchling.com/s/seq-yMKIVqdX7oOIFQiucoDW">https://benchling.com/s/seq-yMKIVqdX7oOIFQiucoDW</a> | 6 and 7B      | Synthesis, Stanton et al., 2013                     |
| Lv0_TetR_BD (No NLS)         | TetR Binding Domain without NLS                               | <a href="https://benchling.com/s/seq-Eb8t9S7syoDaPePhnRNJ">https://benchling.com/s/seq-Eb8t9S7syoDaPePhnRNJ</a> | 6 and 7B      | Synthesis, Stanton et al., 2013                     |
| Lv0-UASGal4*2_BOX            | UAS Gal4 (2 Consecutive Boxes)                                | <a href="https://benchling.com/s/seq-ZxrF71aApZaJ5jh7Lc">https://benchling.com/s/seq-ZxrF71aApZaJ5jh7Lc</a>     | 1 and 11      | Synthesis, Guarente et al., 1982                    |
| Lv0-UASGal4*1_BOX            | UAS Gal4 (1 Box)  | <a href="https://benchling.com/s/seq-4IU7ZWjFh0LCyPZZAG8P">https://benchling.com/s/seq-4IU7ZWjFh0LCyPZZAG8P</a> | 1 and 11      | Synthesis, Guarente et al., 1982                    |
| Lv0-UASHap1*2_BOX            | UAS Hap1 (2 Consecutive Boxes)                                | <a href="https://benchling.com/s/seq-e7V8ERh5Pe67UUfbFz9f">https://benchling.com/s/seq-e7V8ERh5Pe67UUfbFz9f</a> | 1 and 11      | Synthesis, Zhang and Guarente, 1994                 |
| Lv0-UASHap1*1_BOX            | UAS Hap1 (1 Box)  | <a href="https://benchling.com/s/seq-FGq0tITKAxnHyQs0WPbY">https://benchling.com/s/seq-FGq0tITKAxnHyQs0WPbY</a> | 1 and 11      | Synthesis, Zhang and Guarente, 1994                 |
| Lv0-LAF_CKOper_BOX (Split 1) | Cytokinin Operator (Split-Part 1/2)                           | <a href="https://benchling.com/s/seq-mnaN25fE2U0iGnvhVoFK">https://benchling.com/s/seq-mnaN25fE2U0iGnvhVoFK</a> | 1 and Custom  | Synthesis, Muller and Sheen, 2008                   |
| Lv0-LAF_CKOper_BOX (Split 2) | Cytokinin Operator (Split-Part 2/2)                           | <a href="https://benchling.com/s/seq-Q0lllCIVACRY4AEAB07B">https://benchling.com/s/seq-Q0lllCIVACRY4AEAB07B</a> | Custom and 11 | Synthesis, Muller and Sheen, 2008                   |
| Lv0-pMIN35S                  | pMin35S   | <a href="https://benchling.com/s/seq-VvHnlixoCKvxCzcXd9Gp">https://benchling.com/s/seq-VvHnlixoCKvxCzcXd9Gp</a> | 1 and 11      | Plasmid, Federici and Haseloff, unpublished results |
| Lv0-TetROp*2_BOX             | TetR Operator (2 Consecutive Boxes)                           | <a href="https://benchling.com/s/seq-pvgaDFc1IZgBPRBP2slS">https://benchling.com/s/seq-pvgaDFc1IZgBPRBP2slS</a> | 1 and 11      | PCR, Stanton et al., 2013                           |

|                      |  |   |          |                                  |
|----------------------|--|---|----------|----------------------------------|
| Lv0-TetROp*1_BOX     | TetR Operator (1 Box)                                | <a href="https://benchling.com/s/seq-UVjklrsv4b78q7qfjmBq">https://benchling.com/s/seq-UVjklrsv4b78q7qfjmBq</a> | 1 and 11 | PCR, Stanton et al., 2013        |
| Lv0-SprROp*2_BOX     | SprR Operator<br>(2 Consecutive Boxes)               | <a href="https://benchling.com/s/seq-3K1g852Gb74klXmJ3VLh">https://benchling.com/s/seq-3K1g852Gb74klXmJ3VLh</a> | 1 and 11 | PCR, Stanton et al., 2013        |
| Lv0-SprROp*1_BOX     | SprR Operator (1 Box)                                | <a href="https://benchling.com/s/seq-dVe3ykUgCcoKcPYeQYeq">https://benchling.com/s/seq-dVe3ykUgCcoKcPYeQYeq</a> | 1 and 11 | PCR, Stanton et al., 2013        |
| Lv0_AuxREs_BOXS      | Auxin Response Elements from GH3<br>soybean promoter | <a href="https://benchling.com/s/seq-teyDoqqcvD72FEq37kmA">https://benchling.com/s/seq-teyDoqqcvD72FEq37kmA</a> | 1 and 11 | Synthesis, Ishisaki et al., 2012 |
| Lv0_D1b+D1c Prom BOX | ABA response elements from<br>MpDHN1 promoter        | <a href="https://benchling.com/s/seq-iVb2iGrZ85FItNBecHPn">https://benchling.com/s/seq-iVb2iGrZ85FItNBecHPn</a> | 1 and 11 | Synthesis, Ghosh et al., 2016    |
| Lv0_RY+ABRE BOXS     | ABA response elements from Em<br>wheat promoter      | <a href="https://benchling.com/s/seq-zmS4mIOWXpOs9FWO9m0H">https://benchling.com/s/seq-zmS4mIOWXpOs9FWO9m0H</a> | 1 and 11 | Synthesis, Ghosh et al., 2016    |
| Lv0 - pOdd_Spacer    | Lv0 200 bp spacer for Loop<br>Assembly               | <a href="https://benchling.com/s/seq-kLIWCYNX1fA42GAWYZiR">https://benchling.com/s/seq-kLIWCYNX1fA42GAWYZiR</a> | 1 and 11 | Synthesis, This work             |
| Lv0 - Spacer20A      | Lv0 20A bp spacer for Loop<br>Assembly               | <a href="https://benchling.com/s/seq-ux8hmiPoeAmumXIX1aRS">https://benchling.com/s/seq-ux8hmiPoeAmumXIX1aRS</a> | 1 and 11 | Synthesis, This work             |
| Lv0 - Spacer20B      | Lv0 20B bp spacer for Loop<br>Assembly               | <a href="https://benchling.com/s/seq-hynB1GRe4iD0j5ux97ns">https://benchling.com/s/seq-hynB1GRe4iD0j5ux97ns</a> | 1 and 11 | Synthesis, This work             |
| Lv0 - Spacer40B      | Lv0 40A bp spacer for Loop<br>Assembly               | <a href="https://benchling.com/s/seq-Qw4Jn7ZcvcI3fmu296E7">https://benchling.com/s/seq-Qw4Jn7ZcvcI3fmu296E7</a> | 1 and 11 | Synthesis, This work             |
| Lv0 - Spacer40A      | Lv0 40B bp spacer for Loop<br>Assembly               | <a href="https://benchling.com/s/seq-n3RevKvPPVV0zaA3x1Uz">https://benchling.com/s/seq-n3RevKvPPVV0zaA3x1Uz</a> | 1 and 11 | Synthesis, This work             |
| Lv0_GAL4-VP16        | GAL4 (~429 bp BD) + VP16 AD                          | <a href="https://benchling.com/s/seq-hKMSNcQGeQn14O6KV3dQ">https://benchling.com/s/seq-hKMSNcQGeQn14O6KV3dQ</a> | 6 and 9  | Synthesis, This work             |
| Lv0_HAP1-VP16-GR     | HAP1 (BD) + VP16 (AD) + GR (Dex<br>Induction)        | <a href="https://benchling.com/s/seq-AXM0e4ZZKWvD8LfxwHes">https://benchling.com/s/seq-AXM0e4ZZKWvD8LfxwHes</a> | 6 and 9  | Synthesis, This work             |
| Lv0_HAP1-VP16        | HAP1 (BD) + VP16 (AD)                                | <a href="https://benchling.com/s/seq-OT8VcNq7MGZBpuABhpZH">https://benchling.com/s/seq-OT8VcNq7MGZBpuABhpZH</a> | 6 and 9  | Synthesis, This work             |

**Table SIII.** Odd assemblies

| <b>Name</b>                         | <b>Sequence</b>   | <b>Syntax (Donor)</b> |
|-------------------------------------|---|-----------------------|
| LK1_p35S+mTagBFPLti6bCO+Nos_T35S_T  | <a href="https://benchling.com/s/F65BioQ2CcR0mW94RRlw">https://benchling.com/s/F65BioQ2CcR0mW94RRlw</a>         | Alpha and Beta        |
| LK2_p35S+mTurq2+N7+35S_T            | <a href="https://benchling.com/s/RqDsXXRMIU9MrubK29yJ">https://benchling.com/s/RqDsXXRMIU9MrubK29yJ</a>         | Beta and Gamma        |
| LK2_p35S+Hemme+mTurq2+35S_T         | <a href="https://benchling.com/s/SIHiuxwMZ3h8ESI415ej">https://benchling.com/s/SIHiuxwMZ3h8ESI415ej</a>         | Beta and Gamma        |
| LK3_p35S+HemmeYPET+Hsp_T            | <a href="https://benchling.com/s/LywmiVDIdLu2QMtlhyfG">https://benchling.com/s/LywmiVDIdLu2QMtlhyfG</a>         | Gamma and Epsilon     |
| LK3_p35S+Venus+N7+Hsp_T             | <a href="https://benchling.com/s/QCivTnPEAvBpQWohSG4E">https://benchling.com/s/QCivTnPEAvBpQWohSG4E</a>         | Gamma and Epsilon     |
| Lk4_p35S+TagRFPLti+Ubq3_T           | <a href="https://benchling.com/s/seq-fTH4Afd0pQqX6D79degp">https://benchling.com/s/seq-fTH4Afd0pQqX6D79degp</a> | Epsilon and Omega     |
| Lk4_p35S+mRuby3+Ubq3_T              | <a href="https://benchling.com/s/seq-HccCTP2uxuN9doShjSFh">https://benchling.com/s/seq-HccCTP2uxuN9doShjSFh</a> | Epsilon and Omega     |
| LK1_p35S+mTagBFP+Lti6b+Nos_T35S_T   | <a href="https://benchling.com/s/seq-OtjAMzv83IMIC4SQKQn5">https://benchling.com/s/seq-OtjAMzv83IMIC4SQKQn5</a> | Alpha and Beta        |
| LK1_MpEF1+mTagBFPLti6bCO+Nos_T35S_T | <a href="https://benchling.com/s/seq-ADStHJTCchoqoD2ljk6T">https://benchling.com/s/seq-ADStHJTCchoqoD2ljk6T</a> | Alpha and Beta        |
| LK1_MpEF1+HemmeYPET+Nos_T35S_T      | <a href="https://benchling.com/s/seq-rO2XiumLPSrFAtsmAObP">https://benchling.com/s/seq-rO2XiumLPSrFAtsmAObP</a> | Alpha and Beta        |
| LK1_MpEF1+mTagBFP+Lti6b+Nos_T35_T   | <a href="https://benchling.com/s/seq-xN8HveRfgoJFIMAPAYa0">https://benchling.com/s/seq-xN8HveRfgoJFIMAPAYa0</a> | Alpha and Beta        |
| LK1_MpEF1+Venus+Lti6b+Nos_T35_T     | <a href="https://benchling.com/s/seq-ZEN79Im6v7z7j0erK9b6">https://benchling.com/s/seq-ZEN79Im6v7z7j0erK9b6</a> | Alpha and Beta        |
| LK1_MpEF1+mTagBFP2+N7+Nos_T35_T     | <a href="https://benchling.com/s/seq-Ke5woO6xyZ6GIQC1qvNQ">https://benchling.com/s/seq-Ke5woO6xyZ6GIQC1qvNQ</a> | Alpha and Beta        |
| LK1_MpEF1+mRuby3+Nos_T35_T          | <a href="https://benchling.com/s/seq-iYcp2BFH8Z54sA1Okf1f">https://benchling.com/s/seq-iYcp2BFH8Z54sA1Okf1f</a> | Alpha and Beta        |
| LK1_MpEF1+TagRFPLti6bCO+Nos_T35_T   | <a href="https://benchling.com/s/seq-Uf9cxej3jVtotzbW9HxA">https://benchling.com/s/seq-Uf9cxej3jVtotzbW9HxA</a> | Alpha and Beta        |

|   |   |                   |
|---|---|-------------------|
| LK1_MpEF1+Venus+N7+Nos_T35_T            | <a href="https://benchling.com/s/seq-uKv2labjsPEjOB83hORI">https://benchling.com/s/seq-uKv2labjsPEjOB83hORI</a> | Alpha and Beta    |
| LK1_MpEF1+mTurq2+N7+Nos_T35S_T          | <a href="https://benchling.com/s/seq-vWfDAXTB068EliXucZGA">https://benchling.com/s/seq-vWfDAXTB068EliXucZGA</a> | Alpha and Beta    |
| LK1_MpEF1+mTurq2+Lti6b+Nos_T35S_T       | <a href="https://benchling.com/s/seq-acOS3dDp7DjSpS9hGrf8">https://benchling.com/s/seq-acOS3dDp7DjSpS9hGrf8</a> | Alpha and Beta    |
| LK1_MpEF1+Venus+Nos_T35S_T              | <a href="https://benchling.com/s/seq-nTJGREhTTnbjioErfYRH">https://benchling.com/s/seq-nTJGREhTTnbjioErfYRH</a> | Alpha and Beta    |
| LK1_MpEF1+mTurq2+Nos_T35S_T             | <a href="https://benchling.com/s/seq-cmmgPRBqymYywfqSuMIR">https://benchling.com/s/seq-cmmgPRBqymYywfqSuMIR</a> | Alpha and Beta    |
| LK1_MpEF1(1-5)+Hemme+Venus+Nos_T35S_T   | <a href="https://benchling.com/s/seq-yngcWyJcewuDVpKx51Km">https://benchling.com/s/seq-yngcWyJcewuDVpKx51Km</a> | Alpha and Beta    |
| LK1_MpEF1(1-5)+Hemme+mTurq2+Nos_T35S_T  | <a href="https://benchling.com/s/seq-EfEMz7WpEbZGXFAMd0CR">https://benchling.com/s/seq-EfEMz7WpEbZGXFAMd0CR</a> | Alpha and Beta    |
| LK1_MpEF1+TurboRFP+Nos_T35S_T           | <a href="https://benchling.com/s/seq-hGX8MejEJ0LMmHFLqInf">https://benchling.com/s/seq-hGX8MejEJ0LMmHFLqInf</a> | Alpha and Beta    |
| LK1_MpEF1+Citrine+Nos_T35S_T            | <a href="https://benchling.com/s/seq-Sx8afNBzmp3oJ6W3oxXH">https://benchling.com/s/seq-Sx8afNBzmp3oJ6W3oxXH</a> | Alpha and Beta    |
| LK1_MpEF1(1-5)+Hemme+Citrine+Nos_T35S_T | <a href="https://benchling.com/s/seq-EQfXPnxgNtKThJYa5txU">https://benchling.com/s/seq-EQfXPnxgNtKThJYa5txU</a> | Alpha and Beta    |
| LK1_MpEF1+Citrine+N7+Nos_T35S_T         | <a href="https://benchling.com/s/seq-vxT3O9kFnlz34iby9Kp">https://benchling.com/s/seq-vxT3O9kFnlz34iby9Kp</a>   | Alpha and Beta    |
| LK1_MpEF1+Citrine+Lti6b+Nos_T35S_T      | <a href="https://benchling.com/s/seq-JlcUDg6ppleu51EziZJu">https://benchling.com/s/seq-JlcUDg6ppleu51EziZJu</a> | Alpha and Beta    |
| LK1_MpEF1+CyOFP1+Nos_T35S_T             | <a href="https://benchling.com/s/seq-1AFAU24JmlvQV8yXjcgq">https://benchling.com/s/seq-1AFAU24JmlvQV8yXjcgq</a> | Alpha and Beta    |
| LK1_MpEF1+mBeRFP+Nos_T35S_T             | <a href="https://benchling.com/s/seq-bG31DBTd5whEiOTwv1WA">https://benchling.com/s/seq-bG31DBTd5whEiOTwv1WA</a> | Alpha and Beta    |
| LK1_MpEFq+deGFP+Nos_T35S_T              | <a href="https://benchling.com/s/seq-MNaGEZ1rufFyVmv5Rj66">https://benchling.com/s/seq-MNaGEZ1rufFyVmv5Rj66</a> | Alpha and Beta    |
| LK2_MpEF1+mTurq2+N7+Nos_T35S_T          | <a href="https://benchling.com/s/seq-eeGEPDt066Zwl1uNIGdU">https://benchling.com/s/seq-eeGEPDt066Zwl1uNIGdU</a> | Beta and Gamma    |
| LK3_MpEF1+mRuby3+Nos_T35_T              | <a href="https://benchling.com/s/seq-CTkTq1ED2IB5FqhLnR3">https://benchling.com/s/seq-CTkTq1ED2IB5FqhLnR3</a>   | Gamma and Epsilon |

|                                   |   |                   |
|-----------------------------------|---|-------------------|
| LK1_pUBQ10+mTurq2+N7+Nos_T35S_T   | <a href="https://benchling.com/s/seq-4VklWuNX53JoinPn0jbB">https://benchling.com/s/seq-4VklWuNX53JoinPn0jbB</a> | Alpha and Beta    |
| LK2_pUBQ10+mTurq2+N7+Nos_T35S_T   | <a href="https://benchling.com/s/seq-TsJgSluYRguPLTO8FWbF">https://benchling.com/s/seq-TsJgSluYRguPLTO8FWbF</a> | Beta and Gamma    |
| LK3_pUBQ10+mTurq2+N7+Nos_T35S_T   | <a href="https://benchling.com/s/seq-y3rdELRQdWhJAIHYa61H">https://benchling.com/s/seq-y3rdELRQdWhJAIHYa61H</a> | Gamma and Epsilon |
| LK1_MpEF1+Venus+Hsp_T             | <a href="https://benchling.com/s/seq-oMLyDdCkScTKsh18LDMR">https://benchling.com/s/seq-oMLyDdCkScTKsh18LDMR</a> | Alpha and Beta    |
| LK1_MpEF1+HAPI+VP16+Nos_T35S_T    | <a href="https://benchling.com/s/seq-cpyBP7Ro2iEE6QRleT3f">https://benchling.com/s/seq-cpyBP7Ro2iEE6QRleT3f</a> | Alpha and Beta    |
| LK1_MpEF1+HAPI/VP16+Nos_T35S_T    | <a href="https://benchling.com/s/seq-cAyX1gZRUNPkZw8luJxu">https://benchling.com/s/seq-cAyX1gZRUNPkZw8luJxu</a> | Alpha and Beta    |
| LK1_MpEF1+GAL4+VP16+Nos_T35S_T    | <a href="https://benchling.com/s/seq-BbFzoxRvGORZQyf4gvVR">https://benchling.com/s/seq-BbFzoxRvGORZQyf4gvVR</a> | Alpha and Beta    |
| LK1_MpEF1+GAL4/VP16+Nos_T35S_T    | <a href="https://benchling.com/s/seq-owqb1y0i8ReuEOLUMFcZ">https://benchling.com/s/seq-owqb1y0i8ReuEOLUMFcZ</a> | Alpha and Beta    |
| LK1_MpEF1+TetR+VP16+Nos_T35S_T    | <a href="https://benchling.com/s/seq-y1hrwO6COs5EjxqLQPuU">https://benchling.com/s/seq-y1hrwO6COs5EjxqLQPuU</a> | Alpha and Beta    |
| LK1_MpEF1+SprR+EAR+Nos_T35S_T     | <a href="https://benchling.com/s/seq-Ja12cYRf6ve9xZMfa7Mg">https://benchling.com/s/seq-Ja12cYRf6ve9xZMfa7Mg</a> | Alpha and Beta    |
| LK1_MpEF1+SprR+VP16+Nos_T35S_T    | <a href="https://benchling.com/s/seq-OppDZLWUc6yUbSEVbw59">https://benchling.com/s/seq-OppDZLWUc6yUbSEVbw59</a> | Alpha and Beta    |
| LK1_MpEF1+TetR+EAR+Nos_T35S_T     | <a href="https://benchling.com/s/seq-Jd8ozNoDIpLe8NZI25us">https://benchling.com/s/seq-Jd8ozNoDIpLe8NZI25us</a> | Alpha and Beta    |
| LK1_MpEF1+GAL4+EAR+Nos_T35S_T     | <a href="https://benchling.com/s/seq-IHPBC5N93vRSbi6YhbQO">https://benchling.com/s/seq-IHPBC5N93vRSbi6YhbQO</a> | Alpha and Beta    |
| LK1_MpEF1+HAPI+EAR+Nos_T35S_T     | <a href="https://benchling.com/s/seq-qJurIOfPUcY1C5qUEQKb">https://benchling.com/s/seq-qJurIOfPUcY1C5qUEQKb</a> | Alpha and Beta    |
| LK1_MpEF1+HAPI+VP16+GR+Nos_T35S_T | <a href="https://benchling.com/s/seq-eizUMwceTetusUMHxcvk">https://benchling.com/s/seq-eizUMwceTetusUMHxcvk</a> | Alpha and Beta    |
| LK1_MpEF1+HAPI/VP16/GR+Nos_T35S_T | <a href="https://benchling.com/s/seq-tYpB6FKQaZ1Q2TOnZMNA">https://benchling.com/s/seq-tYpB6FKQaZ1Q2TOnZMNA</a> | Alpha and Beta    |
| LK1_MpEF1+GAL4+VP16+GR+Nos_T35S_T | <a href="https://benchling.com/s/seq-dNUBqVA1CQouSVDgx4Jn">https://benchling.com/s/seq-dNUBqVA1CQouSVDgx4Jn</a> | Alpha and Beta    |

|                                   |   |                   |
|-----------------------------------|---|-------------------|
| LK1_MpEF1+TetR+VP16+GR+Nos_T35S_T | <a href="https://benchling.com/s/seq-eguoWRhy4CaXUFCYjJcE">https://benchling.com/s/seq-eguoWRhy4CaXUFCYjJcE</a> | Alpha and Beta    |
| LK1_MpEF1+SprR+VP16+GR+Nos_T35S_T | <a href="https://benchling.com/s/seq-wf5iMZOJMALFvtT9cYBq">https://benchling.com/s/seq-wf5iMZOJMALFvtT9cYBq</a> | Alpha and Beta    |
| LK1_MpEF1+HAPI+EAR+GR+Nos_T35S_T  | <a href="https://benchling.com/s/seq-Cd2bN6ZHK64FG4LwKv5r">https://benchling.com/s/seq-Cd2bN6ZHK64FG4LwKv5r</a> | Alpha and Beta    |
| LK1_MpEF1+GAL4+EAR+GR+Nos_T35S_T  | <a href="https://benchling.com/s/seq-An6OM3VaxvfGaP2FjWsm">https://benchling.com/s/seq-An6OM3VaxvfGaP2FjWsm</a> | Alpha and Beta    |
| LK1_MpEF1+TetR+EAR+GR+Nos_T35S_T  | <a href="https://benchling.com/s/seq-EhV2jQS0v4uOf0sTnToK">https://benchling.com/s/seq-EhV2jQS0v4uOf0sTnToK</a> | Alpha and Beta    |
| LK1_MpEF1+SprR+EAR+GR+Nos_T35S_T  | <a href="https://benchling.com/s/seq-bqACxidnBbsbKgN3gGY5">https://benchling.com/s/seq-bqACxidnBbsbKgN3gGY5</a> | Alpha and Beta    |
| LK1_UASHap1*2_BOX                 | <a href="https://benchling.com/s/seq-HtJNdhgc7S6lioYyaC3U">https://benchling.com/s/seq-HtJNdhgc7S6lioYyaC3U</a> | Alpha and Beta    |
| LK2_UASHap1*2_BOX                 | <a href="https://benchling.com/s/seq-9mwYUE3FICxaKeKExl24">https://benchling.com/s/seq-9mwYUE3FICxaKeKExl24</a> | Beta and Gamma    |
| LK3_UASHap1*2_BOX                 | <a href="https://benchling.com/s/seq-IS1UAiSjQrxA8ReZkOld">https://benchling.com/s/seq-IS1UAiSjQrxA8ReZkOld</a> | Gamma and Epsilon |
| LK4_UASHap1*2_BOX                 | <a href="https://benchling.com/s/seq-xSzKHMrhEevVdYy1EPsq">https://benchling.com/s/seq-xSzKHMrhEevVdYy1EPsq</a> | Epsilon and Omega |
| LK1_UASGal4*2_BOX                 | <a href="https://benchling.com/s/seq-leZ5QZee3ZRGoPRQCgFm">https://benchling.com/s/seq-leZ5QZee3ZRGoPRQCgFm</a> | Alpha and Beta    |
| LK2_UASGal4*2_BOX                 | <a href="https://benchling.com/s/seq-KKLitHpB3UvxU40LPCCU">https://benchling.com/s/seq-KKLitHpB3UvxU40LPCCU</a> | Beta and Gamma    |
| LK3_UASGal4*2_BOX                 | <a href="https://benchling.com/s/seq-OznmwY31WIQke70r7dlo">https://benchling.com/s/seq-OznmwY31WIQke70r7dlo</a> | Gamma and Epsilon |
| LK4_UASGal4*2_BOX                 | <a href="https://benchling.com/s/seq-xDK2BBRPKAYMfWKBjzEi">https://benchling.com/s/seq-xDK2BBRPKAYMfWKBjzEi</a> | Epsilon and Omega |
| LK1_SprROp*1_BOX                  | <a href="https://benchling.com/s/seq-VqGqBMTXE2fVgiEfeFx6">https://benchling.com/s/seq-VqGqBMTXE2fVgiEfeFx6</a> | Alpha and Beta    |
| LK2_SprROp*1_BOX                  | <a href="https://benchling.com/s/seq-PflbnIDK3deLzV0rkbMu">https://benchling.com/s/seq-PflbnIDK3deLzV0rkbMu</a> | Beta and Gamma    |
| LK3_SprROp*1_BOX                  | <a href="https://benchling.com/s/seq-9zdtj4c03M1YpoqQurXC">https://benchling.com/s/seq-9zdtj4c03M1YpoqQurXC</a> | Gamma and Epsilon |

|                      |   |                   |
|----------------------|---|-------------------|
| LK4_SprROp*1_BOX     | <a href="https://benchling.com/s/seq-rC61RFcmNvTNGa07Lf5x">https://benchling.com/s/seq-rC61RFcmNvTNGa07Lf5x</a> | Epsilon and Omega |
| LK1_TetROp*1_BOX     | <a href="https://benchling.com/s/seq-czL8W0onm17tn8CCksEa">https://benchling.com/s/seq-czL8W0onm17tn8CCksEa</a> | Alpha and Beta    |
| LK2_TetROp*1_BOX     | <a href="https://benchling.com/s/seq-PflbnIDK3deLzV0rkbMu">https://benchling.com/s/seq-PflbnIDK3deLzV0rkbMu</a> | Beta and Gamma    |
| LK3_TetROp*1_BOX     | <a href="https://benchling.com/s/seq-ls486LCmaEXgNmV1gwTJ">https://benchling.com/s/seq-ls486LCmaEXgNmV1gwTJ</a> | Gamma and Epsilon |
| LK4_TetROp*1_BOX     | <a href="https://benchling.com/s/seq-rC61RFcmNvTNGa07Lf5x">https://benchling.com/s/seq-rC61RFcmNvTNGa07Lf5x</a> | Epsilon and Omega |
| LK4_pMin35S          | <a href="https://benchling.com/s/seq-u3qeEO0syAlMg2OPE1CD">https://benchling.com/s/seq-u3qeEO0syAlMg2OPE1CD</a> | Epsilon and Omega |
| LK1_AuxREs_BOXs      | <a href="https://benchling.com/s/seq-8WwekfkSa5QGEnyt8Clo">https://benchling.com/s/seq-8WwekfkSa5QGEnyt8Clo</a> | Alpha and Beta    |
| LK2_AuxREs_BOXs      | <a href="https://benchling.com/s/seq-3jUtzfSur2oTrMlqiT9t">https://benchling.com/s/seq-3jUtzfSur2oTrMlqiT9t</a> | Beta and Gamma    |
| LK3_AuxREs_BOXs      | <a href="https://benchling.com/s/seq-dhYV96qzR4zZu8gVTFHb">https://benchling.com/s/seq-dhYV96qzR4zZu8gVTFHb</a> | Gamma and Epsilon |
| LK4_AuxREs_BOXs      | <a href="https://benchling.com/s/seq-5zMAbri5obL79cbGbMi8">https://benchling.com/s/seq-5zMAbri5obL79cbGbMi8</a> | Epsilon and Omega |
| LK1_RY+ABRE BOXS     | <a href="https://benchling.com/s/seq-loErzJTmze2mzfpfn6gB">https://benchling.com/s/seq-loErzJTmze2mzfpfn6gB</a> | Alpha and Beta    |
| LK2_RY+ABRE BOXS     | <a href="https://benchling.com/s/seq-3tfHsdMfz6tVfvd8dFCh">https://benchling.com/s/seq-3tfHsdMfz6tVfvd8dFCh</a> | Beta and Gamma    |
| LK3_RY+ABRE BOXS     | <a href="https://benchling.com/s/seq-7URhhAG5vOgE1e1QckSy">https://benchling.com/s/seq-7URhhAG5vOgE1e1QckSy</a> | Gamma and Epsilon |
| LK4_RY+ABRE BOXS     | <a href="https://benchling.com/s/seq-yxpd1wF8JzRnMkJ4eVAZ">https://benchling.com/s/seq-yxpd1wF8JzRnMkJ4eVAZ</a> | Epsilon and Omega |
| LK1_D1b+D1c Prom BOX | <a href="https://benchling.com/s/seq-rTINAKnwjPfmz7pBNOP1">https://benchling.com/s/seq-rTINAKnwjPfmz7pBNOP1</a> | Alpha and Beta    |
| LK2_D1b+D1c Prom BOX | <a href="https://benchling.com/s/seq-2rYTiLdRYeoffECvBJWW">https://benchling.com/s/seq-2rYTiLdRYeoffECvBJWW</a> | Beta and Gamma    |
| LK3_D1b+D1c Prom BOX | <a href="https://benchling.com/s/seq-fbBdwFSZmlsUircHTlgG">https://benchling.com/s/seq-fbBdwFSZmlsUircHTlgG</a> | Gamma and Epsilon |

|                      |   |                   |
|----------------------|---|-------------------|
| LK4_D1b+D1c Prom BOX | <a href="https://benchling.com/s/seq-8p7nsuZeCqotlnHKrh9a">https://benchling.com/s/seq-8p7nsuZeCqotlnHKrh9a</a> | Epsilon and Omega |
| LK1_UASHap1*1_BOX    | <a href="https://benchling.com/s/seq-GjdYyhvXH66OVVwBaNpw">https://benchling.com/s/seq-GjdYyhvXH66OVVwBaNpw</a> | Alpha and Beta    |
| LK2_UASHap1*1_BOX    | <a href="https://benchling.com/s/seq-1RSVTfwr8xGfugywVZjb">https://benchling.com/s/seq-1RSVTfwr8xGfugywVZjb</a> | Beta and Gamma    |
| LK3_UASHap1*1_BOX    | <a href="https://benchling.com/s/seq-ecQfDFZO6kWsFJrcYfO">https://benchling.com/s/seq-ecQfDFZO6kWsFJrcYfO</a>   | Gamma and Epsilon |
| LK4_UASHap1*1_BOX    | <a href="https://benchling.com/s/seq-G6agFMS1qYfol3s6jRt4">https://benchling.com/s/seq-G6agFMS1qYfol3s6jRt4</a> | Epsilon and Omega |
| LK1_UASGal4*1_BOX    | <a href="https://benchling.com/s/seq-Y07MgxcaGDSe2V5L3t8Z">https://benchling.com/s/seq-Y07MgxcaGDSe2V5L3t8Z</a> | Alpha and Beta    |
| LK2_UASGal4*1_BOX    | <a href="https://benchling.com/s/seq-Oae5G8TrnfUdVxHYzn6W">https://benchling.com/s/seq-Oae5G8TrnfUdVxHYzn6W</a> | Beta and Gamma    |
| LK3_UASGal4*1_BOX    | <a href="https://benchling.com/s/seq-di76h9Mz2tFQJedu6CgB">https://benchling.com/s/seq-di76h9Mz2tFQJedu6CgB</a> | Gamma and Epsilon |
| LK4_UASGal4*1_BOX    | <a href="https://benchling.com/s/seq-UKnxEojjoehqOrF0gjVp">https://benchling.com/s/seq-UKnxEojjoehqOrF0gjVp</a> | Epsilon and Omega |
| LK1_CKOper_Full_BOX  | <a href="https://benchling.com/s/seq-PfUhPpZzxBaxJ78taGCs">https://benchling.com/s/seq-PfUhPpZzxBaxJ78taGCs</a> | Alpha and Beta    |
| LK2_CKOper_Full_BOX  | <a href="https://benchling.com/s/seq-CI2rUWHoWkK0FL0mDUQR">https://benchling.com/s/seq-CI2rUWHoWkK0FL0mDUQR</a> | Beta and Gamma    |
| LK3_CKOper_Full_BOX  | <a href="https://benchling.com/s/seq-fJxlfLC462K6wHxUaT2">https://benchling.com/s/seq-fJxlfLC462K6wHxUaT2</a>   | Gamma and Epsilon |
| LK4_CKOper_Full_BOX  | <a href="https://benchling.com/s/seq-4paayyYyrNeGQ0MM9AfA">https://benchling.com/s/seq-4paayyYyrNeGQ0MM9AfA</a> | Epsilon and Omega |
| LK1_SprROp*2_BOX     | <a href="https://benchling.com/s/seq-BmZhCXIkcuY6nGO3KEr3">https://benchling.com/s/seq-BmZhCXIkcuY6nGO3KEr3</a> | Alpha and Beta    |
| LK2_SprROp*2_BOX     | <a href="https://benchling.com/s/seq-9YIpLGRRUqrdNLFmajc6">https://benchling.com/s/seq-9YIpLGRRUqrdNLFmajc6</a> | Beta and Gamma    |
| LK3_SprROp*2_BOX     | <a href="https://benchling.com/s/seq-Q2JlG5wklb8vJstmGK">https://benchling.com/s/seq-Q2JlG5wklb8vJstmGK</a>     | Gamma and Epsilon |
| LK4_SprROp*2_BOX     | <a href="https://benchling.com/s/seq-Nvi8Uk7NgBxXEjxb2cLz">https://benchling.com/s/seq-Nvi8Uk7NgBxXEjxb2cLz</a> | Epsilon and Omega |

|   |   |                   |
|---|---|-------------------|
| LK1_TetROp*2_BOX                          | <a href="https://benchling.com/s/seq-cU7DIs5Xzfszymke6vds">https://benchling.com/s/seq-cU7DIs5Xzfszymke6vds</a> | Alpha and Beta    |
| LK2_TetROp*2_BOX                          | <a href="https://benchling.com/s/seq-SM5gFgeX0zvbkMGeSPhh">https://benchling.com/s/seq-SM5gFgeX0zvbkMGeSPhh</a> | Beta and Gamma    |
| LK3_TetROp*2_BOX                          | <a href="https://benchling.com/s/seq-XmEhgze4hnZBHwz3v4am">https://benchling.com/s/seq-XmEhgze4hnZBHwz3v4am</a> | Gamma and Epsilon |
| LK4_TetROp*2_BOX                          | <a href="https://benchling.com/s/seq-w3SF4Sk1V36D9GE5SX4s">https://benchling.com/s/seq-w3SF4Sk1V36D9GE5SX4s</a> | Epsilon and Omega |
| LK1_MpEF1+Venus+GR+Nos_T35S_T             | <a href="https://benchling.com/s/seq-nyniAw255TbD3njse1uY">https://benchling.com/s/seq-nyniAw255TbD3njse1uY</a> | Alpha and Beta    |
| LK2_MpEF1+Venus+GR+Nos_T35S_T             | <a href="https://benchling.com/s/seq-RMtCVeskiDCEFsVlkwc2">https://benchling.com/s/seq-RMtCVeskiDCEFsVlkwc2</a> | Beta and Gamma    |
| LK2_p4BOX_TetROp*2+Venus+Nos_T35S_T       | <a href="https://benchling.com/s/seq-l8VYpp05iL5SnntRJWho">https://benchling.com/s/seq-l8VYpp05iL5SnntRJWho</a> | Beta and Gamma    |
| LK2_p4BOX_TetROp*1+Venus+Nos_T35S_T       | <a href="https://benchling.com/s/seq-di3XOvB17soAk7NWcu3j">https://benchling.com/s/seq-di3XOvB17soAk7NWcu3j</a> | Beta and Gamma    |
| LK2_p4BOX_SprROp*2+Venus+Nos_T35S_T       | <a href="https://benchling.com/s/seq-LvOTHGqjlp7yDkXveKey">https://benchling.com/s/seq-LvOTHGqjlp7yDkXveKey</a> | Beta and Gamma    |
| LK2_p4BOX_SprROp*1+Venus+Nos_T35S_T       | <a href="https://benchling.com/s/seq-4OG221nltdB8ghmrbjl6">https://benchling.com/s/seq-4OG221nltdB8ghmrbjl6</a> | Beta and Gamma    |
| LK2_p4BOX_UASGal4*1+Venus+Nos_T35S_T      | <a href="https://benchling.com/s/seq-tATLKUVKQdVphr5trS31">https://benchling.com/s/seq-tATLKUVKQdVphr5trS31</a> | Beta and Gamma    |
| LK2_p4BOX_UASGal4*2+Venus+Nos_T35S_T      | <a href="https://benchling.com/s/seq-aPC0tHFgT6yPkAdF26fh">https://benchling.com/s/seq-aPC0tHFgT6yPkAdF26fh</a> | Beta and Gamma    |
| LK2_p4BOX_UASHapl*1+Venus+Nos_T35S_T      | <a href="https://benchling.com/s/seq-o9Ktmu5qeiGM4XoCaYGH">https://benchling.com/s/seq-o9Ktmu5qeiGM4XoCaYGH</a> | Beta and Gamma    |
| LK2_p4BOX_UASHapl*2+Venus+Nos_T35S_T      | <a href="https://benchling.com/s/seq-gnx9o4bAZGJK6rNtTLmf">https://benchling.com/s/seq-gnx9o4bAZGJK6rNtTLmf</a> | Beta and Gamma    |
| LK2_p7BOX_20B+Venus+Nos_T35S_T            | <a href="https://benchling.com/s/seq-yc1aFlmjkGUoho3GcUP">https://benchling.com/s/seq-yc1aFlmjkGUoho3GcUP</a>   | Beta and Gamma    |
| LK3_MpEF1a+SYNZIP18+VP16+HspT             | <a href="https://benchling.com/s/seq-DmIr1wSmXyxHEkFCWQPJ">https://benchling.com/s/seq-DmIr1wSmXyxHEkFCWQPJ</a> | Gamma and Epsilon |
| LK1_MpEF1a+TetR(NO NLS)+SYNZIP17+NosT35ST | <a href="https://benchling.com/s/seq-PKbDT4PZewaAs53mftm8">https://benchling.com/s/seq-PKbDT4PZewaAs53mftm8</a> | Alpha and Beta    |

|  |   |                   |
|--|---|-------------------|
| LK1_MpEF1a+Gal4 short +SYNZIP17+NosT35ST | <a href="https://benchling.com/s/seq-Lj3w90cWLqfnHgIIPSP7">https://benchling.com/s/seq-Lj3w90cWLqfnHgIIPSP7</a>   | Alpha and Beta    |
| LK1_MpEF1a+TetR+SYNZIP17+NosT35ST        | <a href="https://benchling.com/s/seq-8wE5UVua1P3L9KTZqHhE">https://benchling.com/s/seq-8wE5UVua1P3L9KTZqHhE</a>   | Alpha and Beta    |
| LK1_MpEF1a+Gal4+SYNZIP17+NosT35ST        | <a href="https://benchling.com/s/seq-Jli5azUZUxRLsBj4v4wu">https://benchling.com/s/seq-Jli5azUZUxRLsBj4v4wu</a>   | Alpha and Beta    |
| LK2_p7BOX_D1b+D1c+Venus+NosT35ST         | <a href="https://benchling.com/s/seq-07sComldTwTNdMivf3oD">https://benchling.com/s/seq-07sComldTwTNdMivf3oD</a>   | Beta and Gamma    |
| LK2_p7BOX_CKOper+Venus+NosT35ST          | <a href="https://benchling.com/s/seq-OFn2Z05wgOivXoDeUdzJ">https://benchling.com/s/seq-OFn2Z05wgOivXoDeUdzJ</a>   | Beta and Gamma    |
| LK2_p7BOX_AuxREs+Venus+NosT35ST          | <a href="https://benchling.com/s/seq-yKe1Gk6KBaBKeMtRgD20">https://benchling.com/s/seq-yKe1Gk6KBaBKeMtRgD20</a>   | Beta and Gamma    |
| LK2_p7BOX_RY+ABRE+Venus+NosT35ST         | <a href="https://benchling.com/s/seq-cxH9W3VX0fv6GSdFVoph">https://benchling.com/s/seq-cxH9W3VX0fv6GSdFVoph</a>   | Beta and Gamma    |
| LK1_MpEF1a+Venus+GR (NO NLS)+NosT35ST    | <a href="https://benchling.com/s/seq-bjv1zhznaddqEmJqs1xt">https://benchling.com/s/seq-bjv1zhznaddqEmJqs1xt</a>   | Alpha and Beta    |
| LK3_pUbq10+mRuby3+HspT                   | <a href="https://benchling.com/s/seq-jAJm85sKvGXeAEjkZtQC?m=slm-U4biRN3aB5iVVPcYrbg6">https://benchling.com/s/seq-jAJm85sKvGXeAEjkZtQC?m=slm-U4biRN3aB5iVVPcYrbg6</a> | Gamma and Epsilon |
| LK1_MpEF1a+TetR(NO_NLS)+VP16+GR+NosT35ST | <a href="https://benchling.com/s/seq-83jmWkf0joaW9WcTGUne?m=slm-b5KIL94APRDKqDCTolhU">https://benchling.com/s/seq-83jmWkf0joaW9WcTGUne?m=slm-b5KIL94APRDKqDCTolhU</a> | Alpha and Beta    |
| LK1_MpEF1a+TetR+VP16+GR(NO_NLS)+NosT35ST | <a href="https://benchling.com/s/seq-ZVNp707pWXBjYDKDxY6F?m=slm-IQLNdt2DGOW1eBGnB4vm">https://benchling.com/s/seq-ZVNp707pWXBjYDKDxY6F?m=slm-IQLNdt2DGOW1eBGnB4vm</a> | Alpha and Beta    |

**Table SIV.** Even assemblies

| Name  | Sequence  | Syntax (Donor) |
|---|---|----------------|
| LS1_p35S+mTagBFPLti6bCO+Nos_T35S_T/_p35S+Hemme+mTurq2+35S_T/_p35S+Venus+N7+Hsp_T/_p35S+mRuby3+Ubq3_T  | <a href="https://benchling.com/s/seq-qKHAsWcsrJVxx6h0HzFr">https://benchling.com/s/seq-qKHAsWcsrJVxx6h0HzFr</a> | 1 and 4        |
| LS1_p35S+mTagBFPLti6bCO+Nos_T35S_T/_p35S+mTurq2+N7+35S_T/_p35S+HemmeYPET+Hsp_T/_p35S+mRuby3+Ubq3_T    | <a href="https://benchling.com/s/seq-2nDYb0dHNyCv4HJhnXmc">https://benchling.com/s/seq-2nDYb0dHNyCv4HJhnXmc</a> | 1 and 4        |
| LS1_p35S+mTagBFPLti6bCO+Nos_T35S_T/_p35S+mTurq2+N7+35S_T/_p35S+HemmeYPET+Hsp_T/_p35S+TagRFPLti+Ubq3_T | <a href="https://benchling.com/s/seq-qpVpqHoU91KH5ZbrRuO7">https://benchling.com/s/seq-qpVpqHoU91KH5ZbrRuO7</a> | 1 and 4        |
| LS1_p35S+mTagBFPLti6bCO+Nos_T35S_T/_p35S+mTurq2+N7+35S_T/_p35S+Venus+N7+Hsp_T/_p35S+TagRFPLti+Ubq3_T  | <a href="https://benchling.com/s/seq-dJiPfaDI0DW50c4OeifB">https://benchling.com/s/seq-dJiPfaDI0DW50c4OeifB</a> | 1 and 4        |
| LS1_MpEF1+Venus+Nos_T35S_T/Cassette Hygro   | <a href="https://benchling.com/s/seq-K1Owcaiz7pb8SrKzizO6">https://benchling.com/s/seq-K1Owcaiz7pb8SrKzizO6</a> | 1 and 4        |
| LS1_MpEF1+Venus+Lti6b+Nos_T35_T/Cassette Hygro  | <a href="https://benchling.com/s/seq-CbDBHnB4ceSkUXp3G2Pq">https://benchling.com/s/seq-CbDBHnB4ceSkUXp3G2Pq</a> | 1 and 4        |
| LS1_MpEF1+Venus+N7+Nos_T35_T/Cassette Hygro   | <a href="https://benchling.com/s/seq-VT1tTvOET9uw4onqyeHs">https://benchling.com/s/seq-VT1tTvOET9uw4onqyeHs</a> | 1 and 4        |
| LS1_MpEF1+mRuby3+Nos_T35_T/Cassette Hygro   | <a href="https://benchling.com/s/seq-wipFNZ0k3RnBK1rZQmXy">https://benchling.com/s/seq-wipFNZ0k3RnBK1rZQmXy</a> | 1 and 4        |
| LS1_MpEF1+mTagBFP+Lti6b+Nos_T35_T/Cassette Hygro  | <a href="https://benchling.com/s/seq-8gBQ3ivSoXRHzdZMfYBJ">https://benchling.com/s/seq-8gBQ3ivSoXRHzdZMfYBJ</a> | 1 and 4        |
| LS1_MpEF1+mTagBFPLti6bCO+Nos_T35S_T/Cassette Hygro  | <a href="https://benchling.com/s/seq-fhga21tQ4Bpa4B0PRL3v">https://benchling.com/s/seq-fhga21tQ4Bpa4B0PRL3v</a> | 1 and 4        |
| LS1_MpEF1+TagRFPLti6bCO+Nos_T35_T/Cassette Hygro  | <a href="https://benchling.com/s/seq-hYabITR0FbHwuu1HqAkj">https://benchling.com/s/seq-hYabITR0FbHwuu1HqAkj</a> | 1 and 4        |

|  |   |         |
|--|---|---------|
| LS1_MpEF1+mTurq2+Nos_T35S_T/Cassette Hygro   | <a href="https://benchling.com/s/seq-jPubpjclTFAzXKcl5cVN">https://benchling.com/s/seq-jPubpjclTFAzXKcl5cVN</a> | 1 and 4 |
| LS1_MpEF1+HemmeYPET+Nos_T35S_T/Cassette Hygro  | <a href="https://benchling.com/s/seq-xPsusLtcNn6Qj49qS2rU">https://benchling.com/s/seq-xPsusLtcNn6Qj49qS2rU</a> | 1 and 4 |
| LS1_MpEF1+mTurq2+Lti6b+Nos_T35S_T/Cassette Hygro   | <a href="https://benchling.com/s/seq-GdnXPQqYZ6wjfeEwDzZB">https://benchling.com/s/seq-GdnXPQqYZ6wjfeEwDzZB</a> | 1 and 4 |
| LS1_MpEF1+mTagBFP2+N7+Nos_T35_T/Cassette Hygro   | <a href="https://benchling.com/s/seq-plaxdUy0C6uSXC346D9f">https://benchling.com/s/seq-plaxdUy0C6uSXC346D9f</a> | 1 and 4 |
| LS1_MpEF1+mTurq2+N7+Nos_T35S_T/Cassette Hygro  | <a href="https://benchling.com/s/seq-v4gfgUiUhpdwSaRBIWIU">https://benchling.com/s/seq-v4gfgUiUhpdwSaRBIWIU</a> | 1 and 4 |
| LS1_MpEF1+TurboRFP+Nos_T35S_T/Cassette Hygro   | <a href="https://benchling.com/s/seq-pySvFBkmcDk0iNFGYFEG">https://benchling.com/s/seq-pySvFBkmcDk0iNFGYFEG</a> | 1 and 4 |
| LS1_MpEF1+Citrine+Nos_T35S_T/Cassette Hygro  | <a href="https://benchling.com/s/seq-xchNEoAgcjiViTIRUJiy">https://benchling.com/s/seq-xchNEoAgcjiViTIRUJiy</a> | 1 and 4 |
| LS1_MpEF1+Citrine+N7+Nos_T35S_T/Cassette Hygro   | <a href="https://benchling.com/s/seq-vv49aKz8q6LnnKgYVQWd">https://benchling.com/s/seq-vv49aKz8q6LnnKgYVQWd</a> | 1 and 4 |
| LS1_MpEF1+Citrine+Lti6b+Nos_T35S_T/Cassette Hygro  | <a href="https://benchling.com/s/seq-yZE4Zg66rPbluo43l6zZ">https://benchling.com/s/seq-yZE4Zg66rPbluo43l6zZ</a> | 1 and 4 |
| LS1_MpEF1+mBeRFP+Nos_T35S_T/Cassette Hygro   | <a href="https://benchling.com/s/seq-t2WWBiEdJ7VCmYeVlkvO">https://benchling.com/s/seq-t2WWBiEdJ7VCmYeVlkvO</a> | 1 and 4 |
| LS1_MpEF1+deGFP+Nos_T35S_T/Cassette Hygro  | <a href="https://benchling.com/s/seq-ApcDM6FIq2tTsV6l6He">https://benchling.com/s/seq-ApcDM6FIq2tTsV6l6He</a>   | 1 and 4 |
| LS1_MpEF1+CyOFP1+Nos_T35S_T/Cassette Hygro   | <a href="https://benchling.com/s/seq-4n77AONzwn8dmyM1aCa6">https://benchling.com/s/seq-4n77AONzwn8dmyM1aCa6</a> | 1 and 4 |
| LS1_MpEF1+Venus+Lti6b+Nos_T35_T/MpEF1+mTurq2+N7+Nos_T35S_T/MpEF1+mRuby3+Nos_T35_T/Cassette Hygro | <a href="https://benchling.com/s/seq-NwoQaEHF0l0bRiHvZoeC">https://benchling.com/s/seq-NwoQaEHF0l0bRiHvZoeC</a> | 1 and 4 |

|   |  |         |
|---|--|---------|
| LS1_pUBQ10+mTurq2+N7+Nos_T35S_T/Cassette Hygro                                    | <a href="https://benchling.com/s/seq-3FnTlPENovYzvu5Ds4LV">https://benchling.com/s/seq-3FnTlPENovYzvu5Ds4LV</a>  | 1 and 4 |
| LS1_MpEF1+Venus+Nos_T35S_T/pUBQ10+mTurq2+N7+Nos_T35S_T/Cassette Hygro (LK3-Dummy) | <a href="https://benchling.com/s/seq-kkQcYoECFre1cQPkJihI">https://benchling.com/s/seq-kkQcYoECFre1cQPkJihI</a>  | 1 and 4 |
| LS1_MpEF1+Venus+Nos_T35S_T/pUBQ10+mTurq2+N7+Nos_T35S_T/Cassette Hygro (LK3-20A)   | <a href="https://benchling.com/s/seq-429AN55KcmFNG8HSnwjc">https://benchling.com/s/seq-429AN55KcmFNG8HSnwjc</a>  | 1 and 4 |
| LS1_UASHap1*2_BOX/Spacer20A/UASHap1*2_BOX/Spacer20A                               | <a href="https://benchling.com/s/seq-9D52thCusn1e6vAzhLw0">https://benchling.com/s/seq-9D52thCusn1e6vAzhLw0</a>  | 1 and 4 |
| LS1_UASHap1*2_BOX/Spacer20B/UASHap1*2_BOX/Spacer20B                               | <a href="https://benchling.com/s/seq-YX9gOxirwA35bvXAedK">https://benchling.com/s/seq-YX9gOxirwA35bvXAedK</a>  | 1 and 4 |
| LS1_UASHap1*2_BOX/Spacer40B/UASHap1*2_BOX/Spacer40B                               | <a href="https://benchling.com/s/seq-GMbqHYnEXFPEmpJZtdPE">https://benchling.com/s/seq-GMbqHYnEXFPEmpJZtdPE</a>  | 1 and 4 |
| LS1_UASHap1*2_BOX/Spacer40A/UASHap1*2_BOX/Spacer40A                               | <a href="https://benchling.com/s/seq-Zv2nQlJuObTOYsn98Kbk">https://benchling.com/s/seq-Zv2nQlJuObTOYsn98Kbk</a>  | 1 and 4 |
| LS2_UASHap1*2_BOX/Spacer20B/UASHap1*2_BOX/pMin                                    | <a href="https://benchling.com/s/seq-eR6uyk59EyoufRPpSL6E">https://benchling.com/s/seq-eR6uyk59EyoufRPpSL6E</a>  | 4 and 6 |
| LS2_UASGal4*2_BOX/Spacer20B/UASGal4*2_BOX/pMin                                    | <a href="https://benchling.com/s/seq-uHoUPtAZ8xJrcrMXjjxc">https://benchling.com/s/seq-uHoUPtAZ8xJrcrMXjjxc</a>  | 4 and 6 |
| LS1_UASGal4*2_BOX/Spacer20B/UASGal4*2_BOX/Spacer20B                               | <a href="https://benchling.com/s/seq-RmQAU6QzY01BBAix7pww">https://benchling.com/s/seq-RmQAU6QzY01BBAix7pww</a><br><a href="https://benchling.com/s/seq-RmQAU6QzY01BBAix7pww">https://benchling.com/s/seq-RmQAU6QzY01BBAix7pww</a> | 1 and 4 |
| LS1_SprROp*1_BOX/Spacer20B/SprROp*1_BOX/Spacer20B                                 | <a href="https://benchling.com/s/seq-KbWHEFN1BrL2LwmW48m6">https://benchling.com/s/seq-KbWHEFN1BrL2LwmW48m6</a>  | 1 and 4 |
| LS2_SprROp*1_BOX/Spacer20B/SprROp*1_BOX/pMin                                      | <a href="https://benchling.com/s/seq-LLD4z4I3flIOXBnastOnT">https://benchling.com/s/seq-LLD4z4I3flIOXBnastOnT</a>  | 4 and 6 |
| LS2_TetROp*1_BOX/Spacer20B/TetROp*1_BOX/pMin                                      | <a href="https://benchling.com/s/seq-hrFOAmykH4D76pVnDHoe">https://benchling.com/s/seq-hrFOAmykH4D76pVnDHoe</a>  | 4 and 6 |

|   |   |         |
|---|---|---------|
| LS1_TetROp*1_BOX/Spacer20B/TetROp*1_BOX/Spacer20B           | <a href="https://benchling.com/s/seq-tNG2POqpjfrN0V9T5OnX">https://benchling.com/s/seq-tNG2POqpjfrN0V9T5OnX</a> | 1 and 4 |
| LS1_UASHap1*1_BOX/Spacer20B/UASHap1*1_BOX/Spacer20B         | <a href="https://benchling.com/s/seq-bYXB1LBjWxCceY1PhBto">https://benchling.com/s/seq-bYXB1LBjWxCceY1PhBto</a> | 1 and 4 |
| LS2_UASHap1*1_BOX/Spacer20B/UASHap1*1_BOX/pMin              | <a href="https://benchling.com/s/seq-lb8Dci7hDwSldE2uY3wj">https://benchling.com/s/seq-lb8Dci7hDwSldE2uY3wj</a> | 4 and 6 |
| LS1_UASGal4*1_BOX/Spacer20B/UASGal4*1_BOX/Spacer20B         | <a href="https://benchling.com/s/seq-a3GVABEmpiOTWQdAmj0j">https://benchling.com/s/seq-a3GVABEmpiOTWQdAmj0j</a> | 1 and 4 |
| LS2_UASGal4*1_BOX/Spacer20B/UASGal4*1_BOX/pMin              | <a href="https://benchling.com/s/seq-7NkSSZ4BJQDXDMxqRReY">https://benchling.com/s/seq-7NkSSZ4BJQDXDMxqRReY</a> | 4 and 6 |
| LS2_SprROp*2_BOX/Spacer20B/SprROp*2_BOX/pMin                | <a href="https://benchling.com/s/seq-wDltzExsEqDDTupszlmX">https://benchling.com/s/seq-wDltzExsEqDDTupszlmX</a> | 4 and 6 |
| LS1_SprROp*2_BOX/Spacer20B/SprROp*2_BOX/Spacer20B           | <a href="https://benchling.com/s/seq-eQkgnhHtAxNQj6gQAOpJ">https://benchling.com/s/seq-eQkgnhHtAxNQj6gQAOpJ</a> | 1 and 4 |
| LS1_TetROp*2_BOX/Spacer20B/TetROp*2_BOX/Spacer20B           | <a href="https://benchling.com/s/seq-rZJ43e7FmDRYFxeNOZ4f">https://benchling.com/s/seq-rZJ43e7FmDRYFxeNOZ4f</a> | 1 and 4 |
| LS2_TetROp*2_BOX/Spacer20B/TetROp*2_BOX/pMin                | <a href="https://benchling.com/s/seq-HUpyvSJ64VaNGNyu89ac">https://benchling.com/s/seq-HUpyvSJ64VaNGNyu89ac</a> | 4 and 6 |
| LS1_UASHap1*2_BOX/UASHap1*2_BOX/UASHap1*2_BOX/UASHap1*2_BOX | <a href="https://benchling.com/s/seq-iA0nC64Yu6Bw58KEXBVw">https://benchling.com/s/seq-iA0nC64Yu6Bw58KEXBVw</a> | 1 and 4 |
| LS2_UASHap1*2_BOX/UASHap1*2_BOX/UASHap1*2_BOX/pMin          | <a href="https://benchling.com/s/seq-MgfEggyoUKdqJEkYc0E9">https://benchling.com/s/seq-MgfEggyoUKdqJEkYc0E9</a> | 4 and 6 |
| LS2_Spacer20B/Spacer20B/Spacer20B/pMin                      | <a href="https://benchling.com/s/seq-hCJvy9mlxOpfBdj36ndD">https://benchling.com/s/seq-hCJvy9mlxOpfBdj36ndD</a> | 4 and 6 |
| LS1_Spacer20B/Spacer20B/Spacer20B/Spacer20B                 | <a href="https://benchling.com/s/seq-NQUH11dlpaXN0VDS9Opo">https://benchling.com/s/seq-NQUH11dlpaXN0VDS9Opo</a> | 1 and 4 |

|  |   |         |
|--|---|---------|
| LS1_Spacer20B/Spacer20A/Spacer20B/Spacer20A                                    | <a href="https://benchling.com/s/seq-f86sPJBwhZSM3XCEiGe3">https://benchling.com/s/seq-f86sPJBwhZSM3XCEiGe3</a> | 1 and 4 |
| LS2_Spacer20B/Spacer20A/Spacer20B/pMin   | <a href="https://benchling.com/s/seq-GmmedrL20VmoshKemajJ">https://benchling.com/s/seq-GmmedrL20VmoshKemajJ</a> | 4 and 6 |
| LS1_MpEF1+HAPI/VP16+Nos_T35S_T/p4BOX_UASHapl*1+Venus+Nos_T35S_T/Cassette Hygro | <a href="https://benchling.com/s/seq-XbxxXqqeGWOPg2kkJo2P">https://benchling.com/s/seq-XbxxXqqeGWOPg2kkJo2P</a> | 1 and 4 |
| LS1_MpEF1+HAPI/VP16+Nos_T35S_T/p4BOX_UASHapl*2+Venus+Nos_T35S_T/Cassette Hygro | <a href="https://benchling.com/s/seq-kHdmx97ICJQAjpcUucaf">https://benchling.com/s/seq-kHdmx97ICJQAjpcUucaf</a> | 1 and 4 |
| LS1_MpEF1+HAPI+VP16+Nos_T35S_T/p4BOX_UASHapl*2+Venus+Nos_T35S_T/Cassette Hygro | <a href="https://benchling.com/s/seq-60NCfu2z9AB2a40DNoXa">https://benchling.com/s/seq-60NCfu2z9AB2a40DNoXa</a> | 1 and 4 |
| LS1_MpEF1+GAL4/VP16+Nos_T35S_T/p4BOX_UASGal4*1+Venus+Nos_T35S_T/Cassette Hygro | <a href="https://benchling.com/s/seq-2sKoBdXkq3oONPW8MriG">https://benchling.com/s/seq-2sKoBdXkq3oONPW8MriG</a> | 1 and 4 |
| LS1_MpEF1+GAL4/VP16+Nos_T35S_T/p4BOX_UASGal4*2+Venus+Nos_T35S_T/Cassette Hygro | <a href="https://benchling.com/s/seq-DTmYCz1bkhGzF5no2DGN">https://benchling.com/s/seq-DTmYCz1bkhGzF5no2DGN</a> | 1 and 4 |
| LS1_MpEF1+GAL4+VP16+Nos_T35S_T/p4BOX_UASGal4*2+Venus+Nos_T35S_T/Cassette Hygro | <a href="https://benchling.com/s/seq-DTlwiBrpS101h3mSrFuy">https://benchling.com/s/seq-DTlwiBrpS101h3mSrFuy</a> | 1 and 4 |
| LS1_MpEF1+SprR+VP16+Nos_T35S_T/p4BOX_SprROp*1+Venus+Nos_T35S_T/Cassette Hygro  | <a href="https://benchling.com/s/seq-fTozQ8AP4aYY4ZFROHLV">https://benchling.com/s/seq-fTozQ8AP4aYY4ZFROHLV</a> | 1 and 4 |
| LS1_MpEF1+SprR+VP16+Nos_T35S_T/p4BOX_SprROp*2+Venus+Nos_T35S_T/Cassette Hygro  | <a href="https://benchling.com/s/seq-eVYt1UEQMqYvANlzlphu">https://benchling.com/s/seq-eVYt1UEQMqYvANlzlphu</a> | 1 and 4 |
| LS1_MpEF1+TetR+VP16+Nos_T35S_T/p4BOX_TetROp*1+Venus+Nos_T35S_T/Cassette Hygro  | <a href="https://benchling.com/s/seq-oALrCZic2LOhcJwbl1Hx">https://benchling.com/s/seq-oALrCZic2LOhcJwbl1Hx</a> | 1 and 4 |
| LS1_MpEF1+TetR+VP16+Nos_T35S_T/p4BOX_TetROp*2+Venus+Nos_T35S_T/Cassette Hygro  | <a href="https://benchling.com/s/seq-SIF7GPieiQwGeTiTMkEx">https://benchling.com/s/seq-SIF7GPieiQwGeTiTMkEx</a> | 1 and 4 |
| LS1_MpEF1+HAPI+VP16+Nos_T35S_T/p7BOX_20B+Venus+Nos_T35S_T/Cassette Hygro       | <a href="https://benchling.com/s/seq-KuiR7s0IL1Zd86bYCfjL">https://benchling.com/s/seq-KuiR7s0IL1Zd86bYCfjL</a> | 1 and 4 |

|   |   |         |
|---|---|---------|
| LS1_MpEF1+GAL4+VP16+Nos_T35S_T/p7BOX_20B+Venus+Nos_T35S_T/Cassette Hygro          | <a href="https://benchling.com/s/seq-ONQTPJhMKAgc5H1poq7v">https://benchling.com/s/seq-ONQTPJhMKAgc5H1poq7v</a> | 1 and 4 |
| LS1_MpEF1+TetR+VP16+Nos_T35S_T/p7BOX_20B+Venus+Nos_T35S_T/Cassette Hygro          | <a href="https://benchling.com/s/seq-KteQivW6RAD8baqRUqis">https://benchling.com/s/seq-KteQivW6RAD8baqRUqis</a> | 1 and 4 |
| LS1_MpEF1+SprR+VP16+Nos_T35S_T/p7BOX_20B+Venus+Nos_T35S_T/Cassette Hygro          | <a href="https://benchling.com/s/seq-IIBwePIIT2NPNUFqtEG3">https://benchling.com/s/seq-IIBwePIIT2NPNUFqtEG3</a> | 1 and 4 |
| LS1_p7BOX_20B+Venus+Nos_T35S_T/Cassette Hygro                                     | <a href="https://benchling.com/s/seq-eDdLe4xUBcwq3y1jxYp0">https://benchling.com/s/seq-eDdLe4xUBcwq3y1jxYp0</a> | 1 and 4 |
| LS1_MpEF1+HAPI+VP16+GR+Nos_T35S_T/p4BOX_UASHapl*1+Venus+Nos_T35S_T/Cassette Hygro | <a href="https://benchling.com/s/seq-JsF3z3RPMP4Eoiy0k5BL">https://benchling.com/s/seq-JsF3z3RPMP4Eoiy0k5BL</a> | 1 and 4 |
| LS1_MpEF1+HAPI+VP16+GR+Nos_T35S_T/p4BOX_UASHapl*2+Venus+Nos_T35S_T/Cassette Hygro | <a href="https://benchling.com/s/seq-pdNhHcvaxVugC6UWszFr">https://benchling.com/s/seq-pdNhHcvaxVugC6UWszFr</a> | 1 and 4 |
| LS1_MpEF1+HAPI/VP16/GR+Nos_T35S_T/p4BOX_UASHapl*1+Venus+Nos_T35S_T/Cassette Hygro | <a href="https://benchling.com/s/seq-WzF9qCc8rj2UncwDzvbh">https://benchling.com/s/seq-WzF9qCc8rj2UncwDzvbh</a> | 1 and 4 |
| LS1_MpEF1+GAL4+VP16+GR+Nos_T35S_T/p4BOX_UASGal4*1+Venus+Nos_T35S_T/Cassette Hygro | <a href="https://benchling.com/s/seq-FSXM5eKrbclPiYorbzDs">https://benchling.com/s/seq-FSXM5eKrbclPiYorbzDs</a> | 1 and 4 |
| LS1_MpEF1+GAL4+VP16+GR+Nos_T35S_T/p4BOX_UASGal4*2+Venus+Nos_T35S_T/Cassette Hygro | <a href="https://benchling.com/s/seq-x9rp6d3PndTA5ZixcpiQ">https://benchling.com/s/seq-x9rp6d3PndTA5ZixcpiQ</a> | 1 and 4 |
| LS1_MpEF1+TetR+VP16+GR+Nos_T35S_T/p4BOX_TetROp*2+Venus+Nos_T35S_T/Cassette Hygro  | <a href="https://benchling.com/s/seq-qJmflyOATMQPLf6XmxmL">https://benchling.com/s/seq-qJmflyOATMQPLf6XmxmL</a> | 1 and 4 |
| LS1_MpEF1+TetR+VP16+GR+Nos_T35S_T/p4BOX_TetROp*1+Venus+Nos_T35S_T/Cassette Hygro  | <a href="https://benchling.com/s/seq-Pxqj3eNZItEU7J4SfuJ4">https://benchling.com/s/seq-Pxqj3eNZItEU7J4SfuJ4</a> | 1 and 4 |
| LS1_MpEF1+SprR+VP16+GR+Nos_T35S_T/p4BOX_SprROp*2+Venus+Nos_T35S_T/Cassette Hygro  | <a href="https://benchling.com/s/seq-6YDvfeHfne1IAQRsqve">https://benchling.com/s/seq-6YDvfeHfne1IAQRsqve</a>   | 1 and 4 |
| LS1_MpEF1+SprR+VP16+GR+Nos_T35S_T/p4BOX_SprROp*1+Venus+Nos_T35S_T/Cassette Hygro  | <a href="https://benchling.com/s/seq-gNk0rR7UK0VHCyepL5G6">https://benchling.com/s/seq-gNk0rR7UK0VHCyepL5G6</a> | 1 and 4 |

|  |   |         |
|--|---|---------|
| LS1_MpEF1+Venus+GR+Nos_T35S_T/pUBQ10+mTurq2+N7+Nos_T35S_T/Cassette Hygro | <a href="https://benchling.com/s/seq-ajPJu1juZ0smDdWRmTjn">https://benchling.com/s/seq-ajPJu1juZ0smDdWRmTjn</a> | 1 and 4 |
| LS1_MpEF1+Venus+Hsp_T/pUBQ10+mTurq2+N7+Nos_T35S_T/Cassette Hygro         | <a href="https://benchling.com/s/seq-oU586LeoNKkIEBVLS97U">https://benchling.com/s/seq-oU586LeoNKkIEBVLS97U</a> | 1 and 4 |
| LS1_MpEF1+Venus+Nos_T35S_T/pUBQ10+mTurq2+N7+Nos_T35S_T/Cassette Hygro    | <a href="https://benchling.com/s/seq-3ZluZzE3HwDHIDdr0zbM">https://benchling.com/s/seq-3ZluZzE3HwDHIDdr0zbM</a> | 1 and 4 |
| LS1_MpEF1+Venus+GR+Nos_T35S_T/Cassette Hygro                             | <a href="https://benchling.com/s/seq-xt3XtMPmk1zPRuGtFk5H">https://benchling.com/s/seq-xt3XtMPmk1zPRuGtFk5H</a> | 1 and 4 |
| LS1_pUBQ10+mTurq2+N7+Nos_T35S_T/Cassette Hygro                           | <a href="https://benchling.com/s/seq-OiK0I7PfbJqyWyYPvITQ">https://benchling.com/s/seq-OiK0I7PfbJqyWyYPvITQ</a> | 1 and 4 |
| LS1_RY+ABRE Boxes*4  | <a href="https://benchling.com/s/seq-psCh266nlzpjH7Wvvst4">https://benchling.com/s/seq-psCh266nlzpjH7Wvvst4</a> | 1 and 4 |
| LS2_RY+ABRE Boxes*3 + pMin 35S   | <a href="https://benchling.com/s/seq-PjMbRk2SqNT0H9tEokOF">https://benchling.com/s/seq-PjMbRk2SqNT0H9tEokOF</a> | 4 and 6 |
| LS1_AuxREs Boxes*4   | <a href="https://benchling.com/s/seq-SXXZszlrTliropEMnyBO">https://benchling.com/s/seq-SXXZszlrTliropEMnyBO</a> | 1 and 4 |
| LS2_AuxREs Boxes*3 + pMin 35S  | <a href="https://benchling.com/s/seq-sPnXcMd5fLd5P1X6dz3Q">https://benchling.com/s/seq-sPnXcMd5fLd5P1X6dz3Q</a> | 4 and 6 |
| LS1_CKOper*4   | <a href="https://benchling.com/s/seq-tYRNWCscZ2tH3HnLgzHS">https://benchling.com/s/seq-tYRNWCscZ2tH3HnLgzHS</a> | 1 and 4 |
| LS2_CKOper*3 + pMin 35S  | <a href="https://benchling.com/s/seq-uDI7JmgnhhOhKCuk9jjw">https://benchling.com/s/seq-uDI7JmgnhhOhKCuk9jjw</a> | 4 and 6 |
| LS1_D1b+D1c Prom Boxes*4   | <a href="https://benchling.com/s/seq-o59tPsRIR9T9O7mSK2sv">https://benchling.com/s/seq-o59tPsRIR9T9O7mSK2sv</a> | 1 and 4 |
| LS2_D1b+D1c Prom Boxes*3 + pMin 35S                                      | <a href="https://benchling.com/s/seq-Mgbwewp3EpuRIs7aHNE1">https://benchling.com/s/seq-Mgbwewp3EpuRIs7aHNE1</a> | 4 and 6 |

|  |   |         |
|--|---|---------|
| LS1_p4BOX_TetROp*1+Venus+Nos_T35S_T/Cassette Hygro   | <a href="https://benchling.com/s/seq-2vdRpwXpg1eziQAig6dy">https://benchling.com/s/seq-2vdRpwXpg1eziQAig6dy</a> | 1 and 4 |
| LS1_p4BOX_TetROp*2+Venus+Nos_T35S_T/Cassette Hygro   | <a href="https://benchling.com/s/seq-wJUz695Par5xkex6fHB">https://benchling.com/s/seq-wJUz695Par5xkex6fHB</a>   | 1 and 4 |
| LS1_p4BOX_SprROp*1+Venus+Nos_T35S_T/Cassette Hygro   | <a href="https://benchling.com/s/seq-YpJogIPKf6fRQiNhzxK7">https://benchling.com/s/seq-YpJogIPKf6fRQiNhzxK7</a> | 1 and 4 |
| LS1_p4BOX_SprROp*2+Venus+Nos_T35S_T/Cassette Hygro   | <a href="https://benchling.com/s/seq-Vem2ZOdy8aAvsB8orgcq">https://benchling.com/s/seq-Vem2ZOdy8aAvsB8orgcq</a> | 1 and 4 |
| LS1_p4BOX_UASGal4*2+Venus+Nos_T35S_T/Cassette Hygro  | <a href="https://benchling.com/s/seq-WAqA9WKbD0fIjuJkx7M">https://benchling.com/s/seq-WAqA9WKbD0fIjuJkx7M</a>   | 1 and 4 |
| LS1_p4BOX_UASGal4*1+Venus+Nos_T35S_T/Cassette Hygro  | <a href="https://benchling.com/s/seq-BdJKounkEflnCuW7G82d">https://benchling.com/s/seq-BdJKounkEflnCuW7G82d</a> | 1 and 4 |
| LS1_p4BOX_UASHapl*1+Venus+Nos_T35S_T/Cassette Hygro  | <a href="https://benchling.com/s/seq-uATWXB4DSpAkVV0kt8m7">https://benchling.com/s/seq-uATWXB4DSpAkVV0kt8m7</a> | 1 and 4 |
| LS1_p4BOX_UASHapl*2+Venus+Nos_T35S_T/Cassette Hygro  | <a href="https://benchling.com/s/seq-fhZ5OI3hWdiN5XwegXLi">https://benchling.com/s/seq-fhZ5OI3hWdiN5XwegXLi</a> | 1 and 4 |
| LS1_MpEF1a+TetR+SYNZIP17+NosT35ST/p4BOX_TetROp*1+Venus+Nos_T35S_T/MpEF1a+SYNZIP18+VP16+HspT/Cassette Hygro         | <a href="https://benchling.com/s/seq-dXDrx9N1IUGIyQX8sKI">https://benchling.com/s/seq-dXDrx9N1IUGIyQX8sKI</a>   | 1 and 4 |
| LS1_MpEF1a+Gal4 short+SYNZIP17+NosT35ST/p4BOX_UASGal4*1+Venus+Nos_T35S_T/MpEF1a+SYNZIP18+VP16+HspT/Cassette Hygro  | <a href="https://benchling.com/s/seq-yO3gqH0MHgznd4NHEvwU">https://benchling.com/s/seq-yO3gqH0MHgznd4NHEvwU</a> | 1 and 4 |
| LS1_MpEF1a+TetR(NO NLS)+SYNZIP17+NosT35ST/p4BOX_TetROp*1+Venus+Nos_T35S_T/MpEF1a+SYNZIP18+VP16+HspT/Cassette Hygro | <a href="https://benchling.com/s/seq-Cb9vi7FTqifqZsjhKjd6">https://benchling.com/s/seq-Cb9vi7FTqifqZsjhKjd6</a> | 1 and 4 |
| LS1_MpEF1a+Gal4+SYNZIP17+NosT35ST/p4BOX_UASGal4*1+Venus+Nos_T35S_T/MpEF1a+SYNZIP18+VP16+HspT/Cassette Hygro        | <a href="https://benchling.com/s/seq-OYIKoFs9pthn6Adc3XRx">https://benchling.com/s/seq-OYIKoFs9pthn6Adc3XRx</a> | 1 and 4 |

|   |   |         |
|---|---|---------|
| LS1_p7BOX_D1b+D1c+Venus+NosT35ST/MpEF1+mRuby3+Nos_T35_T/Cassette Hygro                    | <a href="https://benchling.com/s/seq-VdjlpyrOhEpNWE9XACZa">https://benchling.com/s/seq-VdjlpyrOhEpNWE9XACZa</a>   | 1 and 4 |
| LS1_p7BOX_CKOper+Venus+NosT35ST/MpEF1+mRuby3+Nos_T35_T/Cassette Hygro                     | <a href="https://benchling.com/s/seq-W0H0SgcCHRwVPtksW5y">https://benchling.com/s/seq-W0H0SgcCHRwVPtksW5y</a>   | 1 and 4 |
| LS1_p7BOX_RY+ABRE+Venus+NosT35ST/MpEF1+mRuby3+Nos_T35_T/Cassette Hygro                    | <a href="https://benchling.com/s/seq-0HTkA1jNXvNGel6sTN2i">https://benchling.com/s/seq-0HTkA1jNXvNGel6sTN2i</a>   | 1 and 4 |
| LS1_p7BOX_AuxREs+Venus+NosT35ST/pUbq10+mRuby3+HspT/Cassette Hygro                         | <a href="https://benchling.com/s/seq-6YR96HnkCTcXzAC8vlet">https://benchling.com/s/seq-6YR96HnkCTcXzAC8vlet</a>   | 1 and 4 |
| LS1_MpEF1a+Venus+GR (NO NLS)+NosT35ST/MpEF1+mRuby3+Nos_T35_T/Cassette Hygro               | <a href="https://benchling.com/s/seq-d2KngMEbVbhcQoOCsRrK">https://benchling.com/s/seq-d2KngMEbVbhcQoOCsRrK</a>   | 1 and 4 |
| LS1_pUbq10+mRuby3+HspT/Cassette Hygro   | <a href="https://benchling.com/s/seq-uauiwni922VNR4Xdm1EZ?m=slm-jSiLKZR73Rb1wa9anB15">https://benchling.com/s/seq-uauiwni922VNR4Xdm1EZ?m=slm-jSiLKZR73Rb1wa9anB15</a> | 1 and 4 |
| LS1_MpEF1a+TetR(NO_NLS)+VP16+GR+NosT35ST/p4BOX_TetROp*1+Venus+Nos_T35S_T/Cassette Hygro   | <a href="https://benchling.com/s/seq-t8PjiqAmbCEjpt8utgcX?m=slm-EEBkYbVFv8vUFhPi2JKx">https://benchling.com/s/seq-t8PjiqAmbCEjpt8utgcX?m=slm-EEBkYbVFv8vUFhPi2JKx</a> | 1 and 4 |
| LS1_MpEF1a+TetR+VP16+GR(NO_NLS)+NosT35ST/p4BOX_TetROp*1+Venus+Nos_T35S_T/Cassette Hygro   | <a href="https://benchling.com/s/seq-zBqanMcLujE0aK9mX0dF?m=slm-1hxSjmFFnY0qA2Icj5vh">https://benchling.com/s/seq-zBqanMcLujE0aK9mX0dF?m=slm-1hxSjmFFnY0qA2Icj5vh</a> | 1 and 4 |
| LS1_MpEF1a+Gal4 short+SYNZIP17+NosT35ST/p4BOX_UASGal4*1+Venus+Nos_T35S_T/Cassette Hygro   | <a href="https://benchling.com/s/seq-Nam8LcTgtUKNBVZ2bEMj?m=slm-arpwN24hfM1iaLBGUct">https://benchling.com/s/seq-Nam8LcTgtUKNBVZ2bEMj?m=slm-arpwN24hfM1iaLBGUct</a>   | 1 and 4 |
| LS1_MpEF1a+Gal4+SYNZIP17+NosT35ST/p4BOX_UASGal4*1+Venus+Nos_T35S_T/Cassette Hygro         | <a href="https://benchling.com/s/seq-Rncg6UCcxgd1RqBYtkPI?m=slm-crkB9GjAmIXxPwpbNf7G">https://benchling.com/s/seq-Rncg6UCcxgd1RqBYtkPI?m=slm-crkB9GjAmIXxPwpbNf7G</a> | 1 and 4 |
| LS1_MpEF1a+TetR(NO NLS)+SYNZIP17+NosT35ST/p4BOX_UASGal4*1+Venus+Nos_T35S_T/Cassette Hygro | <a href="https://benchling.com/s/seq-W8h1UBGuL3ukmzuWACAX?m=slm-Uss3teM72K2aOpEF3G33">https://benchling.com/s/seq-W8h1UBGuL3ukmzuWACAX?m=slm-Uss3teM72K2aOpEF3G33</a> | 1 and 4 |
| LS1_MpEF1a+TetR+SYNZIP17+NosT35ST/p4BOX_UASGal4*1+Venus+Nos_T35S_T/Cassette Hygro         | <a href="https://benchling.com/s/seq-sS9iwpABkuuyJO1ObVB?m=slm-9Ff6x1xkZD7xJmX4AtKZ">https://benchling.com/s/seq-sS9iwpABkuuyJO1ObVB?m=slm-9Ff6x1xkZD7xJmX4AtKZ</a>   | 1 and 4 |